Doctoral Dissertation

Developing a framework for assessing climate change impacts on human health at local and regional levels

Robert Macnee

January 2017

Osaka University

Graduate School of Engineering

Division of Sustainable Energy and Environmental Engineering

Developing a framework for assessing climate change impacts on human health at local and regional levels

Robert Macnee

Abstract

Climate change is complex phenomenon that is driven by variables at all scales. Its impacts can be felt at global, local and even individual levels. If we consider that there is now almost unanimous consensus among scientists that greenhouse gas accumulation in the atmosphere due to anthropogenic emissions is causing the climate to change (McMichael et al. 2006), the main remaining knowledge gaps concern the extent of this change and, specifically, the impacts that it will have on humans and the environment. This presents a problem when attempting to quantify the impact of climate change on specific health outcomes. Therefore, there is now a requirement to develop methodologies to project the impact of climate change at local levels, considering all potential risk factors and health outcomes (Field et al. 2014). The complexity of climate systems means that results or outputs from an assessment of a risk factor or health outcome in one region are not necessarily applicable to other regions, which may have different environmental, social, economic and infrastructural characteristics. This wide range of spatial variety highlights the need for case based research into climate change impacts. However, as with all risk assessments, it is preferable to have a common framework or methodology upon which to base local studies. Another emerging requirement for climate change impact research is the need to place climate change related health risks in context with other sources of risk. All regions and individuals are faced by multiple risks from different sources. Quantifying the risk that climate risk factors pose to different human health outcomes in a unit that is directly comparable to risks from non-climate sources is, therefore, a useful tool for placing climate related health risks in a multiple risk context. This research aims to develop standardised approaches to quantifying the risk of human induced climate change on health at local and regional levels, using an evolutionary, case-based approach. The final outcome of the research is to provide a methodology which enables climate change related health risks to be quantified in a common risk unit, at a local and regional scale.

A case-based approach is taken to analyse two specific risk factors, which are currently difficult to quantify - infectious diseases and heat waves. Building upon the findings of these two studies and the limitations of the quantification methods used, a framework is proposed to quantify the impact of climate change on health outcomes at a local level. Three main objectives are used to formulate the structure of the research, with a final objective developed to collate the findings into higher level implications for research and policy making in the field of climate change impacts on human health and

risk assessment in general. Chapter 1 provides some introduction to climate change and the ways in which it impacts human health. This chapter also describes the problems faced when analysing human health risks from climate change and identifies key research and knowledge gaps. The structure of the study is described and the research questions that it aims to address are explained. In context, this thesis aims to (1) understand the impact of the climate on infectious disease prevalence in two East Asian countries: Japan and the Republic of Korea, with a focus on malaria; (2) determine the variables affecting vulnerability to heat waves and combine and map this vulnerability with heat wave exposure data at a local level; (3) develop a framework that all risk factors and health outcomes can be quantified on the same scale, using Disability Adjusted Life Years (DALYs) as a common unit.

Chapter 2 tackles the first specific objective of understanding the impact of climate on malaria prevalence in Japan and the Republic of Korea includes investigating and comparing past trends of incidence of malaria, the influence of climate, and developing a method to identify areas at risk of re-emergence. The malaria situation in both countries is compared, with reasons for the differences investigated. The link between climatic factors (mean monthly minimum temperature, mean monthly maximum temperature, monthly precipitation and mean monthly relative humidity) and malaria incidence is statistically analysed in the Republic of Korea. Temperature is identified as the major climatic influence on malaria transmission rates at a monthly level for the study region. Based upon this finding, a biological, temperature dependent model - a base reproduction rate model - is combined with climate model outputs to plot current and future climatic suitability for stable malaria transmission in the study regions. This approach to modelling infectious disease risk under climate scenarios is critically assessed.

The second objective is addressed in Chapter 3. This objective is to determine the variables affecting vulnerability to heat waves and to quantify and map these at a local level. The main aim of this Chapter is to produce an output that can be useful for identifying high-risk areas for policy makers and stakeholders. A key facet of this topic is combining a vulnerability assessment with spatial analysis of heat exposure, to provide information that can be used to prioritise countermeasure selection. The analysis is conducted in Osaka City, Japan, to provide real world context and to enable comparison to vulnerability studies in other locations. Principle Component Analysis (PCA) of vulnerability indicators is conducted to construct three principle components determining vulnerability to heat waves. These are (1) socioeconomic factors; (2) social isolation; (3) physical characteristics. The principle components are mapped individually, to identify differences in the spatial distribution of each. They are then weighted, based upon the PCA results, and combined to produce an overall vulnerability index score, which is divided into 8 risk categories, based upon standard deviation of the scores. The vulnerability index score is combined with outputs from a fine scale assessment of exposure to extreme heat across the city, based on observations from weather stations located around the city. The combined output enables the most vulnerable and exposed areas to be identified simultaneously. This method of

quantification and dual vulnerability and exposure assessment is useful for effective implementation of countermeasures to reduce the impact of heat waves at a local scale.

Chapter 4 covers the third research objective. This objective has a broader scope, in that it develops a framework that all risk factors and health outcomes can be quantified on the same scale, using Disability Adjusted Life Years (DALYs) as a common unit. The framework is designed to be transferrable to different regions, which will aid understanding of the spatial differences in risk. Producing DALYs as an output unit also fulfils the requirement to place climate change risks in context with other risks. Cardiovascular disease and meteorological disaster related injuries in Osaka Prefecture, Japan are used as worked examples of how the framework can be used to assess climate change impacts on human health at both a regional and local scale, for two fundamentally different health outcomes. The example health outcomes were selected due to their importance to the study region and the strong differences in the nature of their impact on human health. The idea was to demonstrate the applicability of the suggested framework on a chronic and an acute health outcome, which would produce outputs quantifying the impact of climate change on each, on a common scale. This framework, therefore, provides a useful reference for producing standardised but transferrable human health impact assessments, as well as producing a result to allow for risk comparisons in a multiple risk environment. As a conclusion to the study, the limitations and key contributions of the methods and findings are discussed. Recommendations for the future direction of study are identified and explained in context. Recommendations for the use of the climate change human health impact quantification framework are provided, with a specific focus on the uses for policy makers.

Chapter 5 addresses the final objective of the study. This chapter collates the findings, limitations and implications of the three subsidiary objectives and draws meaningful conclusions. The conclusions in this chapter aim to contribute to scientific advancement in the field of climate change impact assessment and provide direction to organisations and individuals who are required to take action and implement risk reduction policy related to climate change and human health. Recommendations are provided in how to improve the methodologies provided, with particular attention given to real world applicability. Future research pathways are also discussed, based upon the implications of the research conducted in the thesis. These two concepts formed the backbone of the study, as research in the field of risk analysis should be focused on advancing understanding and communicating this understanding in a transparent, clear and unbiased manner to stakeholders and policy makers alike.

Acknowledgements

This thesis exists due to the help, guidance and support of several people and organisations. I would like to take the time to thank them here.

Firstly, I express my great thanks to my supervisor, Professor Akihiro Tokai. His guidance throughout this study has been invaluable. His critical thinking and clear understanding of how to conduct meaningful and applicable research enabled me to continually focus my research on specific, meaningful goals and questions. The structure, content and conclusions of each study in this thesis would be inferior were it not for his contribution. I owe my understanding of the processes involved in producing research that contributes to science and society to him.

I would like to acknowledge the insightful comments and suggestions from the two reviewers of this thesis: Professor Akira Kondo and Professor Yoshiyuki Shimoda. Their contributions helped to further my research. I would also like to thank Dr. Keiko Masumoto at the Osaka City Institute of Public Health and Environmental Sciences for providing invaluable meteorological data for Osaka City.

Thanks must also be expressed to all the members of the Environmental Management Lab at Osaka University, particularly my fellow doctoral students and the staff researchers, who patiently listened to my monthly reports and rehearsal presentations. Their comments helped me to improve my research and focus my mind on important aspects of the studies undertaken.

This dissertation would not have been possible without the financial support of the Ministry of Education, Culture, Sports, Science and Technology: MEXT. I would also like to acknowledge the APEC Climate Center, Busan, South Korea, for their funding, assistance and data sharing for the initial part of the first study in this thesis.

Finally, I would like to thank my close friends and family members for their emotional support during my time in Japan. I wouldn’t have been able to achieve this without them.

Table of Contents

List of Figures

List of Tables

Definitions of relevant key words and acronyms

Definitions and explanations of key words and acronyms found throughout the thesis are provided below. Most of the definitions are acronyms or technical terms, however definitions are provided for some general words that have a specific definition in relation to climate change impact research.

Adaptation:	The process of adjustment to changes in the climate and its effects (Cardona et al. 2012).
Base reproduction rate model:	A method of modelling the number of cases of a disease that could be transmitted per incidence of the disease, based upon the biology of the disease parasite, the biology of the disease vector, and the ambient temperature.
CVD:	Cardiovascular disease.
DALY:	Disability Adjusted Life Years: a measure of overall disease burden, expressed as the number of years lost due to ill-health, disability or early death (GBD, 2013).
Disability Weight:	Weight given to a particular disease or health outcome that reflects the severity of the disease on a scale from 0 (perfect health) to 1 (equivalent to death) (GBD, 2013).
DRR:	Disaster Risk Reduction: An approach to risk management that focuses on hazardous events and reducing their impact (Füssel and Klein, 2006).
Exposure:	The nature and degree to which a system is exposed to significant climatic variations (Füssel and Klein, 2006).
Getis-Ord Hotspot Analysis:	A statistical method of quantifying spatial clustering of data. This method analyses the value of spatial features within the context of neighbouring features. The output, a *z-score*, determines whether each feature is in a cluster of high (+) or low (-) value features (Mitchell, 2005).
GIS:	Geographic Information System - An information system that is designed to work with data referenced by spatial or geographic coordinates (Foote et al. 1996).

Gonotrophic cycle:	A phase of malaria transmission – The interval between a malaria vector (mosquito) laying each egg-batch and each blood meal (Lindsay et al. 2010).
GMST:	Global Mean Surface Temperature: The average surface temperature for the earth, based upon observed values.
Hazard:	Possible, future occurrence of natural or human-induced physical events that may have adverse effects on vulnerable and exposed elements (Cardona et al. 2012).
HVI:	Heat vulnerability index: a measure of the vulnerability of a population to extreme ambient temperatures. It is a function of demographic, socioeconomic and physical factors.
IPCC:	Intergovernmental Panel on Climate Change.
Lowess smoothing:	A Locally weighted regression scatter plot smoothing method (GISS, 2016).
Meteorological DRI:	Disaster related injury - An injury caused as a direct result of a meteorological disaster.
Optimum Temperature:	A daily maximum temperature for a specific location that, based upon observed data, experiences the lowest death rate compared to other daily maximum temperatures in the same location (Honda et al. 2014).
PTSD:	Post-traumatic stress disorder.
RCP:	Representative Concentration Pathways - Emission pathways developed for the climate modelling community as a basis for long-term and near-term modelling experiments (van Vuuren et al. 2011). They forecast different levels of human induced radiative forcing based on literature derived emission scenarios to account for uncertainty in climate model forecasts.
Sporogonic cycle:	A phase of malaria transmission – The period of (malaria) parasite development in adult mosquitoes, in days (Lindsay et al. 2010).
Tmax (Tmin):	Throughout the study, this refers to maximum (minimum) temperature. The temporal association can be annual, monthly or daily and is specified, where relevant, in each chapter.

UHI:	Urban Heat Island: The phenomenon of higher air and surface temperatures in urban areas compared to the surrounding suburban and rural areas (Solecki et al. 2005).
Vector:	Any agent (animal, or microorganism) that carries and transmits an infectious pathogen into another living organism (Roberts et al. 2008).
Vulnerability:	The degree to which a system is susceptible to or unable to cope with the adverse effects of climate change, including climate variability and extremes (Füssel and Klein, 2006; Smith et al. 2013). In the context of climate change research, vulnerability is usually considered exclusive of external factors.
WHO:	World Health Organisation.
YLD:	Years Lost due to Disability: A measure of the impact of a disease due to its length and the amount of disability that it causes (Murray et al. 2013).
YLL:	Years of Life Lost: A measure of the impact of a disease on a population, accounting for demographics. It is a function of the number of deaths due to a selected health outcome and the standard life expectancy at the age of each death (GBD, 2013).

Chapter 1. Introduction

1.1. Background

1.1.1. Climate change overview – The global situation in 2016

The Intergovernmental Panel on Climate Change (IPCC) reports that it is certain that global mean surface temperatures (GMST) have been increasing since the 19th Century and that the past three decades have been the warmest since records began (Stocker et al. 2013). In fact, eight of the ten warmest years on record have occurred in the past ten years (Figure 1.1.1). There is almost universal consensus among scientists that anthropogenic influences, such as changing the composition of the atmosphere (through greenhouse gas emissions) and land use are drivers of this change (Cubasch et al. 2013). Anthropogenic driven warming in GMST has profound impacts on the energy balance in the atmosphere and ocean, which, in turn, create alterations in energy circulation and variability (Stocker et al. 2013). Long-term impacts on the sea level (Church and White, 2011), ice sheet size (Nghiem et al. 2012) and ocean circulation are being observed (Stocker et al. 2013). Observations of the impact of climate change include an increase in the number of hot days and a decrease in the number of cold nights (Field et al. 2013), variation in precipitation regimes (Trenberth, 2011) and intensification of extreme events (Peterson et al. 2012). The magnitude of these observed impacts is projected to increase further due to future climate change (Stocker et al. 2013).

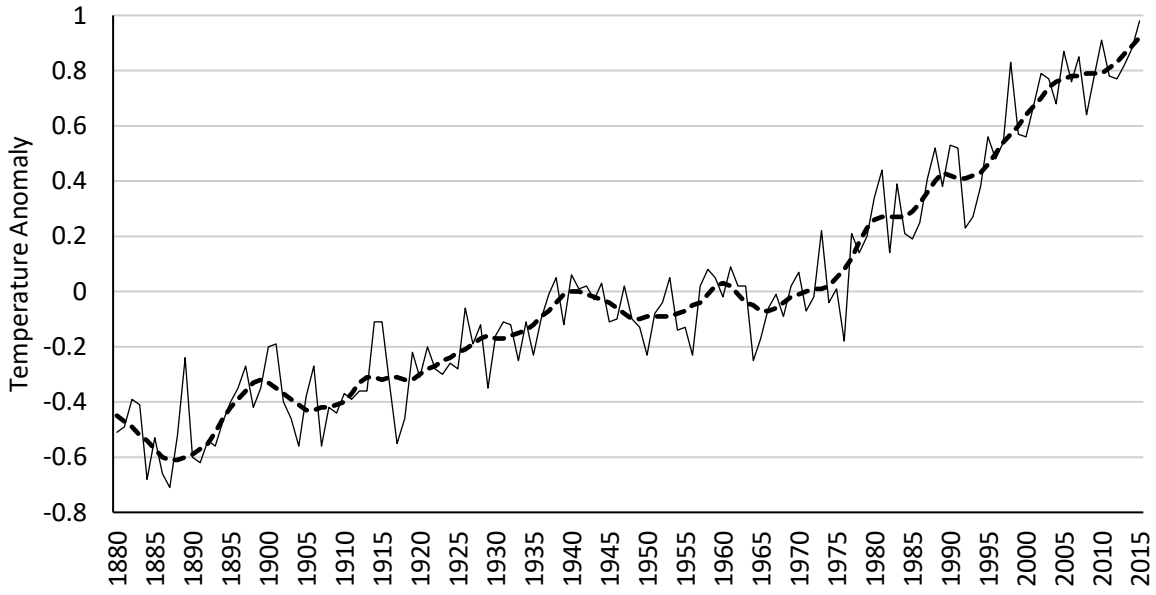

Figure 1.1.1: GMST temperature anomalies 1880-2015 with no smoothing (solid line) and a Lowess-5 smoothing (dashed line) (Data accessed from GISS, 2016).

As a means of projecting the extent of further climate change, the IPCC has developed four scenarios of future emissions, upon which all climate models are built. These scenarios are identified as Representative Concentration Pathways (RCP) and are based upon projections of future socio-economic change, technological change, energy and land use, and emissions of greenhouse gases and air pollutants (van Vuuren et al. 2011). The RCP scenarios are named according to the level of radiative forcing that each scenario projects in 2100, relative to pre-industrial levels (in W/m^2). The scenarios project low (RCP 2.5), medium (RCP 4.5 and 6.0) and high (RCP 8.5) emission scenarios, although the divergence in the pathways is small until 2030-2050 (van Vuuren et al. 2011). The names of each RCP scenario refer to the amount of radiative forcing that each scenario predicts will be attributable to anthropogenic emissions of greenhouse gases (GHG) The scenarios produce projections in temperature increase by 2100 of 0.3 ^oC to 4.8 ^oC, with mean projections of 1.0, 1.8, 2.2 and 3.7 ^oC for RCP 2.5, 4.5, 6.0 and 8.5 respectively (IPCC, 2013). This indicates that the climate will continue to change throughout the century and that only the most drastic emission reduction scenario could limit temperature rise below 1 ^oC. The projected changes in temperature will continue to impact other aspects of the climate, many of which have impacts on human and environmental health.

1.1.2. Climate change and human health – what are the nature of the risks?

Climate change presents a number of risk factors that can impact human health. The key large-scale risk factors that climate change presents are temperature rise, precipitation fluctuations and a change in the frequency and intensity of extreme events (Field et al. 2014). These macroscale risk factors impact other aspects of the climate system, environment and ecosystems (Figure 1.1.2). For example, higher temperatures mean that there is increased evaporation and a greater capacity for the atmosphere to store water vapour (Stocker et al. 2013). Water vapour and its associated latent heat is a driver of atmospheric circulation, from small events such as thunderstorms to global circulation (Stocker et al. 2013). Therefore, we can understand how a rise in GMST can have an impact on precipitation patterns at all scales. When assessing the impact of climate change on human health, it is important to identify risk pathways, such as this, that link an increase in GMST with smaller scale risk factors that have a direct impact on humans.

Essentially, impacts can be categorised as direct or indirect. Examples of direct health impacts include injuries and deaths from flooding and heat waves (McMichael et al. 2006). Indirect impacts include infectious disease spread due to climate change and malnutrition, from climatic influences on agriculture production. Understanding of the impact of climate change on direct hazardous events has developed in the scientific community fairly recently and intensified since the publication of the IPCC Special report on Extreme Events (SREX; IPCC, 2012). It is now possible to quantify the connection between climate change and extreme events through probability calculations (Herring et al. 2014). Extreme heat events are more easily attributable, due to the fact that they are more directly linked to

average global temperatures (Trenberth et al. 2015). Individual thermodynamically created events such as typhoons and storms cannot directly be attributed to climate change, however the probability of such events occurring can be (Trenberth et al. 2015). Two major approaches to attribution exist. The first is a dynamic based approach which considers the underlying atmospheric conditions at the time that a particular event occurred and analyses the impact that climate change has had on these conditions (Trenberth et al. 2015). The second is a statistical approach, based upon observations. The probability of an event occurring at a particular climatic state can be predicted based upon past observations and this can be used to predict the change in the probability of similar events occurring under climate change (Herring et al. 2014). Both approaches are subject to uncertainties, but they provide quantification for the risk of such events occurring in future climate scenarios compared to the present day and past climates. The impact of climate change on indirect health risk factors such as infectious disease, and malnutrition is based largely on changes in average climate conditions over a longer period of time (McMichael et al. 2006). For instance, an increase in average temperatures under climate change will cause alterations to the habitat extent of infectious disease vectors and the growing season length of crops. Through projecting these changes, it is possible to project climate change impacts to indirectly linked health outcomes (McMichael et al. 2006). Figure 1.1.2 identifies pathways linking GMST rise to major human health outcomes, although to fully understand the impacts we must also consider non-climatic factors such as socioeconomics, adaptation and mitigation, and governance (Field et al. 2013).

The traditional approach to tackling climate related risks is through disaster risk reduction (DRR) (IPCC, 2013). This approach focuses on specific hazards and exposed populations and is applicable to event-based risk management (Füssel and Klein, 2006). As understanding of climate change impacts has increased, other risk pathways have been discovered. These include indirect impacts, such as infectious diseases and malnutrition (Smith et al. 2013). Indirect impacts have more complex risk pathways and their impact on a specific population depends heavily on anthropogenic factors. Two health impacts that illustrate the ambiguousness between climate and socioeconomic risks are dengue fever (Bhatt et al. 2013) and malaria (Gething et al. 2010). Trends between climate and dengue (Herrera-Martinez et al. 2010) and malaria (Stern et al. 2011) have been identified; however, anthropogenic influences on both are very strong, meaning that it is often difficult to isolate and quantify the impact of climate related risk factors (Gething et al. 2010). These developments led to the emergence of a new consideration for climate change risk analysis, which included the concept of vulnerability (Füssel and Klein, 2006). The inclusion of vulnerability in climate change risk assessment is an important step forward in developing effective adaptation strategies, as it expands the options available to decision makers. As identified in Figure 1.1.3, the risk for a particular region, population or time is dependent on the exposure, hazard type and underlying vulnerability. Therefore, it is vital to conduct human health impact assessments for different risk pathways and health incomes at regional and local scale, to account for significant variations in exposure and vulnerability.

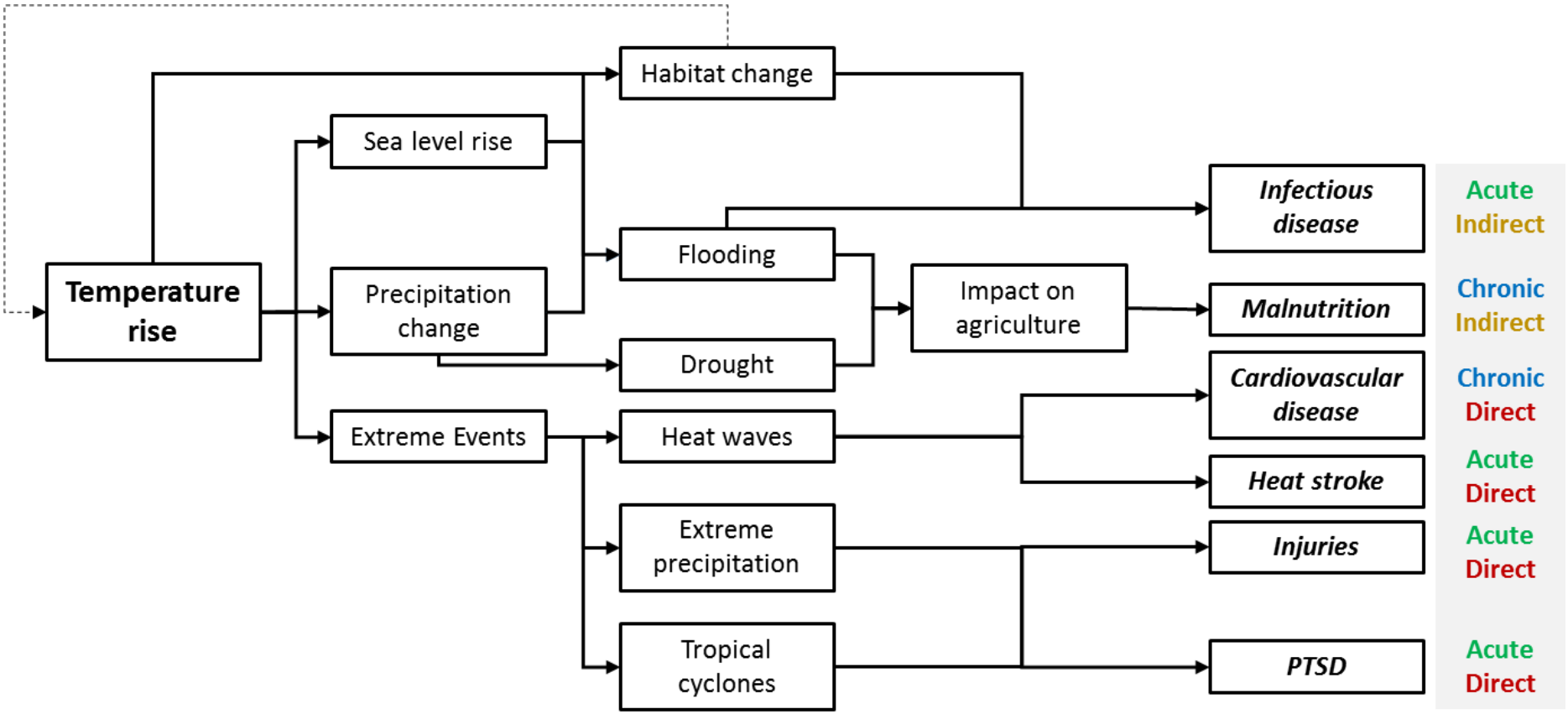

Figure 1.1.2: Impact pathways from anthropogenic induced climate change to human health impacts. Human health endpoints can be categorised into direct, indirect, chronic and acute.

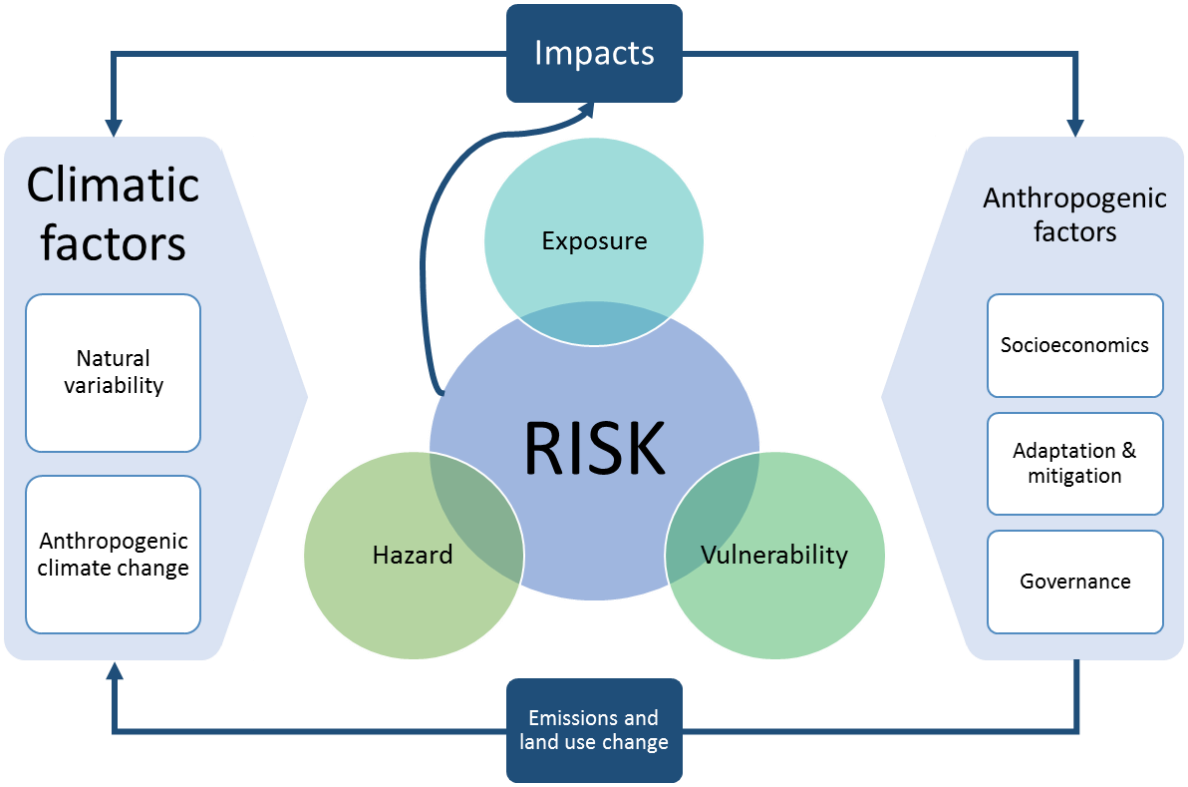

Figure 1.1.3: Conceptual diagram of the influence of climate and human changes on climate change related risks (adapted from Field et al. 2013).

1.1.3. Specific threats to Japan

As a developed country, the most significant climate change risk factors for Japan are increasing mean temperatures, and changes in the frequency and magnitude of extreme events (Campbell-Lendrum et al. 2007). Increasing temperatures will have implications for agriculture (Tanaka et al. 2014), infectious disease prevalence (Bitoh et al. 2011) and heat related illnesses (Honda et al. 2014) in Japan. Extreme events, such as heavy precipitation, tropical storms and typhoons impact Japan several times each year. Under climate change scenarios, the frequency and magnitude of these events is expected to be altered, which has implications for public health and environmental management in Japan.

The mean annual temperature in Japan has increased by 1.15ºC throughout the past century (1898-2010; JMA, 2011). The frequency of > 35ºC days and > 25ºC nights has also increased, and is projected to continue increasing (MEXT et al. 2009). In terms of human health impacts, these risk factors pose two major health impacts to Japan. Increasing mean annual temperature causes an expansion of the habitats of infectious disease transmitting vectors, such as *anopheles albopictus* (dengue fever), and an expansion of the active season of vectors including *anopheles sinensis* (malaria) (Kobayashi et al. 2008). These changes increase the likelihood of imported cases of vector borne diseases being transmitted within Japan (MEXT et al. 2009). Projected increases in the frequency of extremely hot days and nights pose a threat to the health of a large portion of the population of Japan. Takahashi et al. (2007) and

Honda et al. (2014) investigated the concept of an Optimum Temperature for human health (a daily maximum temperature value). The concept of the optimum temperature is that this is the temperature at which the minimum number of daily deaths occur (Honda et al. 2014). Once this temperature is exceeded, the death rate due to heat related illnesses increases exponentially. Temperatures below the optimum temperature also experience an increase in the death rate, but at a much slower rate. Empirical evidence supports the finding that a greater frequency of days above this optimum temperature exposes the population to more dangerous temperatures and increases the risk of succumbing to heat related illnesses (Honda et al. 2014).

The Japan Meteorological Agency defines an extreme heavy precipitation event as an incident of rainfall above 50 mm/hr (JMA, 2016). The frequency of heavy precipitation events (> 50 mm/hr) has increased since the latter half of the 19th Century (JMA, 2016). Iizumi et al (2012) projected that this trend will increase under future climate scenarios. An increase in the number of heavy precipitation events increases the risk of inland flooding and landslides. This has strong implications for Japan, as the population is highly concentrated in many areas that are at risk of flooding (Emori et al. 2005). Tezuka et al. (2014) investigated the relationship between annual precipitation, extreme precipitation events and flood damage costs. Precipitation was found to have a linear relationship with the number of extreme precipitation events. A similar linear relationship was determined to exist between the intensity of an extreme event and the economic cost (Tezuka et al. 2014). This trend was projected to continue beyond 2050 in the study area and provides one way of quantifying the impact of the extreme events risk factor. There is less conclusive evidence of the impact of climate change on the frequency and intensity of tropical storms and typhoons in Japan; however, Mei et al. (2015) projected that climate change is impacting the peak intensity of tropical storms and typhoons. They projected an increase in the frequency of very intense storms and that the actual intensity of the most damaging storms will also exceed current levels. This has the potential to have damaging consequences for Japan, as most of the urban areas are low lying and close to the coast, leaving them vulnerable to strong typhoons and accompanying storm surges.

1.2. Definition of the problem

1.2.1. Problem statement

Climate change is complex phenomenon that is driven a number of variables. Its impacts can also be felt at scales ranging from global to regional, local and even individual levels. This presents a problem in how to quantify the impact of climate change on specific health outcomes. As outlined in Figure 1.1.3.1, there are a complex number of pathways leading from anthropogenic influenced climate change to individual health outcomes. If we consider that there is now almost unanimous consensus among scientists that greenhouse gas accumulation in the atmosphere due to anthropogenic emissions is

causing the climate to change (McMichael et al. 2006), the main uncertainty remains about the extent of this change and the impacts that it will have. Uncertainty in the projected extent of climate change was addressed by the IPCC with the advent of the Special Report of Emissions Scenarios (Nakicenovic and Swart, 2000). This was replaced by the current Representative Concentration Pathways (RCP) in the IPCC Fifth Assessment Report (van Vuuren et al. 2011). The RCPs represent four different emissions scenarios that utilise 95% of the scientific literature on radiative forcing and emissions and include high (RCP 8.5), low (RCP2.5) and two intermediate scenarios (RCP4.5 and RCP6.0). Projections using climate models can be run with all of these scenarios to account for uncertainty, although the variation between the scenarios only becomes significant from between 2030-2050 (van Vuuren (2011). Thus, the main, unaddressed quantification of climate change is the physical impact on the environment and human health. Quantification of this requires an understanding of the pathways with which climate change impacts human health. Identification of the risk factors and their impact on human health outcomes is needed in order to produce meaningful quantifications that have real world uses.

The scientific consensus about global climate change is clear (Ebi et al. 2007). However, differences in local climate, topography, land use, and infrastructure result in different climate change impacts at the regional and local scales. (Ebi et al. 2007). For this reason, general, global scale climate models and projections are inadequate to base adaptation strategies on at a local and regional scale. Due to the complex nature of climate change impact pathways and the wide range of spatially unique influences at different scales, it is important that all methodologies seeking to understand climate change impact are built around real world case studies. The variety of impacts range from direct to indirect and acute to chronic, meaning that generalisations of large scale climate change are inappropriate for basing effective adaptation strategies on. There is a requirement to develop methodologies to project the impact of climate change at local levels, considering all potential risk factors and health outcomes for each location (Field et al. 2014). Results or outputs from an assessment of a risk factor or health outcome in one region are not necessarily applicable to other regions which may have different environmental, social, economic and infrastructural characteristics. This phenomenon highlights the need for case based research into climate change impacts. This, however, does not mean that methodologies of assessments cannot be transferrable to different regions or locations. The whole world is exposed to large scale changes in atmospheric composition and circulation, meaning that generalised global climate models can provide a foundation for local and regional scale assessments (Cubasch et al. 2013). The difficulty arises in converting macroscale projections into something that is applicable to a local environment. Sophisticated downscaling techniques now exist, which can take outputs from global climate models and use them as parameters that drive high resolution regional climate models (RCMs). RCMs can be created by statistical downscaling or dynamic downscaling. As of 2016, dynamically downscaled models are generally perceived to be preferable, as they are based on complex atmospheric physics,

which can replicate microscale and mesoscale atmospheric circulation such as tropical cyclone formation (Knutson et al. 2010). So, downscaling provides a solution to account for differences in local climate and topography, but there is still a requirement to address regional differences in land-use, ecology, social systems, economics and infrastructure. This is where local case study methodology becomes important. Local case studies into climate change are abundant (Basu and Samet, 2002; IPCC, 2014), but there is a lack of cohesion about the end point output of these studies. Different methodologies and units are used as indicators of climate change impacts, which means that decision makers are faced with a difficult task of selecting methodologies and outputs that are applicable to their area of interest and that are comparable to other studies or risk factors. There is a requirement for a universal framework to be developed to assess the impact of different climatic risk factors on different health outcomes at different scales. This would provide organisation and structure to climate change impact studies and increase our understanding of what drives regional differences in impacts.

Further to the development of transferrable frameworks, a common unit that can be used for comparing, combining and contextualising climate change impacts on human health is required. If all regional and local scale studies produced results from a structured and transferable method, that generates a standardised output unit, a much deeper understanding of the nature and spatial components of climate change health impacts would be generated. It would also be much easier to compare the results of different studies, in different locations; an important benefit due to the spatial variety of climate change impacts. Often, poor communication of a risk is a barrier to successful risk reduction policy implementation (Laboy-Nieves et al. 2010). We have seen this in the context of climate change, where, perhaps more than any other global risk, perceptions of the risk and potential impacts have hindered effective mitigation and adaptive action more than any other risk (Weber, 2010). Providing clear, concise and transparent information is a key aspect of influencing peoples' perception of risk. Providing a standardised methodology for assessing climate change risk factors on human health outcomes would be an important step towards improving communication of the nature of risk that people face from climate change in their location. With improved communication would come improved understanding and cooperation, and an increased capacity for providing effective solutions to the risks posed.

Decision makers need knowledge that helps them make informed decisions at the appropriate scale, with the appropriate course of action. This requires them to be able to prioritise allocation of resources to the most pressing risks for each spatial area. In the context of climate change, a decision maker requires knowledge about both the nature and extent of the impact upon a health outcome. Understanding the nature and extent of the impact can help to identify which health outcomes are most affected by climate change and also identify the impact that a climate risk factor has compared to other risk factors (dietary, genetic or chemical, for example). Quantifying the impact of climate change on health outcomes on a comparable scale and using a common unit would provide a solution to this.

1.2.2. Research question

Although climate change is a global phenomenon, its impacts are felt at local and regional scales. This research aims to understand how climate change impacts different health outcomes at a regional and local scale. The pressing question is:

Can the impact of climate change on different health outcomes be quantified using a common unit at a local and regional scale?

From a risk management perspective, it is important to develop a system that enables disparate and dissimilar health outcomes to be quantified and compared on a common scale, in order to increase the understanding of impact pathways of climate change and to place the current and projected impacts in context with other risks. For instance, if we look at cardiovascular disease (CVD) as a health outcome; the risk of suffering from this disease is dependent on a number of risk factors. These risk factors include environmental, physiological, dietary and behavioural risks (GHDx, 2016). In order to prioritise countermeasures, we must consider the impact of each risk factor on the disease separately and also inclusively. By quantifying the impact of the climate and climate change on the disease, using a common unit, we can understand the risk that this poses to CVD in context with the other risks. Furthermore, quantifying the impact of different climatic risk factors on different health outcomes will aid decision from an adaptation perspective. The uses of such a methodology are therefore applicable to public health services, targeting specific health outcomes, as well as to risk management services looking to pursue effective climate change adaptation strategies. As climate change will affect different regions and populations differently, a methodology to provide a clear quantification at a local and regional scale is required. Once developed, the framework can provide a tool to promote targeted and well informed actions, based upon empirical projections of risk on a common scale.

1.2.3. Research objectives

In order to address the research question, this research undertakes investigations into climate change impact pathways at a local and regional scale that currently pose a problem to quantification. A case-based approach is taken to analyse two specific risk factors, which are currently difficult to quantify (infectious diseases and heat waves). Building upon the findings of these two studies and the limitations of the quantification methods used, a method is proposed to quantify the impact of climate change on health outcomes at a local level. The study objectives are as follows:

- Understand the impact of climate on infectious disease prevalence in two East Asian countries: Japan and the Republic of Korea. This aim includes investigating and comparing past trends of incidence of malaria, the influence of climate, and developing a method to identify areas at risk of re-emergence.

- Determine the variables affecting vulnerability to heat waves and map these at a local level. This objective attempts to quantify vulnerability to a risk factor and produce an output that can be useful for identifying high-risk areas. The vulnerability assessment is combined with a spatial analysis of exposure to provide information that can be used to prioritise countermeasure selection.
- Develop a transferrable framework to quantify the impact of climate change on health outcomes at a local and regional scale, using a common unit. The common unit selected is Disability Adjusted Life Years (DALY), which will produce a quantified value of the impact of climate change that can be directly compared to other risks.
- Provide recommendations for policy makers and researchers in this field and suggest future research advancement requirements and direction. The recommendations will be based upon limitations in the research and the findings that open up new research pathways.

1.2.4. Scope of the research

This research is confined geographically to Japan and the Republic of Korea, with a particular focus on the urbanised prefecture of Osaka. The frameworks and methodologies employed are designed to be transferrable to other regions and scales. Thus, discussion and conclusions drawn from the methodologies are universally applicable unless stated otherwise. However, specific interpretations of the results are limited to the study regions in question and do not necessarily apply to other regions. These implications are discussed where applicable in the studies conducted, with any broader ranging conclusions highlighted where necessary. Regarding the use of climate models; the data heavy nature of climate model outputs, particularly at high resolution, required a narrowed scope to be applied to the scenarios studied. For this reason, one climate scenario was employed for each investigation. The scenario selection process is justified where applicable in the text of each study and was selected to represent the *most probable* scenario in each case.

1.3. Research framework

This study is composed of three main areas of focus, which aim to target specific research areas that require further investigation. A more generalised and higher level information provided as an introduction and in a concluding section to summarise the implications and scope of the research conducted and to place the implications in scientific and policy implementation contexts.

Chapter 1 introduces a background to climate change and the ways in which it impacts human health. This chapter also highlights past research and current research gaps. The problem that this study seeks to address is identified and an outline of steps taken to address this problem is presented.

Chapter 2 presents the findings of a study into the impact of the climate and climate change on malaria (an infectious disease) in Japan and the Republic of Korea. This topic was selected as an example of an

emerging climate related health risk that is difficult to quantify. The topic initially investigates regional differences and the observed impact of climate on malaria transmission, before developing a prediction model to identify the areas that are climatically the most at risk to malaria transmission under climate change.

Chapter 3 provides an assessment of heat waves in Osaka City, Japan. This topic was selected to highlight the differences in assessing a direct impact risk factor to an indirect one (infectious diseases). The chapter develops a method to quantify risk at a local level based upon the concepts of vulnerability and exposure to a direct climate related risk factor. The assessment is undertaken at a very fine scale (neighbourhood level) in order to demonstrate the applicability of climate change health risk quantification at a community level. A novel approach of combining a vulnerability assessment with fine temporal and spatial scale exposure observations is pursued and the implications of such an approach are discussed.

Chapter 4 builds upon the findings of the two previous chapters to develop a framework for quantifying all types of climate change health impacts in a common unit. The chapter demonstrates this method at a local and regional scale for a chronic (cardiovascular disease) and acute (meteorological disaster related injuries) health impact, with Osaka Prefecture used as a case study site. The two health outcomes are selected due to their importance in the study area and their fundamental differences. Selecting two dissimilar health outcomes as case studies highlights the adaptability of the climate change risk quantification framework that is discussed in this chapter. Conclusions are drawn on the methodology, including the limitations and implications. Location specific observations and conclusions are also drawn, indicating some of the applicable uses of this framework method to local level studies of climate change health risks.

Chapter 5 summarises the results from the thesis and combines the findings into a broader, high level conclusion. The main contributions of the whole study are discussed and recommendations are proposed to both policy makers and researchers. The thesis structure, identifying the flow of research, is indicated in Figure 1.3.1.

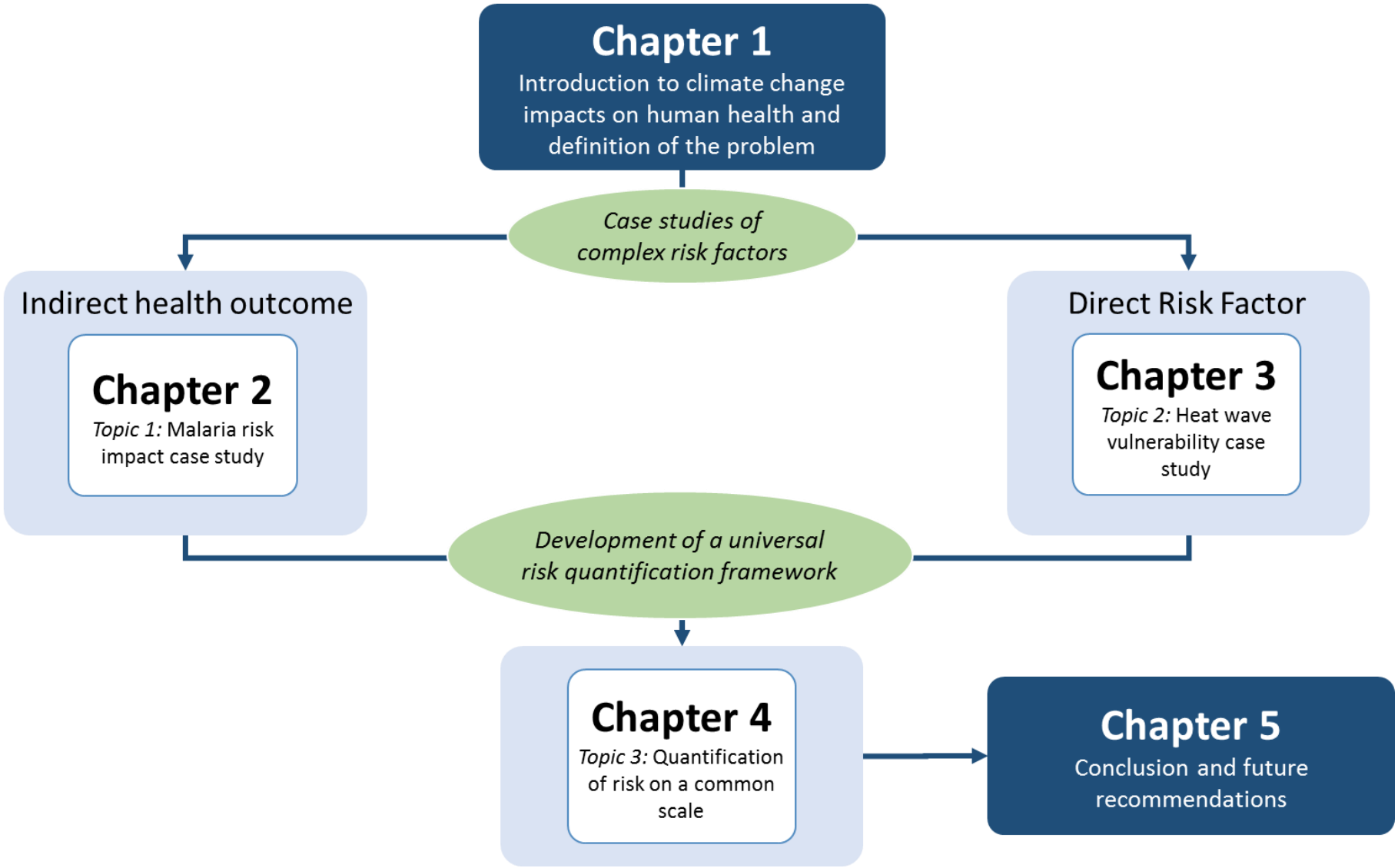

Figure 1.3.1: Thesis structure and flow of the research

References

Bhatt, S., Gething, P.W., Brady, O.J., Messina, J.P., Farlow, A.W., Moyes, C.L., Drake, J.M., Brownstein, J.S., Hoen, A.G., Sankoh, O., Myers, M.F., George, D.B., Jaenisch, T., Wint, G.R.W., Simmons, C.P., Scott, T.W., Farrar, J.J., and Hay, S.I., 2013. The global distribution and burden of dengue. *Nature*, **496**(7446), pp.504-507.

Bitoh, T., Fueda, K., Ohmae, H., Watanabe, M. and Ishikawa, H., 2011. Risk analysis of the re-emergence of Plasmodium vivax malaria in Japan using a stochastic transmission model. *Environmental health and preventive medicine*, **16**(3), pp.171-177.

Campbell-Lendrum, D., Woodruff, R., Prüss-Üstün, A. and Corvalán, C., 2007. Quantifying the health impact at national and local levels. *WHO Environmental Burden of Disease Series*, (14).

Cardona, O.D., van Aalst, M.K., Birkmann, J., Fordham, M., McGregor, G., Perez, R., Pulwarty, R.S., Schipper, E.L.F. and Sinh, B.T., 2012. Determinants of risk: exposure and vulnerability. In: Managing the Risks of Extreme Events and Disasters to Advance Climate Change Adaptation [Field, C.B., V. Barros, T.F. Stocker, D. Qin, D.J. Dokken, K.L. Ebi, M.D. Mastrandrea, K.J. Mach, G.-K. Plattner, S.K. Allen, M. Tignor, and P.M. Midgley (eds.)]. *A Special Report of Working Groups I and II of the Intergovernmental Panel on Climate Change (IPCC)*. Cambridge University Press, Cambridge, UK, and New York, NY, USA, pp. 65-108.

Church, J.A. and White, N.J., 2011. Sea-level rise from the late 19th to the early 21st century. *Surveys in Geophysics*, **32**(4-5), pp.585-602.

Cubasch, U., Wuebbles, D., Chen, D., Facchini, M.C. Frame, D., Mahowald, N. and Winther, J.-G. (2013) Introduction. In: *Climate Change 2013: The Physical Science Basis. Contribution of Working Group I to the Fifth Assessment Report of the Intergovernmental Panel on Climate Change* [Stocker, T.F., D. Qin, G.-K. Plattner, M. Tignor, S.K. Allen,J. Boschung, A. Nauels, Y. Xia, V. Bex and P.M. Midgley (eds.)]. Cambridge University Press, Cambridge, UnitedKingdom and New York, NY, USA.

Emori, S., Kimoto, M., Hasegawa, A., Nozawa, T., Sumi, A., Oki, T., Takahashi, K. and Harasawa, H., 2005. Japan as a possible hot spot of flood damage in future climate illustrated by high-resolution climate modeling using the Earth Simulator. In *conference abstract for 'Avoiding Dangerous Climate Change.*

Ebi, K.L., Meehl, G., Bachelet, D., Twilley, R. and Boesch, D.F., 2007. Regional impacts of climate change: four case studies in the United States. *Pew Center on Global Climate Change*.

Field, C.B., Barros, V.R., Mach, K.J., Mastrandrea, M.D., van Aalst, M., Adger, W.N., Arent, D.J., Barnett, J., Betts, R., Bilir, T.E., Birkmann, J., Carmin, J., Chadee, D.D., Challinor, A.J., Chatterjee, M., Cramer, W., Davidson, D.J., Estrada, Y.O., Gattuso, J.-P., Hijioka, Y., Hoegh-Guldberg, O., Huang, H.Q., Insarov, G.E., Jones, R.N., Kovats, R.S., Romero-Lankao, P., Larsen, J.N., Losada, I.J., Marengo, J.A., McLean, R.F., Mearns, L.O., Mechler, R., Morton, J.F., Niang, I., Oki, T., Olwoch, J.M., Opondo, M., Poloczanska, E.S., Pörtner, H.-O., Redsteer, M.H., Reisinger, A., Revi, A., Schmidt, D.N., Shaw, M.R., Solecki, W., Stone, D.A., Stone, J.M.R., Strzepek, K.M., Suarez, A.G., Tschakert, P., Valentini, R., Vicuña, S., Villamizar, A., Vincent, K.E., Warren, R., White, L.L., Wilbanks, T.J., Wong, P.P. and Yohe, G.W., 2014 Technical summary. In: *Climate Change 2014: Impacts, Adaptation, and Vulnerability. Part A: Global and Sectoral Aspects. Contribution of Working Group II to the Fifth Assessment Report of the Intergovernmental Panel on Climate Change* [Field, C.B., V.R. Barros, D.J. Dokken, K.J. Mach, M.D. Mastrandrea, T.E. Bilir, M. Chatterjee, K.L. Ebi, Y.O. Estrada, R.C. Genova, B. Girma, E.S. Kissel, A.N. Levy, S. MacCracken, P.R. Mastrandrea, and L.L.White (eds.)]. Cambridge University Press, Cambridge, United Kingdom and New York, NY, USA, pp. 35-94.

Foote, K.E. and Lynch, M., 1996. Geographic information systems as an integrating technology: context, concepts, and definitions. *Austin, University of Texas*, pp.40-44.

Füssel, H.M. and Klein, R.J., 2006. Climate change vulnerability assessments: an evolution of conceptual thinking. *Climatic change*, **75**(3), pp.301-329.

GBD, 2013. Global, regional, and national incidence, prevalence, and years lived with disability for 301 acute and chronic diseases and injuries in 188 countries, 1990–2013: a systematic analysis for the Global Burden of Disease Study 2013 [Global Burden of Disease Study 2013 Collaborators, and others], *The Lancet*, **386**(9995), pp.743-800.

Gething, P.W., Smith, D.L., Patil, A.P., Tatem, A.J., Snow, R.W. and Hay, S.I., 2010. Climate change and the global malaria recession. *Nature*, **465**(7296), pp.342-345.

GHDx, 2016. GBD Results Tool, Global Health Data Exchange. http://ghdx.healthdata.org/gbd-results-tool

GISS, 2016. *GISS Surface Temperature Analysis*, Goddard Institute for Space Studies. Accessed from http://data.giss.nasa.gov/gistemp/graphs/

Golledge, N.R., Kowalewski, D.E., Naish, T.R., Levy, R.H., Fogwill, C.J. and Gasson, E.G., 2015. The multi-millennial Antarctic commitment to future sea-level rise. *Nature*, **526**(7573), pp.421-425.

Herrera-Martinez, A.D. and Rodriguez-Morales, A.J., 2010. Potential influence of climate variability on dengue incidence registered in a western pediatric hospital of Venezuela, *Tropical Biomedicine*, **27**(2), pp.280-286.

Honda, Y., Kondo, M., McGregor, G., Kim, H., Guo, Y.-L., Hijioka, Y., Yoshikawa, M., Oka, K., Takano, S., Hales, S. and Kovats, R.S., 2014. Heat-related mortality risk model for climate change impact projection, *Environ Health Prev Med*, **19**, pp.56–63.

Iizumi, T., Takayabu, I., Dairaku, K., Kusaka, H., Nishimori, M., Sakurai, G., Ishizaki, N.N., Adachi, S.A. and Semenov, M.A., 2012. Future change of daily precipitation indices in Japan: A stochastic weather generator‐based bootstrap approach to provide probabilistic climate information. *Journal of Geophysical Research: Atmospheres*, **117**(D11).

IPCC, 2012. Managing the Risks of Extreme Events and Disasters to Advance Climate Change Adaptation. A Special Report of Working Groups I and II of the Intergovernmental Panel on Climate Change [Field, C.B., V. Barros, T.F. Stocker, D. Qin, D.J. Dokken, K.L. Ebi, M.D. Mastrandrea, K.J. Mach, G.-K. Plattner, S.K. Allen, M. Tignor, and P.M. Midgley (eds.)]. Cambridge University Press, Cambridge, UK, and New York, NY, USA, p. 582.

IPCC, 2013. Summary for Policymakers. In: *Climate Change 2013: The Physical Science Basis. Contribution of Working Group I to the Fifth Assessment Report of the Intergovernmental Panel on Climate Change* [Stocker, T.F., D. Qin, G.-K. Plattner, M. Tignor, S.K. Allen, J. Boschung, A. Nauels, Y. Xia, V. Bex and P.M. Midgley (eds.)]. Cambridge University Press, Cambridge, United Kingdom and New York, NY, USA.

JMA, 2011. *Climate Change Monitoring Report 2010*. Japan Meteorological Agency, Tokyo, Japan, pp.106.

JMA, 2016. Heavy Rain Trend, Japan Meteorological Agency. http://www.jma.go.jp/jma/kishou/info/heavyraintrend.html (Japanese)

Knutson, T.R., McBride, J.L., Chan, J., Emanuel, K., Holland, G., Landsea, C., Held, I., Kossin, J.P., Srivastava, A.K. and Sugi, M., 2010. Tropical cyclones and climate change, *Nature Geoscience*, **3**, pp.157 – 163.

Kobayashi, M., Komagata, O. and Nihei, N., 2008. Global warming and vector-borne infectious diseases, *Journal of Disaster Research*, **3**, pp.105–112.

Laboy-Nieves, E.N., Goosen, M.F.A. and Emmanuel, E., 2010. *Environmental and Human Health: Risk Management in Developing Countries*, CRC Press, The Netherlands, pp. 271.

Lindsay, S.W., Hole, D.G., Hutchinson, R.A., Richards, S.A. and Willis, S.G., 2010. Assessing the future threat from vivax malaria in the United Kingdom using two markedly different modelling approaches. *Malaria journal*, **9**(1), p.1.

McMichael, A. J., Woodruff, R. E. and Hales, S., 2006. Climate change and human health: present and future risks, *The Lancet*, **367**(9513), pp.859-869.

Mei, W., Xie, S.P., Primeau, F., McWilliams, J.C. and Pasquero, C., 2015. Northwestern Pacific typhoon intensity controlled by changes in ocean temperatures. *Science advances*, **1**(4), p.e1500014.

MEXT, JMA, and MOE. (2009) *Climate Change and Its Impacts in Japan*. Ministry of Education, Culture, Sports, Science and Technology (MEXT), Japan Meteorological Agency (JMA), Ministry of the Environment (MOE), Tokyo, Japan, 74 pp.

Mitchell, A., 2005. *The ESRI guide to GIS analysis, Volume 2: Spatial Measurements and Statistics*. Redlands, ESRI Press, CA, USA.

Murray, C.J., Vos, T., Lozano, R., Naghavi, M., Flaxman, A.D., Michaud, C., Ezzati, M., Shibuya, K., Salomon, J.A., Abdalla, S. and Aboyans, V., 2013. Disability-adjusted life years (DALYs) for 291 diseases and injuries in 21 regions, 1990–2010: a systematic analysis for the Global Burden of Disease Study 2010. *The lancet*, **380**(9859), pp.2197-2223.

Nakicenovic, N. and Swart, R., 2000. Special report on emissions scenarios. *Special Report on Emissions Scenarios*, Edited by Nebojsa Nakicenovic and Robert Swart, pp. 612. ISBN 0521804930. Cambridge, UK: Cambridge University Press, July 2000., 1.

Nghiem, S.V., Hall, D.K., Mote, T.L., Tedesco, M., Albert, M.R., Keegan, K., Shuman, C.A., DiGirolamo, N.E. and Neumann, G., 2012. The extreme melt across the Greenland ice sheet in 2012. *Geophysical Research Letters*, **39**(20).

Peterson, T., Scott, P. and Herring, S., 2012. Explaining extreme events of 2011 from a climate perspective. *Bulletin of the American Meteorological Society*, **93**, pp.1041-1067.

Roberts, L.S., Janovy, J., Schmidt, G.D. (2008) *Foundations of Parasitology*.

Schmidt, G.D. and Roberts, L.S., 1985. *Foundations of parasitology*. Parasitology Today, **3**(2), McGraw Hill. New York, NY, USA, p.987.

Smith, K.R., Woodward, A., Campbell-Lendrum, D., Chadee, D.D., Honda, Y., Liu, Q., Olwoch, J.M., Revich, B. and Sauerborn, R., 2014. Human health: impacts, adaptation, and co-benefits. In: *Climate Change 2014: Impacts, Adaptation, and Vulnerability. Part A: Global and Sectoral Aspects. Contribution of Working Group II to the Fifth Assessment Report of the*

Intergovernmental Panel on Climate Change [Field, C.B., V.R. Barros, D.J. Dokken, K.J. Mach, M.D. Mastrandrea, T.E. Bilir, M. Chatterjee, K.L. Ebi, Y.O. Estrada, R.C. Genova, B. Girma, E.S. Kissel,A.N. Levy, S. MacCracken, P.R. Mastrandrea, and L.L.White (eds.)]. Cambridge University Press, Cambridge, United Kingdom and New York, NY, USA, pp. 709-754.

Solecki, W.D., Rosenzweig, C., Parshall, L., Pope, G., Clark, M., Cox, J. and Wiencke, M., 2005. Mitigation of the heat island effect in urban New Jersey. *Global Environmental Change Part B: Environmental Hazards*, **6**(1), pp.39-49.

Stern, D.I., Gething, P.W., Kabaria, C.W., Temperley, W.H., Noor, A.M., Okiro, E.A., Shanks, G.D., Snow, R.W. and Hay, S.I., 2011. Temperature and malaria trends in highland East Africa. *PLoS One*, **6**(9), p.e24524.

Stocker, T.F., Qin, D., Plattner, G.-K., Alexander, L.V., Allen, S.K., Bindoff, N.L., Bréon, F.-M., Church, J.A., Cubasch, U., Emori, S., Forster, P., Friedlingstein, P., Gillett, N., Gregory, J.M., Hartmann, D.L., Jansen, E., Kirtman, B., Knutti, R., Krishna Kumar, K., Lemke, P., Marotzke, J., Masson-Delmotte, V., Meehl, G.A., Mokhov, I.I., Piao, S., Ramaswamy, V., Randall, D., Rhein, M., Rojas, M., Sabine, C., Shindell, D., Talley, L.D., Vaughan, D.G. and Xie, S.-P., 2013. Technical Summary. In: *Climate Change 2013: The Physical Science Basis. Contribution of Working Group I to the Fifth Assessment Report of the Intergovernmental Panel on Climate Change* [Stocker, T.F., D. Qin, G.-K. Plattner, M. Tignor, S.K. Allen, J. Boschung, A. Nauels, Y. Xia, V. Bex and P.M. Midgley (eds.)]. Cambridge University Press, Cambridge, United Kingdom and New York, NY, USA.

Takahashi, K., Honda, Y. and Emori, S., 2007. Mortality Risk from Heat Stress due to Global Warming, *Journal of Risk Research*, **10**(3), pp.339-354.

Tanaka, A., Sato, T., Nemoto, M. and Yamanaka, Y., 2014. Sensitivity of cool summer-induced sterility of rice to increased growing-season temperatures: A case study in Hokkaido, Japan. *J. Agr. Meteorol*, **70**(1), pp.25-40.

Tezuka, S., Takiguchi, H., Kazama, S., Sato, A., Kawagoe, S. and Sarukkalige, R., 2014. Estimation of the effects of climate change on flood-triggered economic losses in Japan. *International Journal of Disaster Risk Reduction*, **9**, pp.58-67.

Herring, S.C., Hoerling, M.P., Peterson, T.C. and Stott, P.A., 2014. Explaining extreme events of 2013 from a climate perspective. *Bulletin of the American Meteorological Society*, **95**(9), pp.S1-S104.

Trenberth, K.E., 2011. Changes in precipitation with climate change. *Climate Research*, **47**(1), pp.123-138.

van Vuuren, D.P., Edmonds, J., Kainuma, M., Riahi, K., Thomson, A., Hibbard, K., Hurtt, G.C., Kram, T., Krey, V., Lamarque, J.F. and Masui, T., 2011. The representative concentration pathways: an overview. *Climatic change*, **109**, pp.5-31.

Weber, E.U., 2010. What shapes perceptions of climate change? *Wiley Interdisciplinary Reviews: Climate Change*, **1**(3), pp.332–342.

Chapter 2. A comparative analysis of malaria risk in Japan and the Republic of Korea: current trends and future risk in the context of climate change

2.1. Context setting

In the context of climate change health impacts research, infectious diseases such as malaria and dengue fever pose a complex issue. Malaria and dengue are pressing health issues in many developing countries, where sanitary and health system conditions are lower (McMichael et al. 2006). However, they have largely been eradicated in developed countries (WHO, 2014). Studies have indicated that in some developing countries the area where malaria is endemic has expanded, due to climate change (Siraj et al. 2014). Research has also shown that the area of vector habitation has increased in developed countries, including Japan (Kobayashi et al. 2008). In these countries, the season of vector activity is also expanding. Thus, there is an increased risk of an imported case from an endemic region being transmitted within a current malaria-free area. Such cases have been identified in countries including France (Poncon et al. 2008), Greece (Danis et al. 2011) and the Republic of Korea (Feigner et al. 1998). This presents a problem in quantifying the impact that climate change may pose to infectious disease prevalence in developed countries. The risk of imported cases being transmitted is increasing, but it is difficult to quantify by exactly how much, due to the fact that these incidences are currently sporadic. Add to this the increase in the number of antimalarial drug resistant strains of malaria (Park et al. 2009), and medical professionals' unfamiliarity with the disease in countries like Japan (Kano and Kimura, 2004), and it becomes clear that some quantification of the risk is required. This chapter compares the current situation Japan and the Republic of Korea, analyses reasons for the differences, determines the main climatological parameters controlling malaria prevalence and makes predictions of the climatic suitability of further re-emergence in the region as a result of climate change. Future projections of risk are made using a climatically sensitive base-reproduction rate model for malaria.

2.2. Introduction

Malaria is the most prevalent parasitic vector borne disease in the world, with an estimated 207 million reported cases per year (WHO, 2014). Despite increased global spending, there has not been a significant decrease in cases annually. In addition to this, the influence of the climate on a number of the parameters controlling transmission means that there is potential for malaria to spread to previously malaria free regions (Lieshout et al., 2004). For this reason, it is important to investigate malaria trends in areas on the periphery of the current endemic region and determine the risk of re-emergence in these areas. Indigenous malaria was eradicated from Japan in 1961 and from South Korea in 1979. However,

malaria (Plasmodium vivax strain) re-emerged in South Korea in 1993 (Feigner et al. 1998). The incidence of malaria outbreaks in South Korea has fluctuated since re-emergence, suggesting that re-emergence in similar geographic areas is possible (Feigner et al. 1998; Han et al. 2006). Research comparing reasons for differences in prevalence between countries is important for understanding the variables that control malaria prevalence, and has not been undertaken between South Korea and Japan.

Several studies that propose that there is a strong link between the climate and the distribution of malaria (Lieshout et al. 2004; Jones and Morse, 2010; Parham and Michael, 2010). This is particularly true in terms of temperature, monthly rainfall and humidity (Kleinschmidt et al. 2000). Changes to the climate are most likely to have an impact on the spatio-temporal distribution of malaria in areas at the fringes of current endemic regions (Lindsay and Birley, 1996; Martens et al. 1999). These are areas where climatic conditions are seasonally suitable for malaria outbreaks (Guerra et al. 2006), where malaria transmission vectors are present. With an anticipated increase of global temperatures of between 1.1-2.9ºC and 2.4-6.4ºC by 2100 (Representative Concentration Pathway (RCP) climate scenarios), the area of the world at risk from re-emerging malaria is expected to increase. Therefore, it is important to understand the relationship between malaria and the climate to identify areas at the pole-ward and altitudinal limit of malaria distribution which could be at risk to future epidemics.

Malaria can be controlled by anthropogenic factors, including medical treatments, vaccinations and control of potential vector populations (Han et al. 2006; Emert et al. 2011). These all have financial costs. Therefore, being able to identify areas at different risk levels is vital in ensuring that financial resources are allocated to malaria control efficiently (Guerra et al. 2006). This is particularly relevant to South Korea and Japan, where increased international travel and the presence of malaria vectors (Anopheles sinensis mosquito) makes re-emergence through imported malaria a potential threat (Kano and Kimura, 2004).

The aim of this research is to compare the malaria situation in Japan and South Korea, and to analyse the risk of re-emergence occurring in Japan under climate change. The potential risk of malaria re-emergence in an area can be estimated by calculating the base-reproduction rate model (Lindsay et al. 2010). This model simulates the effect of temperature on the transmission rate of malaria (Lindsay and Birley, 1996). Therefore, it is an indicator of which areas could support transmission of malaria if subjected to an imported case, assuming the vector is present. A number of the parameters (human biting rate, gonotropic cycle and sporogonic cycle) are temperature dependent. Thus, climate can be used as a predictor of risk.

2.3. Methods

A research framework was developed to compare and explain the differences between malaria transmission trends in Japan and South Korea and to project the future risk of outbreaks occurring in

these areas as a result of climate change. An initial comparative analysis was conducted, including a quantitative analysis of the relationship between temperature and malaria transmission. Based upon this analysis, it was deemed appropriate to produce risk projections by combining a malaria transmission model with climate model outputs to identify changes in future risk from climate change. Finally, to identify the key uncertainties and focus future model improvement research, a full literature review of the sensitivity of the malaria transmission model components was conducted.

2.3.1. Direct comparison

Observational data of reported malaria cases were collated from the Korean Center for Disease Control (KCDC, 2014) and the Japanese Infectious Disease Surveillance Center (IDSC, 2014). A comparison of annual trends in Japan and South Korea was made to determine the differences in occurrence of malaria in both countries. In order to attempt to explain the differences, statistical analysis and a literature review were conducted.

2.3.2. Quantitative assessment of cases and climatic factors

The initial comparison revealed the need for a more detailed analysis of annual and monthly trends of reported malaria cases in South Korea to be conducted. Particular focus was placed on the trend of malaria cases in relation to known factors in malaria transmission: near surface air temperature; precipitation; and relative humidity. Monthly values for minimum temperature, maximum temperature, precipitation and relative humidity (KMA, 2011) were obtained for each region for the period corresponding with the available malaria records (2001-2010). The relationship between each of these values and the number of malaria cases was then statistically analysed using regression analysis at a monthly and early level to assess the correlation between each variable and the number of malaria cases.

2.3.3. Base reproduction rate model risk projections

The statistical analysis revealed that it was appropriate to use a process-based malaria transmission model to project future risk of re-emergence in the region based upon monthly temperature projections. The principal theory behind the process-based method is the concept of the basic reproduction rate of malaria (R_0) (Lindsay and Thomas, 2001; Anderson and May, 1991) R_0 is calculated using an equation to represent the temperature dependent cycles in the process of malaria transmission. The value of R_0 represents the average number of infections that are produced from the introduction of a single infected individual into a potential host population (van Lieshout et al, 2004). Any R_0 value that is greater than 1 means that malaria can proliferate indefinitely. If the value of R_0 is less than 1 then the disease will die out without further external introductions (Parham and Michael, 2010).

The formula used to calculate the basic reproduction rate (R_0) is explained below (derived from Lindsay and Birley, 1996; Lindsay et al. 2010; Lindsay and Thomas, 2001):

$$R_0 = \frac{ma^2bp^n}{-ln(p)\,r} \tag{1}$$

Where m is the number of vectors per person and a represents the number of mosquito bites per person per day (Lindsay and Birley, 1996). When the population of mosquitoes is unknown then ma is assumed to be one[17]. When ma is assumed to be one, the female mosquito feeding rate (a) must be calculated. In this study, ma is assumed to be 1, due to the lack of available mosquito population data and to enable comparison with previous studies (Lindsay and Birley, 1996, Lindsay and Thomas, 2001). The feeding rate is calculated by using the following equation:

$$a = \frac{h}{u} \tag{2}$$

In this equation, h represents the proportion of female mosquito feeding incidences (blood meal) that are taken from humans. An accepted constant value for this is 0.42 (Lindsay et al. 2010). u is the length of time in days that it takes for a mosquito to complete the gonotrophic cycle (time between taking a blood meal, laying eggs and taking the next blood meal (Lindsay and Birley, 1996). The gonotrophic cycle length is calculated by using the following formula:

$$u = \frac{f_1}{T - g_1} \tag{3}$$

Here, f_1 is a thermal sum, measured in degree days, representing the accumulation of temperature units over time that is required for the gonotrophic cycle to be completed (36.5ºC (Lindsay and Thomas, 2001)). T represents the ambient temperature and g_1 is a temperature threshold below which development ceases (9.9ºC) (Lindsay et al. 2010). In the R_0 formula, b is the proportion of female mosquitoes that develop parasites after taking an infective blood meal (0.19). p is the daily survival probability for adult mosquitoes which, for this model, is calculated by a formula using the ambient temperature as a factor (Lindsay and Birley, 1996):

$$p = exp\left(\frac{-1}{-4.4 + 1.31T} - 0.03T^2\right) \tag{4}$$

In the initial equation, n represents the sporogonic cycle (the length, in days, of the period of parasite development in adult mosquitoes) and is given by:

$$n = \frac{f_2}{T - g_2} \tag{5}$$

Where f_2 is a thermal sum representing the accumulation of temperature units over time to complete the sporogonic cycle (105 degree days) (Lindsay et al. 2010), T is the ambient temperature and g_2 is a temperature threshold below which the cycle cannot be completed (14.5ºC). r is the average recovery rate of humans once they have been infected with malaria (0.0167 recovery per day).

For the risk map projections, climate model outputs (monthly average temperature) from the Korean Meteorological Agency (MM5 Regional Climate Model (RCM) (Koo et al. 2009)), for South Korea, and the CMIP5 CCSM4 model run for RCP 8.5, to show maximum potential comparative risk (for the comparative maps of Japan and Korea) were incorporated into the temperature dependent parameters in the formulae to represent the temperature components of the model. Once run, time-slices of malaria risk were generated. The measure of risk was designated as the number of months that malaria transmission could be supported ($R_0 > 1$), if a case of malaria was imported into the study area. The high resolution projections of South Korea were produced from a RCM using dynamical downscaling for South Korea (full methodology in Koo et al. 2009). The larger scale comparative projections, displaying Japan and South Korea on the same map were run from a global Climate Model (GCM): CMIP5 CCSM4. This separate, comparative projection, was produced in a larger scale to ensure that the results for both countries could be directly compared on a projection using the same climate projection methodology for both areas at the same scale.

2.4. Results

2.4.1. Direct comparison

Annual reported cases of malaria in Japan and South Korea differ greatly, with Japan averaging 99 cases per year and South Korea averaging 1,575 cases per year (Figure 2.4.1). In addition to this, the annual variation between cases in South Korea is much greater than in Japan (Standard deviation: 1239.5 and 23.4 respectively). Further analysis was undertaken to understand the nature of malaria cases in both countries. This revealed that 100% of the cases of malaria reported in Japan since 1990 were imported cases. When compared to imported cases in South Korea, it becomes clear that a vast majority of cases reported in South Korea are indigenous cases (Figure 2.4.2). Only 2.9% of cases reported in South Korea in 2010 were recorded as imported cases. Previous studies (Yeom et al, 2012; Jun et al. 2009) propose that the initial re-emergence of malaria in South Korea was caused by transmission from the Democratic Peoples' Republic of Korea (North Korea). The cause of the outbreak in North Korea, which triggered the re-emergence in South Korea cannot be quantitatively attributed to a single cause due to the lack of data, though it has been proposed that it was a combination of a collapse of the medical care system, poor sanitation and a number of floods 1993-1996 (Feigner et al. 1998). These events produced more breeding sites for mosquito vectors in the vicinity of the border, which enabled the transfer of infected vectors into South Korea (Feigner et al. 1998). In order to understand the difference

in malaria transmission patterns between Japan and South Korea, comparisons of other known malaria transmission parameters were made between both countries. This revealed that the land-use in both countries is distributed similarly, with the only significant difference being the percentage of the population living in urban areas - a poor land-use classification for malaria transmission. (92% in Japan, compared to 83% in South Korea (CIA World Factbook, 2014)).

Figure 2.4.1: Annual reported cases of malaria in Japan (solid line) South Korea (dashed line) and North Korea (dotted line, right axis) 1990-2010 (KCDC, 2014; IDSC, 2014; Pant et al, 2014).

Figure 2.4.2: Imported cases of malaria in Japan (solid line) and South Korea (dashed line) 1990-2010 (KCDC, 2014; IDSC, 2014).

2.4.2. Quantitative assessment of cases and climatic factors

A strong seasonal trend in the number of reported cases of malaria was found in all provinces. July and August were found to be the most prevalent months for malaria, with an average of 390.8 and 404.5 cases respectively (Figure 2.4.3). Multiple regression analysis was undertaken to determine the relationships between monthly reported malaria cases and the corresponding monthly average values of four climatic variables: Minimum and maximum temperature; precipitation; relative humidity. The variables statistically significantly predicted 11.1% (R^2) of the variation in malaria cases. The low R^2 values can be explained by the vast regional differences in the number of cases recorded each month. Multiple regression analysis was re-run with the regions selected as nominal value variables. The statistically significant regression (R^2 = 13.1%) identified the region variable as the most significantly significant predictor of cases (β = -0.159). To investigate the climatic impact at a regional level, multiple regression analysis was performed for each region. This identified a stronger relationship between the four climate variables and malaria prevalence (Table 2.4.1). A strong relationship was found between average monthly minimum and maximum temperature and malaria prevalence, particularly in Gyeonggi province (R^2 68.7% and 61.2% respectively; Figure 2.4.4). Other provinces showed similar trends, though with lower R^2 values. Regression analysis of precipitation and relative humidity and malaria prevalence showed that a significant relationship existed, although it was weaker than the relationship with temperature variables. This provided the foundation for producing a prediction model based upon temperature.

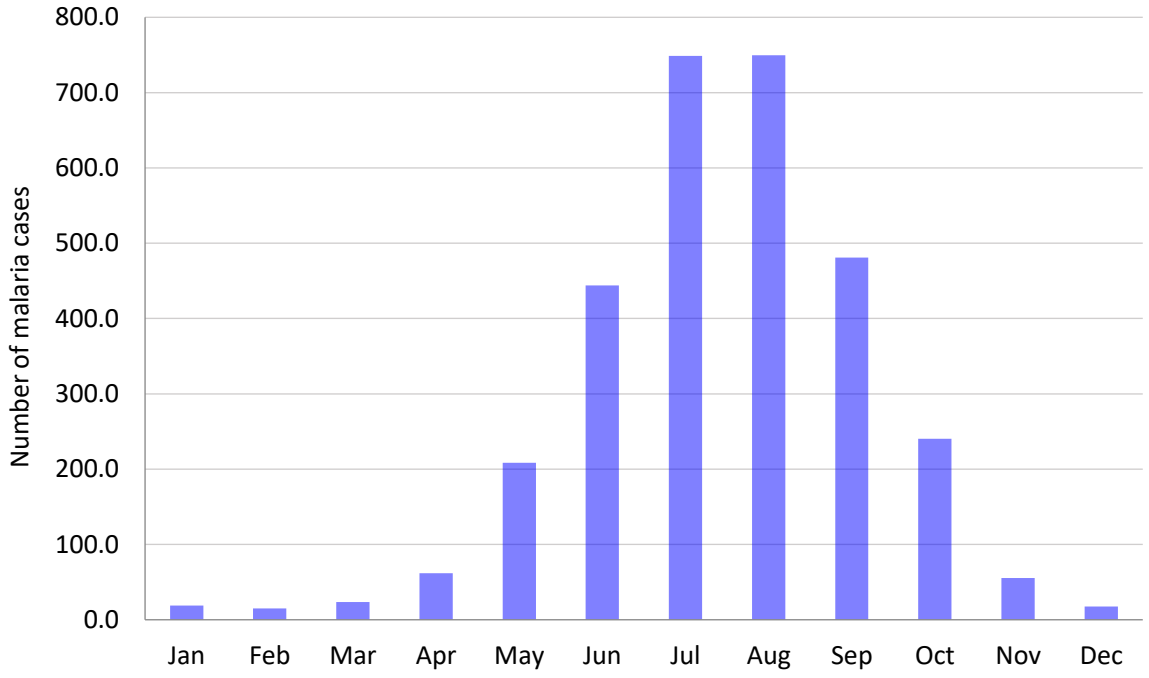

Figure 2.4.3: Average reported cases per month in South Korea 1993-2010 (KCDC, 2014).

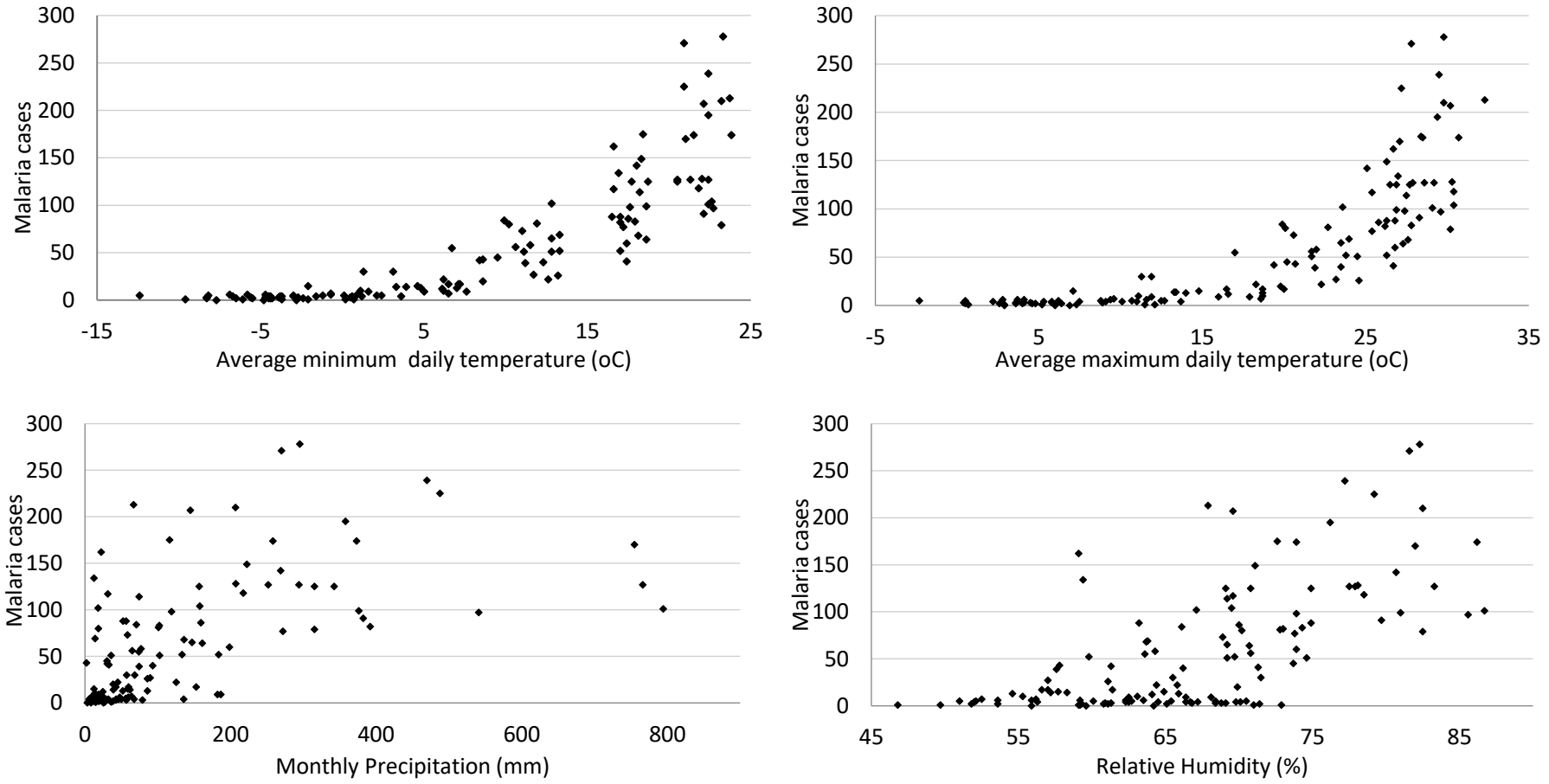

Figure 2.4.4: Relationship between monthly cases of malaria and average minimum (a) and maximum temperatures (b), precipitation (c) and relative humidity (d) respectively for Gyeonggi Provence.

Table 2.4.1: Multiple regression analysis of climatic variables and regional malaria prevalence (2001-2010).

Region	R^2 %	Total malaria cases
Gyeonggi	76.2	7423
Incheon	56.4	2693
Seoul	66.5	2444
Gangwon	36.9	1827
Busan	51.6	420
South Gyeongsang	41.7	304
North Gyeongsang	17.6	285
North Jeolla	53.3	240
Daegu	57.3	232
South ChungChong	51.7	221
South Jeolla	51.1	210
North Chungcheong	47.7	196
Daejon	47.2	175
Ulsan	39.7	163
Gwangju	35.5	145

2.4.3. Base reproduction rate model risk projections

The projections show the number of months per year that malaria transmission can be sustained based upon monthly average temperature. The projections were initially computed for South Korea for the time slice 2001-2010 by combining the base-reproduction rate model with a Regional Climate Model output, MM5 (Koo et al. 2009). When 2001-2010 projections are compared with observations of malaria cases it can be seen that temperature is not currently the limiting factor for malaria prevalence in South Korea. The projection indicates that there is more malaria transmission potential in the South and West, whereas observations show that most cases occur in the North and North-west. However, when analysing the most prevalent areas (37-38^{o} North), the trend is represented well in the projections (Figure 2.4.5).

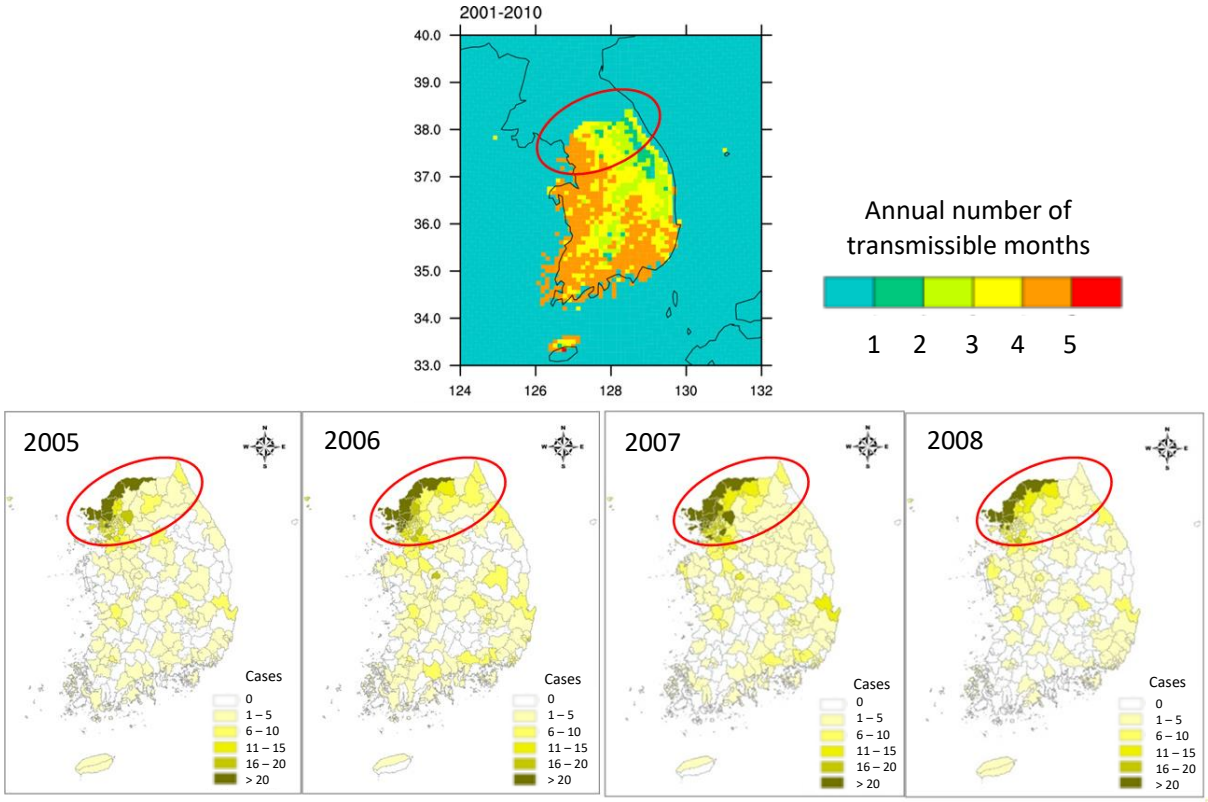

Figure 2.4.5: Projected 2001-2010 malaria transmission climate suitability and 2005-2008 observed prevalence (KCDC, 2014).

The number of months that the R0 value is greater than 1 was computed as an average for ten-year time slices 2001-2010 to 2091-2100 (Figure 2.4.6). The projections indicate that South Korea will become more suitable for supporting malaria transmission in the future. Areas that are most suitable for transmission appear to be located more towards the South and West of the country and in low-lying regions. To further compare the risk of an outbreak of malaria arising from an imported case, projections of Japan and South Korea as a whole were made at a larger scale from the CMIP5 CCSM4 model. The resulting projections show similar trends of a lengthening transmission season based on the climate in both countries, with a greater extension of the season being projected in Southern and Western Japan (Figure 2.4.7).

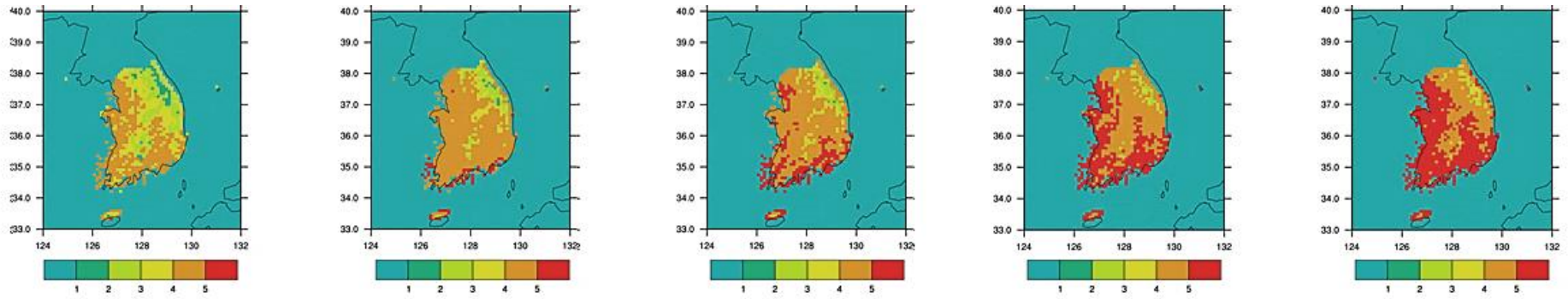

Figure 2.4.6: Projections of the estimated number of months that malaria transmission can be supported in South Korea based upon monthly average temperature generated from an MM5 downscaled climate model for 2001-2010, 2021-2030, 2041-2050, 2061-2070 and 2091-2100 respectively.

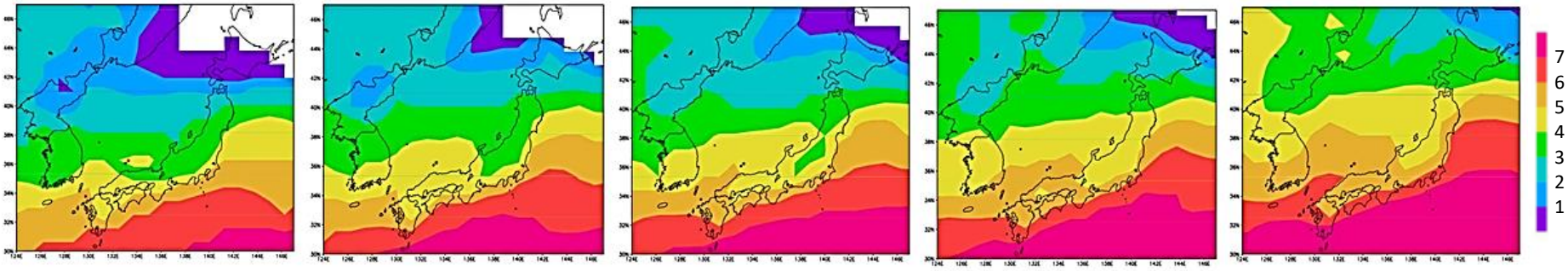

Figure 2.4.7: Projections of the estimated number of months that malaria transmission can be supported in Japan and South Korea based upon monthly average temperature generated from the CCSM4 climate model for 2001-2010, 2021-2030, 2041-2050, 2061-2070 and 2091-2100 respectively.

2.5. Discussion

2.5.1. Direct comparison

South Korea has substantially more cases of malaria reported each year. Almost all of these are indigenous cases of malaria (Park, 2011). Due to the similar environmental, climatic and demographic conditions between Japan and South Korea, South Korea's proximity to North Korea can be identified as the main cause of the variation between Japan and South Korea (Yeom et al. 2012; Park et al. 2009). Due to the similar climatic and environmental conditions in Japan and South Korea, Japan is potentially vulnerable to an outbreak of malaria from imported cases (Kano and Kimura, 2004). The distribution of mosquito vectors in has not been mapped, although evidence of mosquito vectors has been discovered in both countries (Kano and Kimura, 2004; Park, 2011; Rueda et al. 2006) and is evidenced in South Korea by the fact that 97.1% of reported cases were classified as internal transmission cases.

The nature of reported cases in South Korea has changed since it re-emerged (Park, 2011), with over 60% of cases in 2010 being civilian (compared to 100% of cases initially being in the military). This indicates that conditions in South Korea are suitable for sustaining malaria transmission. The pattern of malaria transmission in South Korea is heavily influenced by the conditions in North Korea; however, there is evidence of local transmission, as the pattern of cases in 2009 was different between the two countries (Yeom et al. 2012). Therefore, the occurrence of malaria in South Korea is influenced by both local transmission and the malaria situation in North Korea (Yeom et al. 2012). Two studies (Park, 2011; Yeom et al. 2012) reported that the transmission season in South Korea extended annually 1993-2010, meaning that the length of time that malaria transmission can be supported is extending as a result of climate change. Japan is also experiencing climate change, suggesting that it could become more at risk from malaria outbreaks in the future, as the mosquito vector species is widespread and abundant in both Japan and Korea (Rueda et al. 2006). However, vector population density needs to be fully analysed in order to comprehensively determine the risk of malaria re-emergence in Japan and transmission in South Korea. An assessment of climatic suitability can be used as the first stage of analysis, to target areas for more detailed analysis of vector density, environmental conditions and medical care status.

2.5.2. Quantitative assessment of climatic factors

A statistically significant relationship between monthly minimum and maximum temperatures and the number of malaria cases exists at a regional level in South Korea. This is supported in the literature through statistical studies (Kleinschmidt et al. 2000) and biological studies (Rúa et al. 2005; Bayoh and Lindsay, 2004). The sensitivity of both the mosquito vector and the malaria parasite to temperature is strong, meaning that small temperature increases can extend the transmission season of the parasite (van Lieshout et al. 2004; Zhou et al, 2004). The climate of South Korea currently does not support

year-round transmission of malaria, meaning that it is climatically vulnerable to an extended transmission season (Park et al. 2009). A significant relationship between temperature and the number of malaria cases found in this study also suggests that the distribution of malaria could spread to areas where it is currently limited by temperature (Kovats et al, 2001). There appears to be a significant trend between both relative humidity and malaria prevalence at a seasonal level (Table 2.4.2). This trend can be explained by the link between increased humidity and precipitation and the amount of standing water on the ground surface (Lindsay and Birley, 2008). The relationship between precipitation and malaria prevalence is less clear due to the uncertainty of the impact of heavy rain on transmission rates (Singh and Sharma, 2002). The transmission rate of malaria is dependent on a wide variety of factors, including the level of medical controls, vector density, and the environmental characteristics. Annual trends indicate that temperature is not the main factor in determining the prevalence of malaria in the studied region (Figure 2.4.1.1). However, the analysis of climatic factors and malaria in South Korea displayed that prevalence is linked to climate, particularly temperature at a monthly level. Therefore, it is possible to use the temperature dependent base reproduction rate model as an indicator of the climatic suitability of a region to malaria transmission, if separated from the other variables.

2.5.3. Base reproduction rate prediction model

The model identifies areas that are climatically vulnerable to malaria outbreaks if other conditions are met. Potential risk areas are identified easily, enabling a preliminary assessment of malaria transmission potential. The main practical use of the model is as the initial component of a vulnerability assessment of an area to a vector borne disease (van Lieshout et al. 2004). In this study, an assumption was made to calculate *ma,* due to the lack of available data on the population distribution of the *Anopheles* mosquito. The resulting map projections should be taken as a guide depicting relative climatic suitability (Figure 2.4.3.1). With this caveat taken into account, the model projections provide a useful overview and highlight the relative suitability of each location for malaria transmission based on temperature projections.

In order to address model uncertainty, a review of the biological components of the model was conducted (Rúa et al. 2005; Lindsay et al. 2004; Chitnis et al. 2008; Poncon et al. 2008). The human biting rate is the most sensitive parameter. This indicates that the suitability of the model is highly dependent on this calculation. Future improvements to this model would be to include human and mosquito population density data in order to more accurately depict *ma*. This would greatly improve the ability of the model to predict malaria risk. This data would also enable projections of actual prevalence to be made, rather than transmission potential. Identifying the human biting rate as the most sensitive parameter also identifies this as a key parameter to target for potential countermeasures, such as those that limit human-mosquito contacts (Chitnis et al. 2008, Sharma et al. 2005).

Despite temperature not being identified as the principle controlling variable, it is important to analyse trends in potential transmissivity due to the risk of imported cases of malaria transmitting locally (Danis et al. 2011). There is evidence of independent transmission within South Korea and other temperate, developed countries, including Greece (Danis et al. 2011), France and Germany (Zoller et al. 2009). These factors highlight the importance of modelling malaria risk and the base reproduction rate model provides an important first step towards comprehensive risk assessments of malaria. Future studies should focus on improving the validity of *ma*, as this is the most influential variable and is highly dependent on data limitations. Vector and human population distribution data is required to improve the applicability of the model to real world scenarios that rely on robust models. Once this function is developed, the model can be more comprehensively validated.

2.6. Conclusion

This research compared malaria transmission in South Korea and Japan and analysed reasons for the differences. The results showed that South Korea experiences significantly more annual cases of malaria than Japan. Temperature was not identified as the main variable affecting annual trends in malaria prevalence, indicating that other factors have a greater impact. The proximity of South Korea to North Korea was identified as a cause of the initial re-emergence of malaria in 1993 (Yeom et al. 2012). The differences between the other known variables of malaria transmission were small. Temperature was not shown to be a major factor in annual trends of malaria; however, multiple regression analysis indicated that climatic factors have a significant influence on the monthly trends in South Korea (R^2 = 11.1%) and the individual regions (R^2 = 17.3-76.4%). The differences in prevalence between regions indicates that although the climate has an impact, it is not the limiting factor. The base reproduction rate model projected that the length of the potential transmission season would increase by up to two months annually by 2100. Sensitivity studies have identified the limitations of the prediction model used in this study, particularly regarding the assumptions made in calculating ma. Future studies should focus on improving the robustness of this parameter and conducting site specific model sensitivity analyses. The model provides an important insight into impact of climate on malaria transmission. This is the first step towards assessing malaria risk, which can be followed up by collecting vector mosquito population and habitat data to investigate other controls on transmission.

References

Anderson, R.M., May, R.M. and Anderson, B., 1992. *Infectious diseases of humans: dynamics and control* (Vol. 28). Oxford: Oxford university press.

Bayoh, M.N. and Lindsay, S.W., 2004. Temperature‐related duration of aquatic stages of the Afrotropical malaria vector mosquito Anopheles gambiae in the laboratory. *Medical and veterinary entomology*, **18**(2), pp.174-179.

Chitnis, N., Hyman, J.M. and Cushing, J.M., 2008. Determining important parameters in the spread of malaria through the sensitivity analysis of a mathematical model. *Bulletin of mathematical biology*, **70**(5), pp.1272-1296.

CIA World Factbook, 2014. Available at: https://www.cia.gov/library/publications/the-world-factbook/rankorder/rankorderguide.html.

Danis, K., Baka, A., Lenglet, A., Van Bortel, W., Terzaki, I., Tseroni, M., Detsis, M., Papanikolaou, E., Balaska, A., Gewehr, S. and Dougas, G., 2011. Autochthonous Plasmodium vivax malaria in Greece, 2011. *Euro Surveill*, **16**(42), pp.1-5.

Ermert, V. Fink, A. H., Jones, A. E. and Morse, A. P., 2011. Development of a new version of the Liverpool Malaria Model II. Calibration and validation for West Africa. *Malaria Journal*, **10**(1), 62.

Feighner, B. H. Pak, S. I., Novakoski, W. L., Kelsey, L. L. and Strickman, D., 1998. Reemergence of Plasmodium vivax malaria in the Republic of Korea. *Emerging Infectious Diseases*, **4**(2), p.295.

Guerra, C. A., Snow, R. W. and Hay, S. I., 2006. Defining the global spatial limits of malaria transmission in 2005. *Advances in Parasitology*, **62**, pp.157-179.

Han, E.T., Lee, D.H., Park, K.D., Seok, W.S., Kim, Y.S., Tsuboi, T., Shin, E.H. and Chai, J.Y., 2006. Reemerging vivax malaria: changing patterns of annual incidence and control programs in the Republic of Korea. *The Korean journal of parasitology*, **44**(4), pp.285-294.

IDSC, 2014. Malaria patient data. Available from: http://idsc.nih.go.jp/.

Jones, A. E. and Morse, A.P., 2010. Application and Validation of a Seasonal Ensemble Prediction System Using a Dynamic Malaria Model. *Journal of Climate*, **23**(15), pp.4202-4215.

Jun, G. Yeom, J. S., Hong, J. Y., Shin, E. H., Chang, K. S., Yu, J. R., Oh, S., Chung, H. and Park, J.W., 2009. Resurgence of Plasmodium vivax Malaria in the Republic of Korea during 2006 – 2007. *American Journal of Tropical Medicine and Hygiene*, **81**(4), pp.605-610.

Kano, S. and Kimura, M., 2004. Trends in malaria cases in Japan. *Acta tropica*, **89**(3), pp.271-278.

KCDC, 2014. Malaria patient data. Available from: http://stat.cdc.go.kr/.

Kleinschmidt, I., Bagayoko, M., Clarke, G.P.Y., Craig, M. and Le Sueur, D., 2000. A spatial statistical approach to malaria mapping. *International Journal of Epidemiology*, **29**(2), pp.355-361.

KMA, 2011. Korean Meteorological Society observation data. Available from: http://www.kma.go.kr/weather/climate/past_table.jsp.

Kobayashi, M., Komagata, O. and Nihei, N., 2008. Global warming and vector-borne infectious diseases, *Journal of Disaster Research*, **3**, pp.105–112.

Koo, G. S., Boo, K. O. and Kwon, W. T. 2009 Projection of temperature over Korea using an MM5 regional climate simulation. *Climate Research*, **40**(2-3), pp.241-248.

Kovats, R.S., Campbell-Lendrum, D.H., McMichel, A.J., Woodward, A. and Cox, J.S.H., 2001. Early effects of climate change: do they include changes in vector-borne disease?. *Philosophical Transactions of the Royal Society of London B: Biological Sciences*, **356**(1411), pp.1057-1068.

Lindsay, S.W. and Birley, M.H., 1996. Climate change and malaria transmission. *Annals of tropical medicine and parasitology*, **90**(6), pp.573-588.

Lindsay, S.W., Hole, D.G., Hutchinson, R.A., Richards, S.A. and Willis, S.G., 2010. Assessing the future threat from vivax malaria in the United Kingdom using two markedly different modelling approaches. *Malaria journal*, **9**(1), p.1.

Lindsay, S., Kirby, M., Baris, E. and Bos, R., 2004. Environmental management for Malaria control in the East Asia and Pacific (EAP) Region. *Health, Nutrition and Population (HNP) Discussion Paper. The World Bank.*

Lindsay, S.W. and Thomas, C.J., 2001. Global warming and risk of vivax malaria in Great Britain. *Global change and human health*, **2**(1), pp.80-84.

Martens, P., Kovats, R.S., Nijhof, S., De Vries, P., Livermore, M.T.J., Bradley, D.J., Cox, J. and McMichael, A.J., 1999. Climate change and future populations at risk of malaria. *Global Environmental Change*, **9**, pp.S89-S107.

McMichael, A. J., Woodruff, R. E. and Hales, S., 2006. Climate change and human health: present and future risks, *The Lancet*, **367**(9513), pp.859-869.

Pant, S. D., Chol, K. Y., Tegegn, Y., Mandal, P. P. and Chol, R. K., 2014. Mass primaquine preventive treatment for control of Plasmodium vivax malaria in the Democratic People's Republic of Korea: a country success story. *WHO South-East Asia J Public Health*, **3**(1), pp.75–80.

Parham, P. E. and Michael, E., 2010. Modeling the Effects of Weather and Climate Change on Malaria Transmission. *Environmental Health Perspectives*, **118**(5), 620-626.

Park, J. W., 2011. Changing Transmission Pattern of Plasmodium vivax Malaria in the Republic of Korea: Relationship with Climate Change. *Environmental health and toxicology*, **26**, p.e2011001.

Park, J. W., Jun, G. and Yeom, J. S., 2009. Plasmodium vivax malaria: status in the Republic of Korea following reemergence. The Korean journal of parasitology, 47(Supplement), pp.S39-S50.

Ponçon, N., Tran, A., Toty, C., Luty, A.J. and Fontenille, D., 2008. A quantitative risk assessment approach for mosquito-borne diseases: malaria re-emergence in southern France. *Malaria journal*, **7**(1), p.1.

Rúa, G.L., Quiñones, M.L., Vélez, I.D., Zuluaga, J.S., Rojas, W., Poveda, G. and Ruiz, D., 2005. Laboratory estimation of the effects of increasing temperatures on the duration of gonotrophic cycle of Anopheles albimanus (Diptera: Culicidae). *Memorias Do Instituto Oswaldo Cruz*, **100**(5), pp.515-520.

Rueda, L.M., Kim, H.C., Klein, T.A., Pecor, J.E., Li, C., Sithiprasasna, R., Debboun, M. and Wilkerson, R.C., 2006. Distribution and larval habitat characteristics of Anopheles Hyrcanus Group and related mosquito species (Diptera: Culicidae) in South Korea. *Journal of Vector Ecology*, **31**(1), pp.198-205.

Sharma, S.K., Upadhyay, A.K., Haque, M.A., Padhan, K., Tyagi, P.K., Batra, C.P., Adak, T., Dash, A.P. and Subbarao, S.K., 2005. Village‐scale evaluation of mosquito nets treated with a tablet formulation of deltamethrin against malaria vectors. *Medical and veterinary entomology*, **19**(3), pp.286-292.

Singh, N. and Sharma, V.P., 2013. Patterns of rainfall and malaria in Madhya Pradesh, central India. *Annals of tropical medicine and parasitology*, **96**(4), pp.349-359.

Siraj, A.S., Santos-Vega, M., Bouma, M.J., Yadeta, D., Carrascal, D.R. and Pascual, M., 2014. Altitudinal changes in malaria incidence in highlands of Ethiopia and Colombia. *Science*, **343**(6175), pp.1154-1158.

van Lieshout, M., Kovats, R.S., Livermore, M.T.J. and Martens, P., 2004. Climate change and malaria: analysis of the SRES climate and socio-economic scenarios. *Global Environmental Change*, **14**(1), pp.87-99.

WHO, 2014. World Malaria Report 2014, *World Health Organization*. Available from: http://www.who.int/malaria/publications/world_malaria_report_2014/en/.

Yeom, J.S., Jun, G., Kim, J.Y., Lee, W.J., Shin, E.H., Chang, K.S., Bang, J.H., Oh, S., Kang, J.Y. and Park, J.W., 2012. Status of Plasmodium vivax malaria in the Republic of Korea, 2008–2009: decrease followed by resurgence. *Transactions of the Royal Society of Tropical Medicine and Hygiene*, **106**(7), pp.429-436.

Zhou, G., Minakawa, N., Githeko, A.K. and Yan, G., 2004. Association between climate variability and malaria epidemics in the East African highlands. *Proceedings of the National Academy of Sciences of the United States of America*, **101**(8), pp.2375-2380.

Zoller, T., Naucke, T.J., May, J., Hoffmeister, B., Flick, H., Williams, C.J., Frank, C., Bergmann, F., Suttorp, N. and Mockenhaupt, F.P., 2009. Malaria transmission in non-endemic areas: case report, review of the literature and implications for public health management. *Malaria journal*, **8**(1), p.1.

Chapter 3. Heat wave vulnerability and exposure mapping for Osaka City, Japan

3.1. Context setting

Chapter 2 investigated a method of quantifying the risk to human health posed by malaria, a climate influenced infectious disease. The problems of quantifying this indirect risk factor were addressed and solutions suggested. Heat waves pose a different health impact. They are direct consequences of atmospheric circulation, which is controlled by the climate. This risk factor is a mesoscale event that, when it occurs, causes excess mortality and morbidity in exposed areas (Bai et al. 1995). Thus, the impact pathway and health outcomes are different. The major health impact is early death or morbidity due to the stress of heat on the body (Wolf and McGregor, 2013). More so than infectious disease in developed countries, heat wave risk to an individual or area is highly dependent on underlying vulnerability. Vulnerability to heat waves is itself dependent on sociodemographic characteristics (age, gender and wealth), physiological characteristics (susceptibility to illness, underlying health conditions), access to support and information, and mobility (Wolf and McGregor, 2013). For this reason, we can use demographic data to determine the vulnerability of a particular region and quantify this. This chapter combines an empirical vulnerability assessment with exposure data to produce a comprehensive assessment of the impact of a heat wave on a particular area: Osaka City, Japan. The study region is selected as a densely populated city, in a country where a study of vulnerability to heat waves using a heat wave index has not previously been conducted. Again, the purpose of such a quantification is to provide information to policy makers and risk management organisations as to what type of countermeasures to employ and to which areas.

This study investigates heat wave exposure and vulnerability in an urban area. The scope is not specifically related to investigating the impact of climate change on heat waves, rather the spatial distribution of vulnerability and exposure to heat wave events. The exposure analysis seeks to develop a temperature profile of Osaka City to identify areas that are most impacted by heat, exacerbated by the Urban Heat Island (UHI) effect. Past research has identified that the UHI effect exacerbates warming due to climate change (Fujibe, 2011). Fujibe (2011) identified that in addition to warming from climate change, meteorological monitoring stations in urban areas experienced further warming of 0.03-0.05 °C/decade. Therefore, urban areas are more exposed to climate change induced warming and contain much larger populations than urban areas. For this reason, it is important to understand the spatial distribution of both exposure and social vulnerability within a large urban area. Developing a method to concurrently analyse the distribution of fine scale exposure and vulnerability is an important

step towards the identification of areas within a city that are suitable for urban planning and social vulnerability reduction adaptation strategies. Areas with the highest exposure to UHI effect are likely to be more affected by climate change induced warming, meaning that they should be prioritised for adaptation planning.

3.2. Introduction

Globally, exposure to extreme heat is a major source of mortality and morbidity (Chestnut et al. 1998). The Intergovernmental Panel on Climate Change (IPCC) has reported an increase in the number of heat waves since the end of the twentieth century and projects that this trend will increase throughout the twenty-first century (IPCC 2014). In Japan, studies have shown that excess deaths during heat wave events can amount to 1.5 times the average mortality rate in urban areas such as Tokyo and Osaka (Bai et al. 1995). Given that Japan has several large metropolitan areas and an ageing population, it is imperative that research into heat wave vulnerability and preparedness be conducted. Furthermore, observations indicate that heat wave events in the Osaka region have become increasingly frequent since 1980 (Figure 3.2.1).

Heat-related excess mortality is primarily caused by cardiovascular and respiratory disorders and heat stroke (Reid et al. 2009). This is of particular concern in large urban areas, where there are large population concentrations and where the urban heat island (UHI) effect exacerbates temperatures (Wolf and McGregor 2013). Epidemiological studies have identified a link between certain demographic characteristics and vulnerability to extreme heat events in the USA (Cutter et al. 2003; Reid et al. 2009), Europe (Huisman et al. 2004) and South Korea (Kim and Joh 2006). Continuities in the findings of these studies enable us to identify key proxy variables that are consistently found to increase sensitivity and, therefore, vulnerability to heat waves. Among the most important characteristics influencing spatial variability are population density (Vescovi et al. 2005), social isolation (Fouillet et al. 2006), age (Hajat et al. 2010), economic status (Kim and Joh 2006) and having an underlying health condition (Reid et al. 2009). Studies have shown that these characteristics are often intrinsically linked and spatially clustered (Vescovi et al. 2005), which means that they can be used to map vulnerability within urban environments. This is an important action to take, because, due to the heterogenic distribution of health risks from heat, identifying the locations of the most vulnerable populations enables city administrations to effectively target appropriate countermeasures to the areas that are most in need.

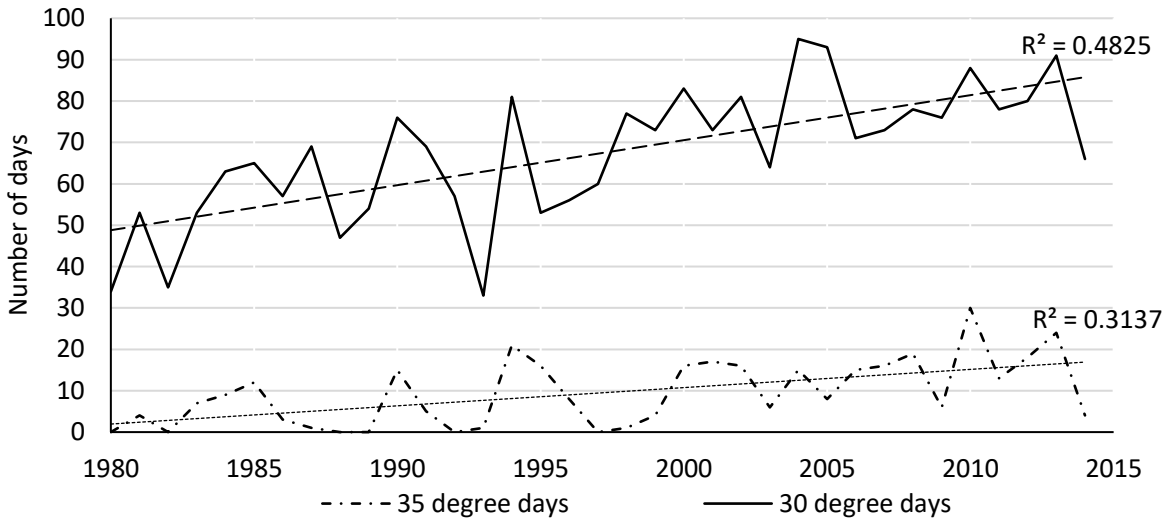

Figure 3.2.1: Annual number of > 30 and > 35°C days and linear regression for Osaka City [Itami Airport Meteorological Station (JMA 2015)].

The existing literature on this topic is focussed on population vulnerability in terms of underlying sensitivity to extreme heat exposure. This is useful, but the exposure of particular areas to heat extremes must also be taken into consideration when developing effective countermeasures. This study maps population vulnerability based on intra-city-scale proxy measures and overlays climate information in order to give a comprehensive indication of the areas of Osaka City that are vulnerable in both sensitivity and exposure. This combined approach has had little coverage in the literature, but provides additional observed exposure information to enhance plot social vulnerability to heat waves more comprehensively.

Two major approaches to adapting to heat wave impacts and the UHI effect exist: increasing preparedness and resilience (Reid et al. 2009) and reducing exposure to extreme temperatures through urban environmental engineering (Han and Huh 2008; Song et al. 2015). The first approach includes public health measures such as preparing emergency action plans, providing education for how the population can protect itself and developing policies to reduce social vulnerability (Ebi et al. 2004). The second approach is urban planning, focussed on reducing the exposure of the population to extreme temperatures and involves engineering the urban environment in order to reduce the impact of the UHI effect. This can include developing green areas within the city, using different less absorptive building materials and creating architecture that improves ground-level ventilation (Song et al. 2015). By examining heat wave sensitivity and exposure, the areas in which these different approaches to adaptation planning should be adopted can be identified clearly. Under acknowledgement of the preceding research above, the purpose of this study is to estimate the heat vulnerability of Osaka City through the practical application of a heat wave vulnerability method that utilises fine-scale temperature observations to identify the most vulnerable areas to heat waves within the city boundary.

3.3. Methods

3.3.1. Development of a heat wave vulnerability index

Epidemiological (Braga et al. 2002; Curriero et al. 2002; Mastrangelo et al. 2007) and demographic studies (Kim and Joh 2006; Vescovi et al. 2005; Wolf and McGregor 2013) have identified key indicators of population vulnerability to extreme temperatures in urban areas. This enables demographic statistics that represent vulnerability to be selected and used as indicators of the vulnerability of a particular area. In this study, we employ this inductive approach, using proxy measures of vulnerability to develop a vulnerability index for Osaka City.

The literature identifies seven main classes of vulnerability indicators (Table 3.3.1). Within these classes, intra-city data can be used as proxy values for each risk class. Census data for the number of households without working air conditioners were not available for this study. However, this is likely to be an insignificant indicator in Osaka City, as the average household in the city contains 3.6 air conditioning units (Matsumoto 2015). Furthermore, a study in Phoenix, Arizona, concluded that the presence of air conditioning units was an insignificant predictor of heat-related illness due to the high prevalence of air conditioning units in the city (Chuang and Gober 2015).

Table 3.3.1: Variables used as proxy indicators of heat wave vulnerability for Osaka City (data from E-Stat, 2015)

Class	Data indicator variables (%)	Scale
Population	Population density (pax/ha)	Chome (Sub-ward)
Age	Population over 65 years old	Chome (Sub-ward)
Economic	Population unemployed	Chome (Sub-ward)
Education	Population who didn't graduate high school	Chome (Sub-ward)
Social isolation	Single person households,	Chome (Sub-ward)
	Over 65 single households	Chome (Sub-ward)
Health	Population receiving home care	Ward
Environment	Green space / open water	Chome (Sub-ward)

Suitable proxy values were extracted from 2010 census data and the National Land Numerical Information download service (NLNI 2016) at the smallest administrative level. The resulting database was subjected to a principle component analysis (PCA). For the PCA, Chome (census) administrative areas were used as fixed parameters and the heat risk factors were considered as variables. Direct health data were not available at a Chome level, so were excluded from the finest scale PCA, as in Harlan et

al. (2013). Some of the input variables had different units of measurements, so a correlation matrix was used as the basis for the PCA, which standardised the data. As in Wolf and McGregor (2013), an orthogonal (Varimax) rotation was used to maximise the dispersion of the variables once loaded into the PCA. The PCA identified key components. The percentage of variance explained by each of these components was used as a weight. Values for each Chome were then combined, with the weights, to calculate a unit-less vulnerability index score. The distribution of the index scores per Chome was analysed and then categorised based on standard deviation from the mean score, producing an index of eight categories of heat vulnerability, from low risk (1) to high risk (8). Eight categories of vulnerability were selected to allow comparisons to studies in other locations. To statistically analyse evidence of clustering in the distribution of the vulnerability index, a Getis-Ord Hot Spot Analysis was conducted in ArcGIS 10.2.2 software.

3.3.2. Mapping heat exposure data

Daily temperature observations at 35 sites in Osaka City were recorded by the Osaka City Institute of Public Health and Environmental Sciences in July, August and September, 2007 (the months defined as summer in Osaka City). The monitoring network of weather stations was established in elementary school playgrounds around the city (Fig. 3.4.2), and temperatures were recorded hourly throughout July, August and September. The year 2007 was selected for this study because this was the year with the most complete database of temperature recordings available for Osaka City. In order to represent different levels of heat exposure, temperature classes defined by the Japan Meteorological Agency (JMA) were used. These classes are defined as 'hot days' [maximum temperature (Tmax) ≥ 30°C], 'extremely hot days' (Tmax ≥ 35°C) and 'hot nights' [minimum temperature (Tmin) ≥ 25°C] (Masumoto et al. 2006). The most appropriate measures of heat exposure were determined to be the cumulative degree hours (DHs) above the 30 and 35ºC thresholds and the number of nights exceeding the 25°C threshold. DH was chosen as a measure for daytime thresholds because this index quantifies the duration and intensity of heat. DH calculated for the entire summer period also helps to account for different micro-meteorological phenomena which may impact local exposure values. The number of nights where Tmin exceeded 25°C was used because this more fully represents night-time temperature exposure. Selecting night-time and daytime thresholds also enables diurnal spatial exposure to be analysed. The selected exposure measures at each site were plotted as point values, using GIS software, and then interpolated, using the inverse distance weighting method, to depict the spatial pattern of exposure for the whole study area.

3.3.3. Combining exposure and sensitivity mapping

In order to maximise risk management applicability of the study, vulnerability and exposure were plotted together on a map of the administrative zones of Osaka City. The vulnerability index was calculated and categorised for each administrative district in Osaka City. This output was then compiled

in GIS software to produce a map displaying the vulnerability index class of each district (1–8). This then enabled relative daytime and night-time heat exposure and the vulnerability index scores to be analysed on the same map. The resulting map can be further manipulated to display all or selected relative risk classes and different temperature thresholds to identify the most vulnerable areas in the city, providing a flexible tool for vulnerability and exposure assessments.

3.4. Results

3.4.1. Vulnerability index

The PCA determined the most influential variable combinations. Three key components, with eigenvalues > 1, were identified from the sub-ward level data. For the purposes of this study they are described as age, education and unemployment (component 1), social isolation (component 2) and density and lack of green space (component 3) (Table 3.4.1). The vulnerability index was developed from weighted sums of the components in the PCA, based upon the variance explained by each (Table 3.4.1). The variable loading numbers for each component are displayed in (Table 3.4.2).

Table 3.4.1: PCA of the proxy measures used, including eigenvalues, % of variance and loadings

Component	Eigenvalue	% of Variance	Cumulative %
1	2.122	30.309	30.309
2	1.855	26.504	56.813
3	1.137	20.326	77.139

Table 3.4.2: Loading numbers for sub-ward-level heat vulnerability variables for each principle component based on data from Chome districts

Proxy variable	Component 1 *(Age, education, unemployment)*	Component 2 *(Social isolation)*	Component 3 *(density, lack of green space)*
Age > 65	**0.871**	0.120	0.052
Did not graduate from high school	**0.909**	-0.062	-0.003
Unemployment	**0.699**	0.446	0.282
Living alone	0.010	**0.916**	0.109
Age > 65 and living alone	0.164	**0.884**	0.081
Density	0.145	0.099	**0.805**
Percentage built up	-0.009	0.083	**0.821**

The resulting vulnerability index scores ranged from 0 to 106.13, with a mean of 53.40, a median of 55.64 and a standard deviation of 13.92 (Figure 3.4.1). The data for the 1904 districts were normally distributed ($p > 0.05$).

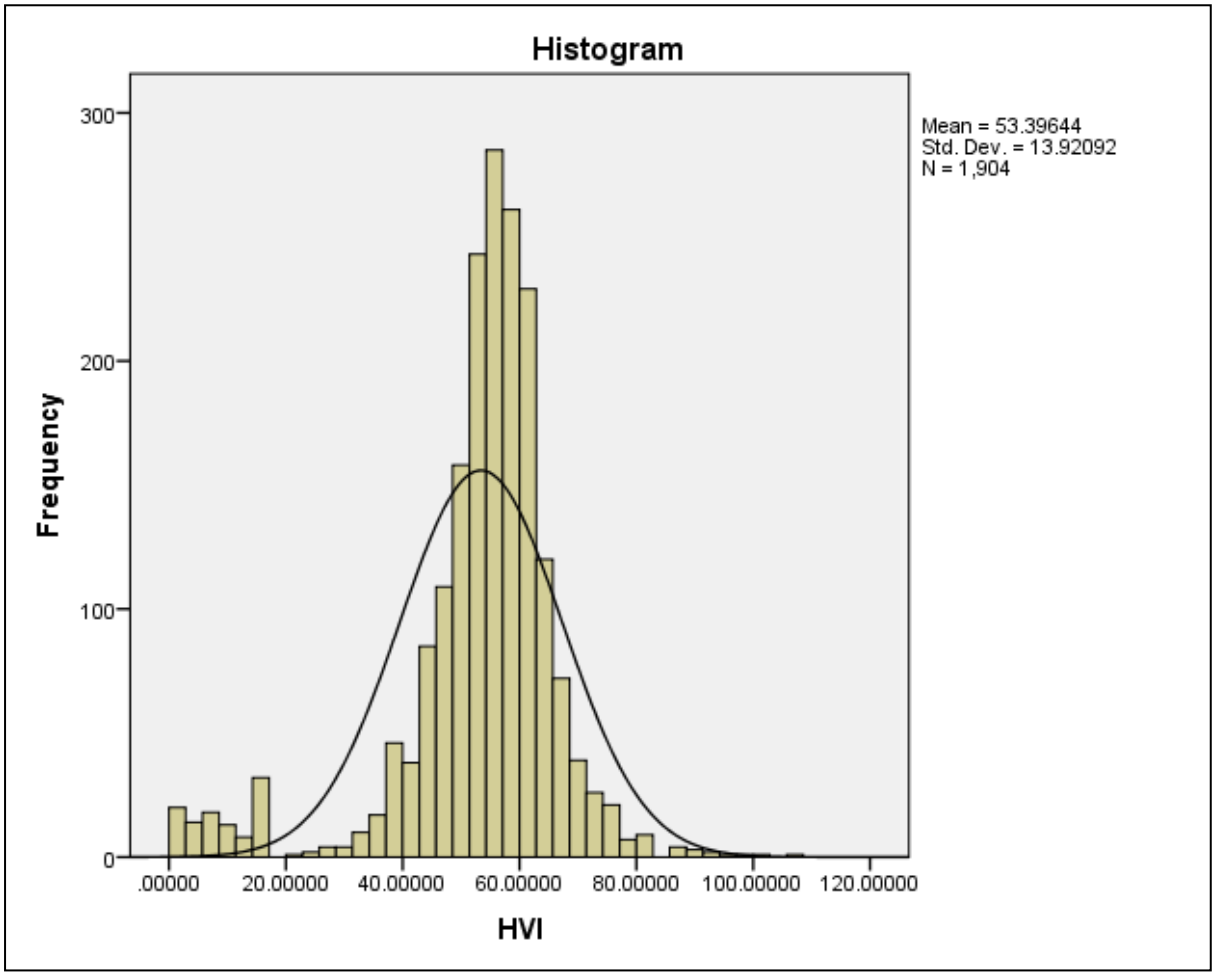

Figure 3.4.1: Value distribution of the calculated Heat Vulnerability Index (HVI).

The spatial distribution of heat vulnerability in Osaka City is uneven and shows clustering of vulnerability in certain areas. A Getis-Ord Hot Spot Analysis revealed clustering of areas with high and low vulnerability. Statistically significant clusters of high (low) vulnerability are identified as areas with a Gi* statistic z score > 2 (< −2) (Figure 3.4.2). The area just south of the Central Business District (CBD) (Nishinari ward) shows the largest cluster of high vulnerability districts in the city. Another small area, east of the CBD, also shows clustering of high vulnerability. The CBD, itself, (particularly in Kita ward) scores low on the vulnerability index. A large cluster of low vulnerability exists along the western boundary of the city. A secondary cluster also appears to the north and north-east of the CBD, with small clusters identified in the far east and far south of the city.

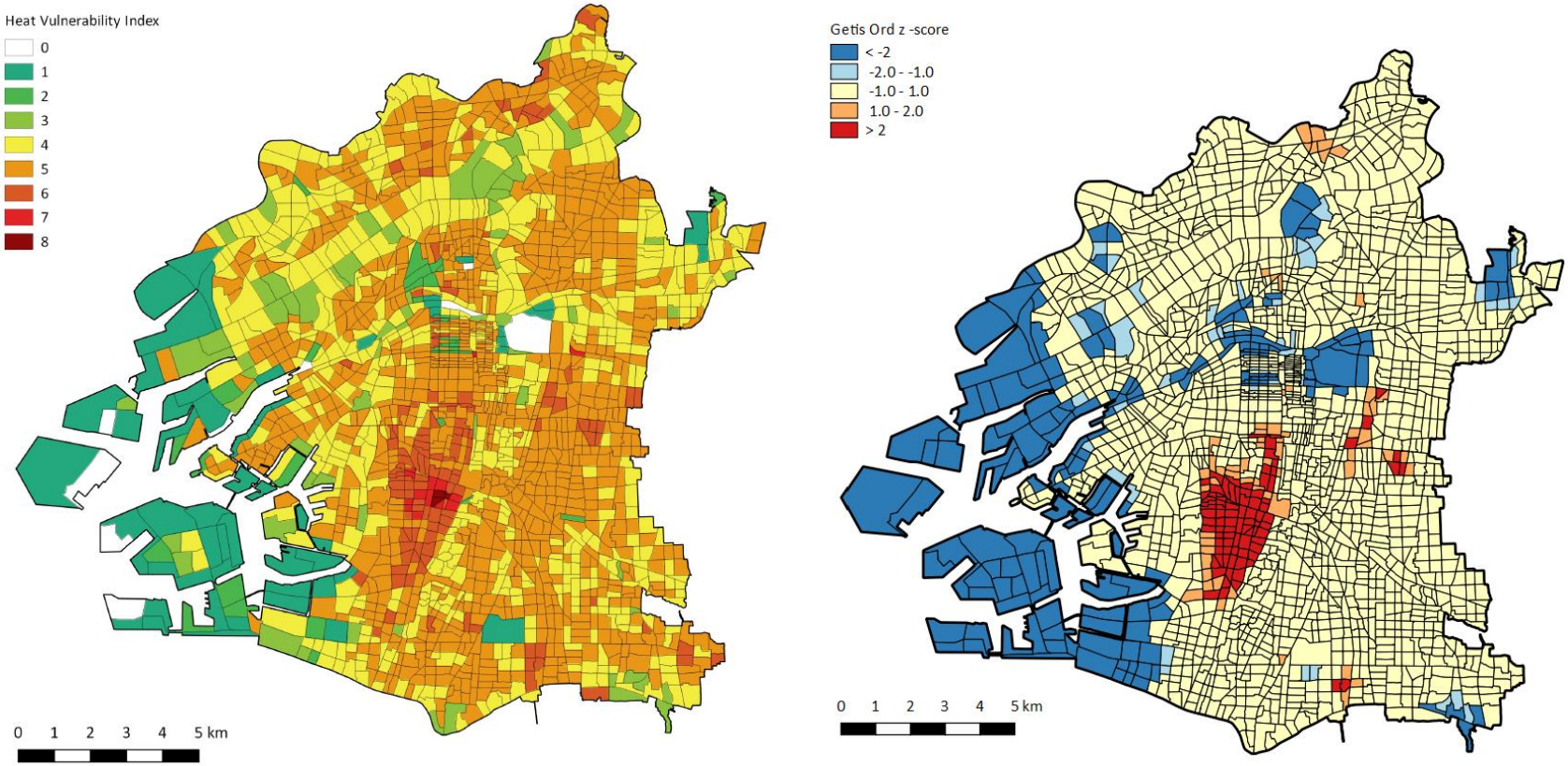

Figure 3.4.2: Output from the vulnerability index calculation, showing low (white, green) to high (orange, red) vulnerability (a); Getis-Ord z score Hot Spot Analysis, showing clusters of high (red) and low (blue) vulnerability (b).

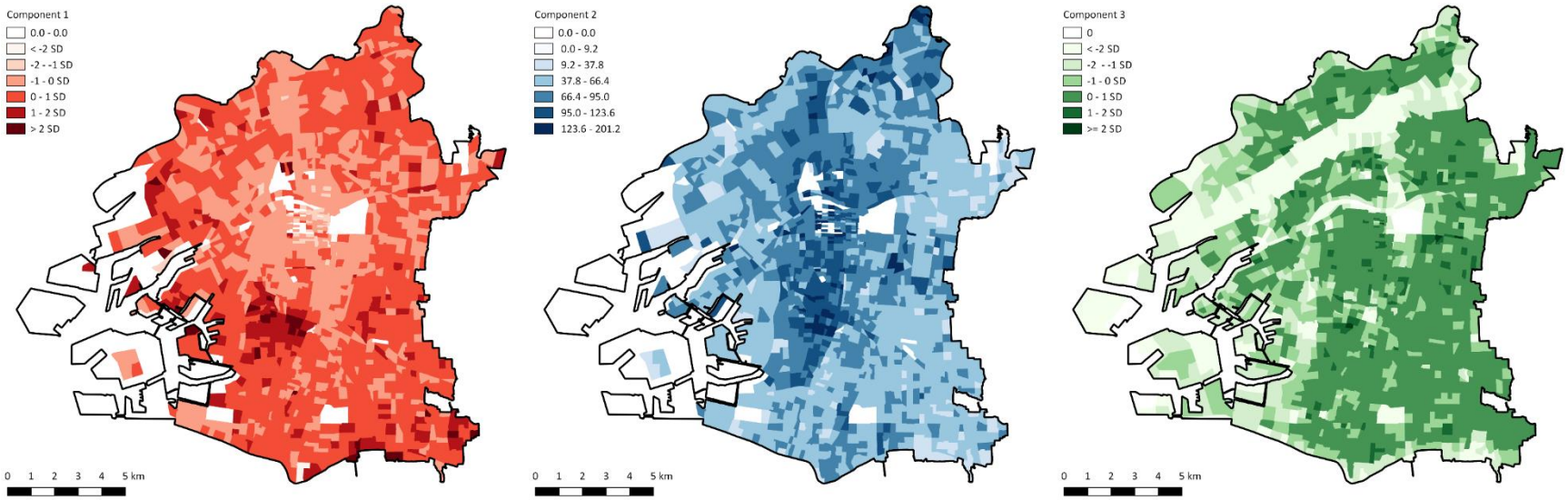

Figure 3.4.3: Spatial distribution of the three key components identified in the PCA; component 1: age, education and unemployment (a), component 2: social isolation (b) and component 3 density and lack of green space (c). The scales are unit-less, displayed as standard deviations from the mean.

In order to investigate the influence of each component on the spatial distribution of the final vulnerability index, the three key components were plotted individually for comparison (Figure 3.4.3). Component 1 (age, education & unemployment) highlights a large area of high vulnerability to the south of the CBD, in Nishinari Ward, with the CBD itself showing low vulnerability. There are small clusters of vulnerability around the periphery of the CBD, although the most pronounced is to the south. Component 2 (social isolation) displays a high concentration of vulnerability in the CBD and, again, in the area to the south of the CBD, which also scored highly in component 1. The east and west of the city show low vulnerability in the social isolation component. Component 3 (density & lack of green space) identifies vulnerability hot spots less clearly than the other two components. However, what is noticeable on this map is the location of the vegetated and low-density areas of the city. The large band of low vulnerability in the north of the city indicates the location of a large river (Yodo River). Other low-scoring areas are situated around the north of the CBD (Osaka Castle Park and the Okawa River). The west of the city also scores low in vulnerability indicated by component 3.

3.4.2. Heat exposure distribution

The spatial distribution of the DH of 'hot days' is displayed in Figure 3.4.2. The eastern and south-eastern areas of the city show the highest DH for temperatures exceeding 30°C, whereas the western, seaward side of the city shows the lowest. The central, CBD area shows a low level of exposure to hourly temperatures above 30°C, relative to the eastern areas of the city. A small pocket of low exposure is identified in the north-east of the city, originating from one particular monitoring station. The number of 'hot nights' shows a more centralised distribution, with the northern and southern CBD districts showing the highest relative exposure (Figure 3.4.4). The area with the lowest exposure to hot nights is in the north-east of the city. Eastern areas of the city generally display lower night-time exposure relative to daytime DH exposure. There is a very pronounced difference in the pattern of exposure to daytime and night-time exposure in the city, which highlights Osaka City's diurnal thermal regime.

3.4.3. Combined vulnerability mapping

Spatial distribution of population vulnerability and spatial exposure were plotted, to enable identification of areas that show high vulnerability and high heat exposure (Figure 3.4.5). Areas that experience the highest exposure to daytime temperatures are concentrated in the east of the city, with a small pocket in the CBD. These areas tend to score lower in the vulnerability index, but there are certain districts located in this high-exposure zone. Areas exposed to high night-time temperatures are concentrated in the CBD and immediate surrounding areas. The cluster of high-scoring vulnerability districts to the south of the CBD is located within one of these zones. This co-occurrence of high vulnerability and high night-time exposure is clearly identified in Figure 3.4.5.

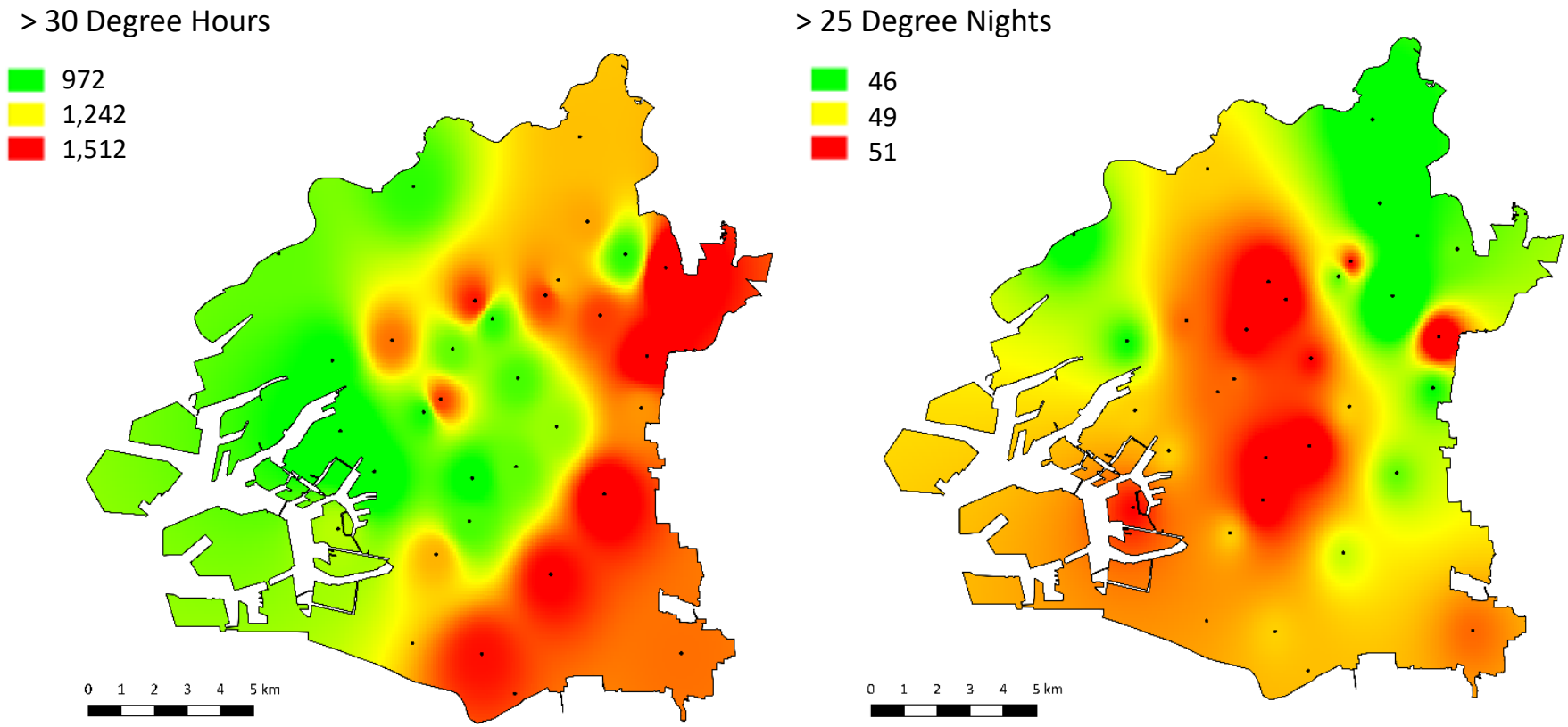

Figure 3.4.4: Interpolated observational data of the number of degree hours > 30°C (a) and the number of days where Tmin > 25°C (b) for Osaka City in summer 2007. The scale indicates the mean (yellow), and 2 SD from the mean (green −2 SD; red +2 SD). Black dots indicate the location of weather recording stations.

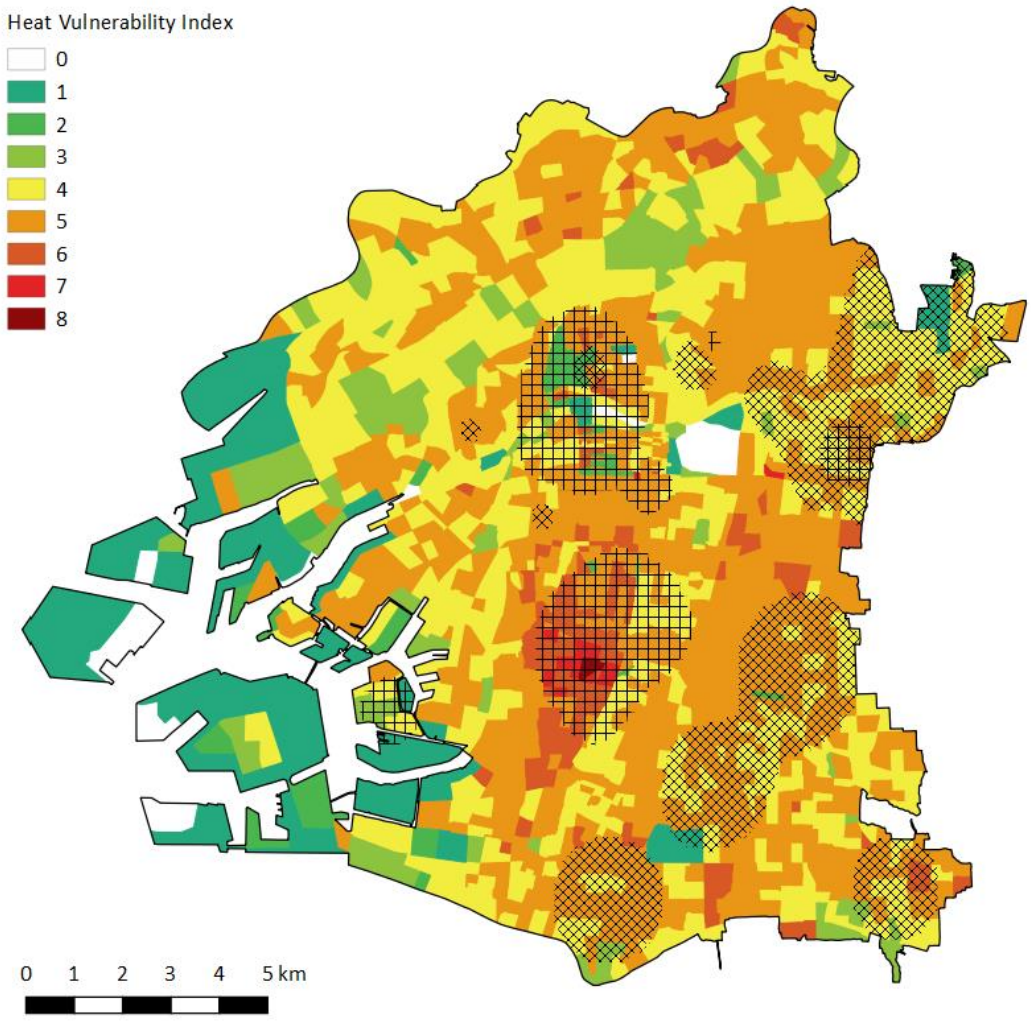

Figure 3.4.5: Overlay of census district HVI scores and heat exposure. Checked areas indicate > 50 days with Tmin > 25°C (> 1 SD above the mean). Diagonal checked areas > 1370 degree hours above 30°C for summer 2007 (> 1 SD above the mean).

3.5. Discussion

This study combines an inductive human vulnerability assessment with an exposure assessment, based on observations from an entire summer season at a daily and hourly scale. Previous studies have looked at single time slice temperatures for a specific hour on a particular day (Wolf and McGregor 2013), and mean temperatures for a summer month (Chow et al. 2012). This study used ground-level observations from a network of meteorological stations to build up a fine temporal scale seasonal profile of temperature variability. Exposure analysis was conducted based upon cumulative hourly exposure to hot temperatures (degree hours of exposure) and the number of nights that residents are exposed to hot

temperatures (Tmin > 25^{o}C). Based on the results of this, we can more strongly identify the areas of the city that are more frequently exposed to heat wave conditions.

3.5.1. Characteristics of the heat wave vulnerability index

Based on this index, the heat vulnerability for Osaka City varies spatially and is clustered in several areas around the CBD area (Figure 3.4.5). Corresponding studies in the USA and UK identified similar spatial distributions of vulnerability (Reid et al. 2009; Wolf and McGregor 2013). In the analysed cities in these regions, the CBD area was found to be the largest cluster of vulnerability, with other, smaller clusters distributed around the central area. The cluster distribution is comparable; however, the largest cluster in Osaka City is just south of the CBD, with the CBD itself scoring lowly on the scale. A key factor in the difference is the population density within the compared cities. In contrast to most of the cities in the USA and UK very few people permanently reside in the most central areas of Osaka City, particularly in Kita ward, where several of the most central districts have no permanent population. As population density in census data is recorded by permanent address, the density of these zones appears to be very low, hence the low vulnerability scores. Access to daytime population data at a sub-ward scale is not currently available, but given that the most vulnerable time for heat wave-related illness is at night-time (Reid et al. 2009), it can be said that the night-time population density used is an appropriate measure of vulnerability.

A further differentiation between this study and most previous studies is the large area of low vulnerability identified in the west of the city. The explanation for this is that this area is predominantly utilised as an industrial port, with some zones designated as recreation (theme parks and museums) and administrative districts. Therefore, there is a low population density in this area, which is reflected in the vulnerability map. Despite the anomaly of CBD vulnerability, the results show similar clustering to previous studies of vulnerability and indicate that proxy indicators based on epidemiological knowledge are a strong indicator of the sensitivity of a population to heat waves in Osaka City.

Further conclusions can be drawn from analysis of the individual components of the vulnerability index. Component 1 (age, education and unemployment) highlights one particular area, to the south of the CBD, with high social vulnerability (Figure 3.4.3). The CBD itself shows low social vulnerability. This contrasts somewhat with several studies in the USA (Harlan et al. 2013; Johnson et al. 2012; Reid et al. 2009), where social vulnerability was found to concentrate more centrally. The finding is, however, similar to a study in the UK (Wolf and McGregor 2013). The very central districts of Osaka City (Kita and Chuo Wards) are relatively affluent areas compared to their surrounding neighbourhoods and, although being highly developed, are not as densely populated as other parts of the city (Figure 3.4.2). The population of elderly in Chuo and Kita wards is also lower than surrounding areas (16.79 and 18.15 %, respectively, compared to a city average of 22.16 %). This finding highlights a difference in the social vulnerability of a Japanese city, compared to cities in the USA. Another contrast between

urban areas in the USA and Osaka is identified by component 2 (social isolation). The population of Osaka City is more socially isolated than the urban US population. Within Osaka City, 46.92 % of people live alone, compared to 10.28 %, for urban populations in the USA (Reid et al. 2009). This can partly be explained by the fact that Osaka City as an administrative zone is not an entire urban area in itself (there are very few suburban areas within the city boundaries), but is still a distinct difference. Comparing Figure 3.4.2 with Figure 3.4.3 enables the strong influence of social isolation to overall heat vulnerability in Osaka City to be visualised. Component 3 (density and lack of green space) enables environmental vulnerabilities to be visualised (Figure 3.4.3). Chomes adjacent to rivers and including parks score low in this component (Appendix 2.3). This component highlights areas of the city that, physically, are more (less) vulnerable to heat waves. Small areas of very high vulnerability exist in central areas. These could be targeted for investigation into potential physical interventions such as urban greening (Declet-Barreto et al. 2013). Individually mapping each component allows hot spots of particular types of vulnerability to be identified and helps to highlight particular areas that could be targeted for investigations into reducing different aspects of heat vulnerability. The three individual components in this study indicate a level of heterogeneity in the distribution of environmental-based vulnerability (component 3) and socioeconomic vulnerability (components 1 and 2) (Figure 3.4.3). Buscail et al. (2012) concluded that exposure and vulnerability to heat require different prevention strategies. Environmental vulnerability is linked more closely to exposure, whereas socioeconomic vulnerability is related to population sensitivity. This study highlights the distributions of environmental- and socioeconomic-based vulnerability, which can raise awareness about the locations in the city which are suitable for different prevention strategies.

3.5.2. Heat exposure distribution

The difference in spatial distribution of ‘hot days’ and ‘hot nights’ is indicative of the strong UHI effect of Osaka City. The UHI effect is more evident at night, primarily due to the absorption and subsequent storing and radiation of heat from buildings and dense infrastructure (Han and Huh 2008). The bias of hot daytime temperatures to the east of the city can be explained by the moderating impact of sea breezes on the western areas of the city during the day (Masumoto 2009). The sea breeze dissipates at night, which can explain why the highest night-time exposure to heat is concentrated in the central area of the city, where the UHI effect is strongest. The small area in the north-east of the city experiencing a large number of ‘hot nights’ was investigated further using satellite imagery Landsat 8 Thermal Infrared Sensor (TIRS) (Appendix 2.3; USGS 2016) and elevation data (Jarvis et al. 2008). No specific causes could be identified for the hot spot. However, the satellite image indicated that the area had a relatively high land surface temperature and is low lying compared to the wider area. It must also be added that the city boundary of Osaka City doesn’t mark the end of the urban area, so this area is under the influence of the UHI effect. Further investigation into the station recording the lowest number of ‘hot nights’ revealed that this station is located adjacent to a large, vegetated park (Osaka Castle Park;

Appendix 2.3), and is close to a river. This finding is supported in the literature, relating to effect of vegetation on temperatures in their vicinity (Buscail et al. 2012; Harlan et al. 2013; Song et al. 2015). This result indicates that the effect of urban green areas may impact the spatial distribution of ambient temperature exposure in Osaka City. However, none of the monitoring sites were located within vegetated areas (all were located in school playgrounds). To investigate the impact of vegetated areas on ambient temperatures within the city, future studies should locate monitoring stations in a greater variety of locations, including within parks, beside bodies of water and in highly developed areas. This would also enable the relationship between remote-sensed land surface temperature and observed air temperature to be analysed in more detail.

The heat exposure mapping results highlight two key points about exposure distribution in Osaka City. The first is that there is a significant influence of sea breezes on daytime summer temperatures (Figure 3.4.4). The second is that the UHI effect is very pronounced at night-time, with the CBD and surrounding areas experiencing the most 'hot nights'. This finding raises awareness about the daily temperature regime of Osaka City, a coastal urban area, which could provide direction to considerations of physical intervention measures. The difference in spatial distribution between daytime and night-time exposures also highlights the requirement to assess exposure in cities at a fine temporal scale over a period of time. A single snapshot is not adequate for understanding the full temperature regime of a city.

3.5.3. Combined vulnerability and exposure analysis

A key analysis to draw from the combined vulnerability and exposure analysis for Osaka City is that the largest cluster of social vulnerability is located in an area of high exposure to night-time heat (Figure 3.4.5). This indicates that on both measures of vulnerability (social and environmental), this area scores highly and is clearly highlighted as the most vulnerable area. This area, in Nishinari Ward, is well documented as one of the most highly deprived areas in Japan (Tabuchi et al. 2012). Therefore, the findings support the theory that vulnerability to heat is concentrated in inner city neighbourhoods that have low income, education and social mobility (Harlan et al. 2013; Reid et al. 2009).

Combined analyses of exposure and social vulnerability, such as the method employed in this study, can be used to prioritise areas that require public health measures and/or urban planning initiatives to reduce vulnerability and exposure (Milan and Creuzig 2015). Public health measures are low-cost, targeted and rapid responses to reduce vulnerability. Urban planning initiatives are costlier (time and capital) and result in larger changes to the urban environment. They are currently infrequently used; however, they have been proven to be more effective at reducing exposure on a larger scale and are effective for a longer time period (Milan and Creuzig 2015). The combined vulnerability map (Figure 3.4.2) can be used as a guideline to identify the areas of Osaka City that could be effectively targeted

with each approach, enabling decision-makers to determine which areas are suitable for further investigation for either measure.

This study is limited by the availability of health data at the smallest scale and could be improved by the inclusion of such data when available. Due to this limitation, the vulnerability map is most suitable for awareness raising and identifying areas of potential vulnerability. The vulnerability index map can be validated in future studies by using local-level ambulance call-out and mortality data for heat wave events (Wolf and McGregor 2013). After more conclusive validation, the map could provide a basis for decision-making. A caveat for the temperature interpolation map is that its accuracy is limited by the number of monitoring stations in the city. Data were recorded from 35 monitoring stations; however, for a more accurate assessment of the temperature regime of the city, more observation sites could be used. Temperature data from the 35 sites were only available for 1 year: 2007. Future studies should aim to develop a heat profile for the target city over a number of years and at a finer scale, to account more strongly for any anomalous results. A further improvement would be to assess the entire *Keihanshin* urban area (including Kyoto and Kobe cities). This would enable a more thorough investigation into the spatial distribution of vulnerability throughout a wider urban area, a megacity, and would indicate the influence of UHI more strongly.

3.6. Conclusion

This study developed and mapped a heat wave vulnerability index derived from a principle component analysis of key variables influencing heat wave vulnerability in Osaka City, Japan. Census data and environmental variables were included in the analysis, and three principle components determining vulnerability were identified as explaining > 77 % of the variance in the eight original variables (age, employment and education; social isolation; density and lack of green space). The vulnerability index was combined with interpolated fine-scale observational air temperature observations. The output identifies the distribution of population vulnerability and exposure simultaneously, highlighting the spatial distribution of vulnerability and exposure in Osaka City. This assessment of vulnerability, combining fine-scale exposure and sensitivity components, can provide precedent for efficient, targeted action to be taken to reduce the impact of heat waves at present and under climate change.

References

Bai, H., Islam, M.N., Kuroki, H., Honda, K. and Wakasugi, C., 1995. [Deaths due to heat waves during the summer of 1994 in Osaka Prefecture, Japan]. *Nihon hoigaku zasshi= The Japanese journal of legal medicine*, **49**(4), pp.265-274.

Braga, A.L., Zanobetti, A. and Schwartz, J., 2002. The effect of weather on respiratory and cardiovascular deaths in 12 US cities. *Environmental health perspectives*, **110**(9), p.859.

Buscail, C., Upegui, E. and Viel, J.F., 2012. Mapping heatwave health risk at the community level for public health action. *International journal of health geographics*, **11**(1), p.1.

Chestnut, L.G., Breffle, W.S., Smith, J.B. and Kalkstein, L.S., 1998. Analysis of differences in hot-weather-related mortality across 44 US metropolitan areas. *Environmental Science & Policy*, **1**(1), pp.59-70.

Chow, W.T., Chuang, W.C. and Gober, P., 2012. Vulnerability to extreme heat in metropolitan Phoenix: spatial, temporal, and demographic dimensions. *The Professional Geographer*, **64**(2), pp.286-302.

Chuang, W.C. and Gober, P., 2015. Predicting hospitalization for heat-related illness at the census-tract level: Accuracy of a generic heat vulnerability index in phoenix, Arizona (USA). *Environmental Health Perspectives (Online)*, **123**(6), p.606.

Curriero, F.C., Heiner, K.S., Samet, J.M., Zeger, S.L., Strug, L. and Patz, J.A., 2002. Temperature and mortality in 11 cities of the eastern United States. *American journal of epidemiology*, **155**(1), pp.80-87.

Cutter, S.L., Boruff, B.J. and Shirley, W.L., 2003. Social vulnerability to environmental hazards. *Social science quarterly*, **84**(2), pp.242-261.

Declet-Barreto, J., Brazel, A.J., Martin, C.A., Chow, W.T. and Harlan, S.L., 2013. Creating the park cool island in an inner-city neighborhood: heat mitigation strategy for Phoenix, AZ. *Urban Ecosystems*, **16**(3), pp.617-635.

Ebi, K.L., Teisberg, T.J., Kalkstein, L.S., Robinson, L. and Weiher, R.F., 2004. Heat watch/warning systems save lives. *Bulletin of the American Meteorological Society*, **85**(8), p.1067.

E-Stat, 2015. 2010 Census: Osaka Prefecture list of statistical changes. https://www.e-stat.go.jp/SG1/estat/GL08020103.do?_toGL08020103_&tclassID=000001036634&cycleCode=0&requestSender=search

Fouillet, A., Rey, G., Laurent, F., Pavillon, G., Bellec, S., Guihenneuc-Jouyaux, C., Clavel, J., Jougla, E. and Hémon, D., 2006. Excess mortality related to the August 2003 heat wave in France. *International archives of occupational and environmental health*, **80**(1), pp.16-24.

Fujibe, F., 2011. Urban warming in Japanese cities and its relation to climate change monitoring. *International Journal of Climatology*, *31*(2), pp.162-173.

Hajat, S., O'Connor, M. and Kosatsky, T., 2010. Health effects of hot weather: from awareness of risk factors to effective health protection. *The Lancet*, **375**(9717), pp.856-863.

Han, S.G. and Huh, J.H., 2008. Estimate of the Heat Island and Building Cooling Load Changes due to the Restored Stream in Seoul, Korea. *International Journal of Urban Sciences*, **12**(2), pp.129-145.

Harlan, S.L., Declet-Barreto, J.H., Stefanov, W.L. and Petitti, D.B., 2013. Neighborhood effects on heat deaths: social and environmental predictors of vulnerability in Maricopa County, Arizona. *Environmental Health Perspectives (Online)*, **121**(2), p.197.

Huisman, M., Kunst, A.E. and Mackenbach, J.P., 2003. Socioeconomic inequalities in morbidity among the elderly; a European overview. *Social science & medicine*, **57**(5), pp.861-873.

IPCC, 2014. In: Field, C.B., Barros, V.R., Dokken, D.J., Mach, K.J., Mastrandrea, M.D., Bilir, T.E., Chatterjee, M., Ebi, K.L., Estrada, Y.O., Genova, R.C., Girma, B., Kissel, E.S., Levy, A.N., MacCracken, S., Mastrandrea, P.R., White, L.L. (eds), *Climate change 2014: impacts, adaptation, and vulnerability. Part A: Global and sectoral aspects*. Contribution of Working Group II to the Fifth Assessment Report of the Intergovernmental Panel on Climate Change. Cambridge University Press, Cambridge, United Kingdom; New York, NY, USA, p 1132

JMA, 2015. Japan Meteorological Agency. http://www.data.jma.go.jp/gmd/risk/obsdl/index.php

Jarvis, A., Reuter, H.I., Nelson, A. and Guevara, E., 2008. Hole-filled SRTM for the globe Version 4. *available from the CGIAR-CSI SRTM 90m Database (http://srtm.csi.cgiar.org).*

Johnson, D.P., Stanforth, A., Lulla, V. and Luber, G., 2012. Developing an applied extreme heat vulnerability index utilizing socioeconomic and environmental data. *Applied Geography*, **35**(1), pp.23-31.

Kim, Y. and Joh, S., 2006. A vulnerability study of the low-income elderly in the context of high temperature and mortality in Seoul, Korea. *Science of the total environment*, **371**(1), pp.82-88.

Mastrangelo, G., Fedeli, U., Visentin, C., Milan, G., Fadda, E. and Spolaore, P., 2007. Pattern and determinants of hospitalization during heat waves: an ecologic study. *BMC Public Health*, **7**(1), p.1.

Masumoto, K., Taniguchi, I. and Nomura, T., 2006. Characteristics of air temperature distribution in 2005 and situation of heat island in Osaka City. *Journal of Heat Island Institute International*. **1**, pp.30-35.

Masumoto, K., 2009. Urban heat island in Osaka city distribution of air temperature and west bulb globe temperature. *In The Seventh International Conference on Urban Climate, 29 June-3 July 2009.*

Matsumoto, S., 2015. *Environmental Subsidies to Consumers: How Did They Work in the Japanese Market?* Routledge, New York, NY, USA. 280 pp.

Milan, B.F. and Creutzig, F., 2015. Reducing urban heat wave risk in the 21st century. *Current Opinion in Environmental Sustainability*, **14**, pp.221-231.

NLNI, 2016. National Land Numerical Information download service, Accessed online at: http://nlftp.mlit.go.jp/ksj/jpgis/jpgis_datalist.html [Japanese].

Reid, C.E., O'Neill, M.S., Gronlund, C.J., Brines, S.J., Brown, D.G., Diez-Roux, A.V. and Schwartz, J., 2009. Mapping community determinants of heat vulnerability. *Environmental Health Perspectives* **117**(11), pp.1730-1736.

Song, X., Liu, J., Lin, Y., Liu, L. and Wang, D., 2015. Regional thermal climate prediction and mitigation strategy of local urban heat island, *Harbin Gongye Daxue Xuebao / Journal of Harbin Institute of Technology*, **47**(2), pp.25-30.

Tabuchi, T., Fukuhara, H. and Iso, H., 2012. Geographically-based discrimination is a social determinant of mental health in a deprived or stigmatized area in Japan: A cross-sectional study. *Social Science & Medicine*, **75**(6), pp.1015-1021.

USGS, 2016. United States Geological Survey website (http://landsat.usgs.gov). Satellite data. *Available from: http://earthexplorer.usgs.gov/.*

Vescovi, L., Rebetez, M. and Rong, F., 2005. Assessing public health risk due to extremely high temperature events: climate and social parameters, *Climate Research*, **30**, 71–78.

Wolf, T. and McGregor, G., 2013. The development of a heat wave vulnerability index for London, United Kingdom, *Weather and Climate Extremes*, **1**, 59–68.

Chapter 4. The development of a method to determine the burden of climate change on different health outcomes at a local scale: A case study in Osaka Prefecture, Japan

4.1. Context setting

The case studies presented in chapters 2 and 3 provide in depth research into two different risk factors with distinct health outcomes. Both provide potential solutions in quantifying the risk of climate change on each factor. However, the quantified scales are disparate and cannot be directly compared. There is no way for us to determine which is the greater risk of the two, or which is influenced more strongly by climate change. This chapter outlines a framework whereby the current risk of health outcomes can be calculated, the impact of climate determined and the burden of climate change quantified in a common unit (Disability Adjusted Life Years: DALY). This chapter builds on the issues identified in the findings of the previous two chapters and sets out a framework to address the issues with quantifying, comparing and prioritising climate change related risks at a local level. The study in this chapter uses two major health outcomes related to climate and climate change in Osaka Prefecture: cardiovascular disease and meteorological disaster related injuries. These were selected due to their importance to the region in question; however, the framework presented can be adapted to assess climate change impact on any health outcome, provided the data is available. An additional benefit of the methodology presented in this chapter is that the output of different health outcomes can be combined, using the same unit. This means that the analysis can be extended to isolate specific risk factors and quantify their impact in terms of DALY.

4.2. An introduction to DALY

DALY is a measure of overall disease burden, expressed as the number of years lost due to ill-health, disability or early death (GBD, 2013a). It was developed by the World Health Organisation as a way of comparing the overall health and life expectancy of different countries, but has uses in comparing the burden of health outcome and risk factors at all scales. DALY combines estimates of the number of years of life lost due to premature death (YLL) and the value of life lost due to disability, expressed in years lived with disability (YLD) (Murray et al. 2010). YLL is calculated based upon the number of deaths due to a selected health outcome and the standard life expectancy at the age of each death:

$$YLL = N * L \quad (1)$$

Where N is the number of deaths and L is the life expectancy at death, based on life tables for the study region. YLD is calculated using the following equation:

$$YLD = P * DW \quad (2)$$

Where P is the prevalence of the disease or health outcome and DW is the disability weight given to the disease. The disability weight is based upon a study involving clinical physicians, in which diseases were given a weighting from 0 (full health) to 1 (death), based upon their impact on the quality of life and the duration of the illness (Salomon et al. 2010). YLL and YLD are then combined to quantify the burden of the health outcome in question:

$$DALY = YLL + YLD \quad (3)$$

DALY of different health outcomes can be combined and compared with each other. The proportion of a disease's total burden caused by specific risk factors can also be calculated, to determine the main contributing factors to a particular health outcome's burden. It is this point that makes DALY applicable to climate change health impact research, as in order to implement effective adaptation strategies, the contribution of climate change to particular health outcomes needs to be quantified.

4.3. Study introduction

From a human health perspective, climate change contributes to increases in a range of health outcomes (IPCC, 2014; World Health Organisation, 2012). The impacts can be categorised by risk factors and health impact endpoints. Risk factors are the physical changes to the earth's atmosphere and circulatory system, including rising temperatures, changes in precipitation regimes, sea level rise and altered frequency and intensity of natural disasters (Ezzati et al. 2002). Health outcomes are diseases or human damage influenced by climate change. These include, but are not limited to, cardiovascular disease (CVD), injuries caused by extreme events, infectious diseases and malnutrition (De Schryver et al. 2008). The existence of different risk factors and endpoints presents a problem for comparing the relative risk of each. It also makes it difficult to compare the impact of climate change with other risk factors on particular health outcomes. A solution is provided by the concept of Disability Adjusted Life Years (DALYs) (Murray et al. 2013). This enables different risk factors and health outcomes to be compared on a common scale. The World Health Organisation (WHO) provided an assessment on how to quantify the health impact of climate change (Campbell-Lendrum et al. 2007); however, this does not produce results on a common, fully comparable scale for individual health outcomes. It is vitally important to quantify the impact of climate change on different health outcomes on a common scale that can be combined and compared to the impact of other risk factors. The development of a

transferrable method to calculate the impact of climate change on health outcomes at a local scale will be of great benefit to local authorities and risk management. This study presents a method to calculate the impact of climate change on CVD and meteorological disaster related injuries (DRI), using DALYs as a common unit at a local scale, in Osaka Prefecture, Japan. CVD and DRI were selected as endpoints to demonstrate the method due to their importance to the study area and their fundamental differences: CVD is a chronic illness, whereas DRIs are acute. The results provide a demonstration of the method and show the importance of identifying the impact of climate change at a local scale, to identify hot spots of vulnerability and exposure in populations.

4.4. Methods

The general method for quantifying both CVD and meteorological DRI impacts from climate change in this study, followed the framework identified in Figure 4.4.1. Initially, the exposed population was calculated. This involved identifying the specific climate risk factor that impacts the health outcome concerned. As all areas will be exposed to climate change, the entire population was considered to be exposed. The degree of exposure of populations in different areas was calculated by using the output from a climate model. The current death rate from each health outcome was derived from observed records. The future death rate was projected by calculating the climate-response value. This determined the relationship between the climatic risk factor and the number of deaths for the target health outcomes. This value was combined with the climate model output and the current death rate to produce the projected future death rate. The difference between the current and future death rate was determined as the Relative Risk. This value was then used to calculate the change in DALYs from present values to future estimates, thus deducing the burden of climate change.

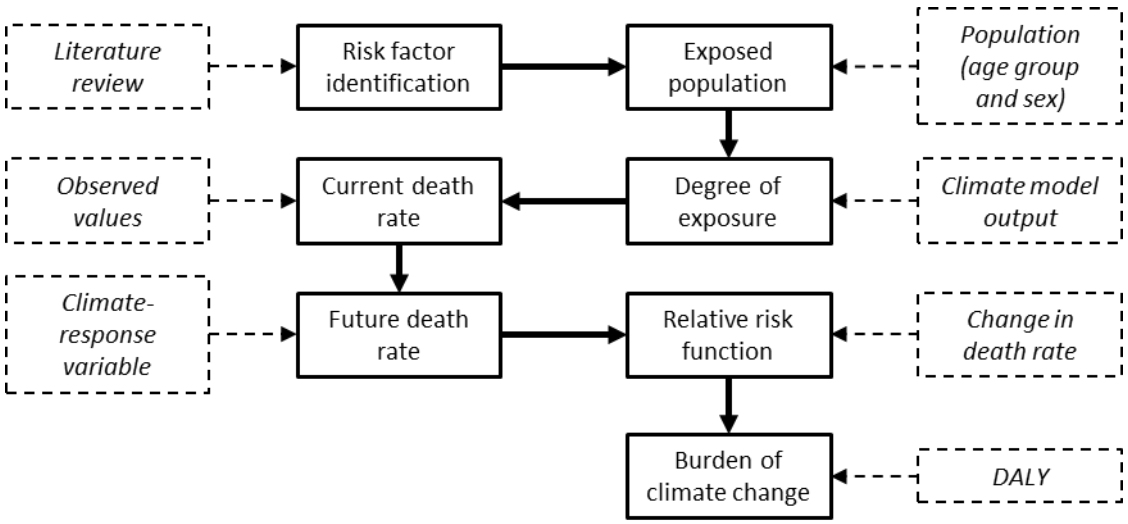

Figure 4.4.1: Framework for calculating the burden of climate change on health outcomes. Dashed boxes indicate inputs and solid boxes indicate processes. The full framework for the two case studies in this topic is displayed in Appendix 3.2.

4.4.1. Risk factor identification

The risk factor for each health outcome was identified through a review of past studies. Temperature was identified as the major risk factor for CVD (Basu & Samet, 2002; McMichael et al. 2006; Patz et al. 2005) and meteorological natural disasters, linked to precipitation, as the risk factor for acute injuries (Campbell-Lendrum et al. 2007). For the purposes of this study, only the negative impacts of climate change on CVD are considered. We propose this approach for two reasons. Firstly, although climate change will reduce exposure to cold temperatures, which will modulate the overall impact of climate change on CVD mortality, this does not impact on the fact that populations will be exposed to higher risk of heat related CVD (McMichael et al, 2006). Heat and cold related CVD have different risk pathways and countermeasures, thus must be considered separately to maximise understanding of the risk of increasing exposure to high temperatures. Secondly, most excess deaths during heat wave events are related to CVD (Haines et al. 2006), meaning that understanding the increased risk under climate change due to higher exposure to heat is of vital importance.

4.4.2. Degree of exposure

Outputs from interpolated observation data at a 1km resolution were used to plot current mean annual temperature, derived from monthly mean temperature for Osaka Prefecture. Administrative zones at the smallest scale for the study area were overlaid on this projection, and the values averaged for each zone. Future temperature projections were calculated in the same manner, using 1km resolution downscaled projection outputs from the Coupled Model Intercomparison Project, Phase 5 (CMIP5) climate model ensemble for 2050, under the four Representative Concentration Pathways (RCP 2.6 (optimistic), 4.5 and 6.0 (most probable) and 8.5 (pessimistic)) (Hijmens, 2005). The model output for this study was produced at 1km resolution but using statistical downscaling of a GCM (full methodology in Hijmens et al. 2005). These outputs were selected due to the extremely high resolution, robust parent GCM ensemble and the high density of observation points in Japan, from which the statistical downscaling was derived (Hijmens et al. 2005). RCP 4.5 was selected for the local scale assessment projections, in this timeframe, as it is a medium stabilisation pathway, within the range of the majority of IPCC scenarios (van Vuuren et al. 2011). The change in average temperature between the current conditions and the 2050 projections was identified as the relative level of exposure for each administrative zone.

For exposure to meteorological natural disasters, the whole region was determined to have the same level of exposure, due to the relatively small area of the Osaka Prefecture (1,899km^2; NLNI, 2016) and the mesoscale nature of events such as typhoons and extreme precipitation related to frontal systems (Sugimoto & Ueno, 2012).

4.4.3. Current death rate

The death rate of CVD varies strongly by age and sex, thus, when projecting the death rate, age and sex demographics must be considered (Campbell-Lendrum, 2007). The current death rate of CVD (per 100,000 population) by sex and five-year age group was deduced from a WHO Global Burden of Disease study (GBD, 2013b). Population demographic data for each zone were accessed from the portal site for the Official Statistics of Japan (e-Stat, 2016). The whole Japan CVD death rate was statistically downscaled to project the death rate in Osaka Prefecture administrative zones by using the death rate of CVD for each five-year age group and sex for Japan, coupled with the population of each age group and sex in each administrative zone. First, the number of deaths per sex and age group in each zone are calculated:

$$D = P * \left(\frac{DR}{100{,}000}\right) \quad (1)$$

Where DR is the whole Japan death rate for the age group and sex and P is the population of the age group and sex in the administrative zone. The total number of deaths for each age group and sex was calculated and summed for each administrative zone. The total death rate for each zone was then calculated by:

$$DR = \left(\frac{D}{P}\right) * 100{,}000 \quad (2)$$

Where D is the total projected deaths per administrative zone and P is the total population of each zone.

The death rate from meteorological DRIs is less related to demographics than CVD, therefore the values were calculated without consideration of age group and sex. Deaths and injuries from meteorological events were accessed from the Japan Meteorological Administration (JMA, 2016a). The record of deaths from DRIs is not continuous for Osaka Prefecture, so the Whole Japan total was used, and the ratio of hospitilisations from DRIs in 2002, 2005 and 2008 (the only available years) was used to calculate the annual death rate for Osaka Prefecture:

$$DR = \left(\frac{D}{P} * 100{,}000\right) * RR \quad (3)$$

Where D is the number of deaths from meteorological DRIs in Japan, P is the Population of Japan and RR is the risk ratio between Japan and Osaka Prefecture.

4.4.4. Future death rate

In order to calculate the future death rate, under climate change, the climate-response value must be calculated (Campbell-Lendrum, 2007). The climate-response value differs by risk factor, health

outcome and location. It is calculated using observed data, to determine the relationship between a risk factor and a health outcome at each location.

Research into the relationship between CVD deaths and temperature is divided into studies which look at specific events (heat waves), those that consider climate change as a binary event and those that calculate a response in the daily number of deaths per degree above a certain threshold (Basu & Samet, 2002; McMichael et al. 2006; Patz et al. 2005). This study employed a threshold approach, with reference to Campbell-Lendrum et al. (2007). Threshold temperature values and a temperature-mortality function were employed from Takahashi et al. (2007). This approach was taken to combine a methodology, originating from the WHO, which is applicable to a local scale (Campbell-Lendrum et al. 2007), with a climate-response function based on observed data from all 47 Prefectures in Japan, 1972-2008 (Takahashi et al. 2007).

The ratio between annual mean temperature and the number of days with a maximum temperature (Tmax) at each degree was calculated, based on observed daily Tmax at a weather station in Osaka City, 1985-2015 (JMA, 2016c). Average annual daily Tmax from the high resolution climate model output was combined with the observed ratio from 1985-2015 data to project the frequency of days at each Tmax degree. This enabled the number of days with a Tmax registering above the designated risk thresholds to be calculated. Takahashi et al. (2007) deduced that the risk ratio between deaths and temperature beyond this threshold was exponential, so suggested a categorical risk function for locations in Japan. This function attributes a relative risk of excess mortality of 1.02 to days with a Tmax of between 0-5ºC above the threshold and a relative risk of 1.10 to days with a Tmax > 5ºC above the threshold. In this study, the relative risk ratio was applied to temperature values above the threshold of 28ºC and 32ºC. For each daily Tmax value (in degrees), the number of CVD deaths was calculated by:

$$D_{total} = \left(D_{avg} * RR\right) * n \quad (4)$$

Where D_{avg} is the average daily number of CVD deaths, RR is the relative risk for the Tmax value. Totals for each Tmax value were summed, to project the annual number of CVD deaths. The difference in the number of days above each threshold between 2000-2010 values and 2050 values was used to project the number of excess deaths attributable to climate change. To single out the climate risk function, no changes in population, or adaptation capacity were considered.

The Death rate for meteorological DRIs was calculated based upon the relationship between the annual precipitation, the number of extreme precipitation events and the number of annual deaths, similar to Campbell-Lendrum et al. (2007). The JMA records the number of times extreme rainfall (> 50 mm/hr) occurs in Japan each year, from over 1000 recording stations. This study identified a linear relationship of annual average precipitation (derived from the 46 prefectures in the four main islands of Japan) with

the number of extreme rainfall events, 1985-2015 (JMA, 2016b). This ratio was combined with climate projections of annual average precipitation in 2050 (calculated from point data at the site of each of the 46 prefectural meteorological stations), to project the number of extreme rainfall events that will occur annually based on the climate in 2050. The linear relationship between the annual number of deaths and the number of events was calculated and combined with this output to estimate the number of meteorological DRIs in 2050 for Japan. This output was downscaled to represent the projected death rate for Osaka Prefecture by the same method identified in equation 3.

4.4.5. Relative risk

The relative risk was calculated from the difference between the current and future death rate for CVD and meteorological DRIs:

$$PAF = \frac{\sum DR_p}{\sum DR_c} \tag{5}$$

Where DR_p is the projected death rate and DR_c is the current death rate.

4.4.6. Burden of climate

The burden of climate on CVD and meteorological DRIs was calculated in disability adjusted life years (DALYs). DALY is a unit that accounts for the years of life lost due to early death and disability (Lim et al. 2012). DALY is used in this study to enable the results to be compared with each other and with risk factors and health outcomes from other studies. DALY values for Japan were accessed from Global Health Data Exchange (GHDx, 2016). The burden of the climate on each health outcome in this study is calculated by using the relative risk:

$$B_{total} = (RR * DALY_i) - DALY_i \tag{6}$$

Where $DALYi$ is the current number of DALYs in each administrative zone and RR is the relative risk. As detailed in section 2.2, DALY for meteorological DRIs was calculated only for the whole prefecture due to data limitations and the difficulty of projecting mesoscale events at a micro scale.

4.4.7. Study location

Osaka Prefecture is located in Western Japan (34-35ºN, 135ºE). Its land area of 1,905 km^2 consists mainly of the Osaka-Kobe metropolitan area (NLNI, 2016). As of 2015, the population is 8,838,908, making it the third most populous prefecture in Japan, and the second most densely populated (4,640 pax/km^2). The majority of the prefecture is a low lying basin, enclosed by forested uplands to the North, East and South, and by Osaka Bay to the West. The basin area is almost entirely developed and densely populated (11,952 pax/km^2 in Osaka City) (OPG, 2016). The prefecture is an industrial hub, with the second largest economy in Japan. Per capita, the economy ranks seventh (Cabinet Office, 2016). This

is a suitable study region due to the large population, dense urban structure and high resolution topographical variations. The area is subject to intense heat in summer and experiences extreme precipitation events and typhoons annually (JMA, 2016c). The hazards faced and the situational characteristics of the prefecture make it a useful study site to apply climate change impact assessment methodologies.

4.5. Results

This study provides a framework for calculating the impact of climate on different health outcomes, using a common unit: DALY. The results of the key steps in the methodology are detailed below, to illustrate the development of the projection model.

4.5.1. Degree of exposure

The frequency distribution of daily Tmax values, averaged for the entire prefecture, for the baseline climate and 2050 was projected to determine the degree of exposure to days with a Tmax above the excess mortality thresholds identified by Takahashi et al. (2007). The regression model was validated against observed frequencies for overall frequency ($R^2 = 0.66$), Tmax > 28°C frequency ($R^2 = 0.74$) and Tmax > 32°C frequency ($R^2 = 0.51$). Based on this linear regression, a shift to a higher frequency of hotter days and lower frequency of cold days is projected in Osaka Prefecture (Figure 4.5.1). The number of days above the lower threshold of 28°C, was projected to increase by 23.67 days annually, and the frequency of days above 32°C was projected to increase by 19.55 days (Table 4.5.1).Baseline and future frequencies of days above both thresholds were calculated for each administrative zone in Osaka Prefecture. This provided the basis for a spatial analysis of the degree of exposure in the baseline and future climate scenario (Figure 4.5.2). Exposure to meteorological extreme events was determined by the number of occurrences of extreme rainfall (> 50 mm/hr). Regression analysis deduced that the number of > 50 mm/hr events in Japan is a function of the annual average rainfall total for Japan ($R^2 = 0.39$). The recorded number of extreme rainfall events in Osaka Prefecture was not available, so downscaling was performed at the next stage of the analysis.

Table 4.5.1: Average annual frequency of excess mortality threshold Tmax days

Time Period	> 28°C Tmax days *(RCP range)*	> 32°C Tmax days *(RCP range)*	28-32°C Tmax days *(RCP range)*
Baseline	101.16	50.16	50.10
2050	124.83 *(119.98 – 135.64)*	69.71 *(65.70 – 78.63)*	55.12 *(54.28 – 57.01)*

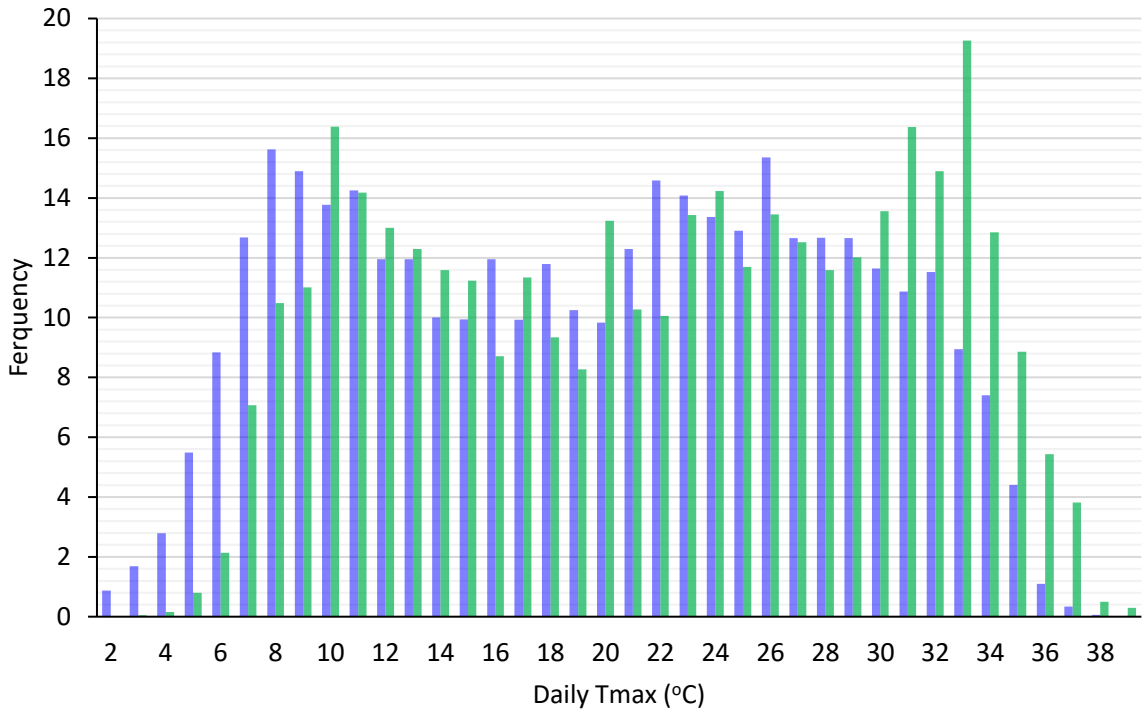

Figure 4.5.1: Frequency distribution of Tmax degree days at the baseline climate (blue) and that produced from CMIP5 2050 projections at RCP 4.5(green).

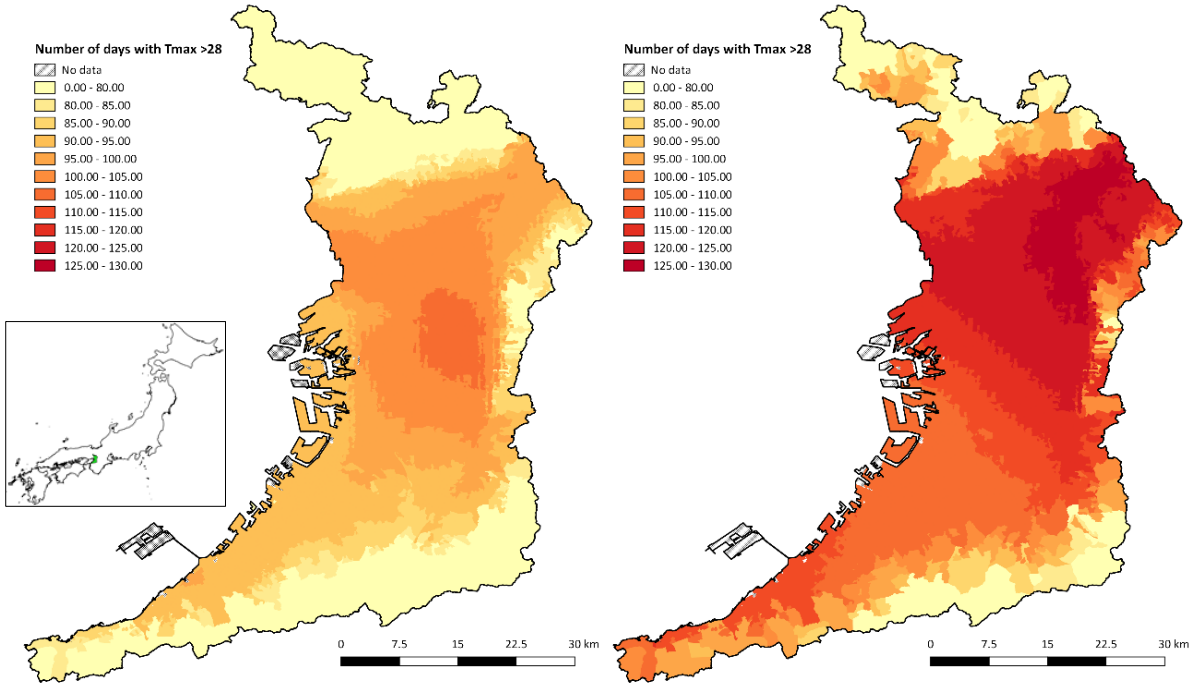

Figure 4.5.2: Projections of the annual number of days with a Tmax > 28oC, averaged for each administrative zone in Osaka Prefecture for the baseline climate (a) and 2050 (b) Inset shows the location of Osaka Prefecture in Japan.

4.5.2. Current death rate

The annual number of deaths caused by CVD for Japan and Osaka Prefecture were accessed from Vital Statistics of Japan (VSJ, 2016). The death rate for each administrative zone in Osaka Prefecture was calculated from the death rate by five-year age groups and sex in Japan. The resulting calculations were summed and validated against Osaka prefecture totals, and were found to overestimate the death rate for the whole prefecture by 13.41%.

The death rate from meteorological DRIs was available for Japan 1989-2013 (JMA, 2016a). The death rate in Osaka Prefecture was estimated from the average ratio of hospitilisations from DRIs in Osaka Prefecture and Japan (1:0.499) (Table 4.5.2).

Table 4.5.2: *Death rate of CVD (2000-2014) and meteorological DRIs (1989-2000).*

Health Outcome	Japan death rate /100,000	Osaka Prefecture death rate /100,000
CVD	271.471	232.607
Meteorological DRI	0.043	0.021

4.5.3. Future death rate and relative risk

The future death rate of CVD in Osaka Prefecture was calculated from the baseline annual number of deaths and the change in the number of days above the 28ºC and 32ºC thresholds (Table 4.5.3). The death rate from meteorological DRIs was calculated from the estimated baseline death rate and the projected number of > 50 mm/hr events in 2050 (Table 4.5.3). The relative risk of climate change on CVD is projected to be lower than that of meteorological DRIs in Osaka Prefecture, although the actual impact is far greater (Table 4.5.3).

Table 4.5.3: Projected death rate of CVD and meteorological DRIs for Osaka Prefecture in 2050.

Health Outcome	Baseline Deaths	2050 Excess deaths *(RCP range)*	2050 Death rate *(RCP range)*	Relative Risk *(RCP range)*
CVD	20,594	114.938 *(91.389 – 167.418)*	233.456 *(233.638 – 234.497)*	1.006 *(1.004 – 1.008)*
Meteorological DRI	1.863	0.489 *(0.467 – 0.536)*	0.027 *(0.026 – 0.027)*	1.263 *(1.251 – 1.288)*

Local scale analysis of the change in the death rate identified the relative risk of climate change in 2050 on CVD in each administrative zone in Osaka Prefecture (Figure 4.5.3). This map identifies the most

vulnerable areas to climate change impacts on CVD, based upon the population demographics and the projected changes in temperature.

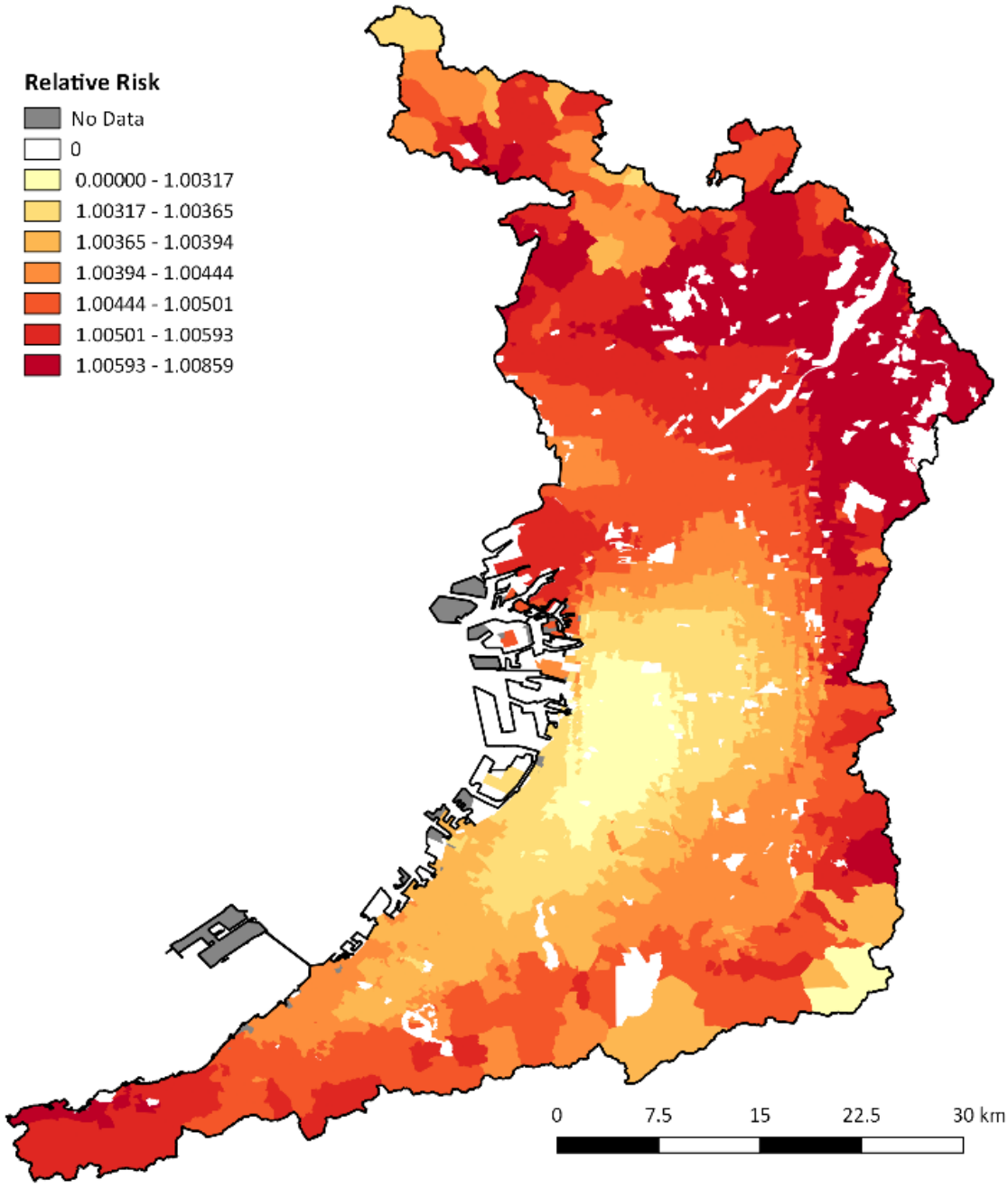

Figure 4.5.3: Relative risk of climate change on CVD in Osaka Prefecture in 2050.

4.5.4. Burden of climate change

The burden of climate was calculated from the change in the DALY /100,000 population rate (DALY rate). For Osaka Prefecture, the burden of CVD due to climate change was projected to increase by an average of 16.87 DALY/100,000 by 2050. The burden of meteorological DRIs due to climate change was projected to increase by an average of 0.65 DALY/100,000 by 2050 (Table 4.5.4).

Table 4.5.4: The burden of climate change on CVD and meteorological DRIs in Osaka Prefecture in 2050.

Health Outcome	Baseline DALY /100,000	2050 DALY /100,000 *(RCP range)*	Burden of climate change (DALY /100,000) *(RCP Range)*
CVD	3,024.21	3,041.08 *(3037.62 – 3048.78)*	16.866 *(13.408 – 24.573)*
Meteorological DRI	2.554	3.199 *(3.169 – 3.264)*	0.645 *(0.615 – 0.710)*

The burden of climate change on CVD was estimated for each administrative zone in Osaka Prefecture. The range was 0-114.29 DALY/100,000, with a mean value of 16.10 DALY/100,000 and a standard deviation of 8.46. Areas in the extreme North, East and South of the region were projected to have the largest increase in the DALY rate, due to climate change (Figure 4.5.4). Due to the low population and rural location of the peripheral administrative zones in Osaka Prefecture, the maps were reproduced for the areas defined by the Ministry of Land, Infrastructure, Transport and Tourism (MILT) as urban (NLNI, 2016). This gave a more representative projection of the variations in CVD and the impact of climate change on the metropolitan area of Osaka Prefecture (

Figure 4.5.5). To further investigate the spatial variety in the impact of climate change on CVD in the Osaka metropolitan area, a Getis-Ord cluster analysis was performed, which identified hot spots of high and lower impact areas in the area (Figure 4.5.5).

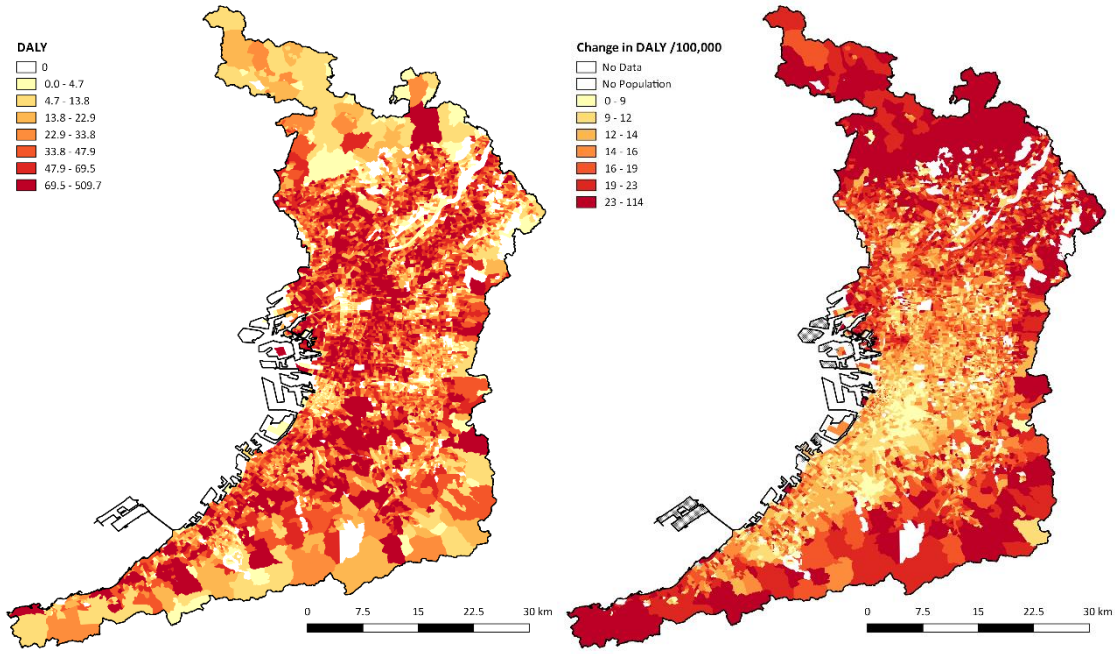

Figure 4.5.4: Total DALY estimates for 2010 (a), and projected change in the rate of DALY /100,000 in 2050 (b).

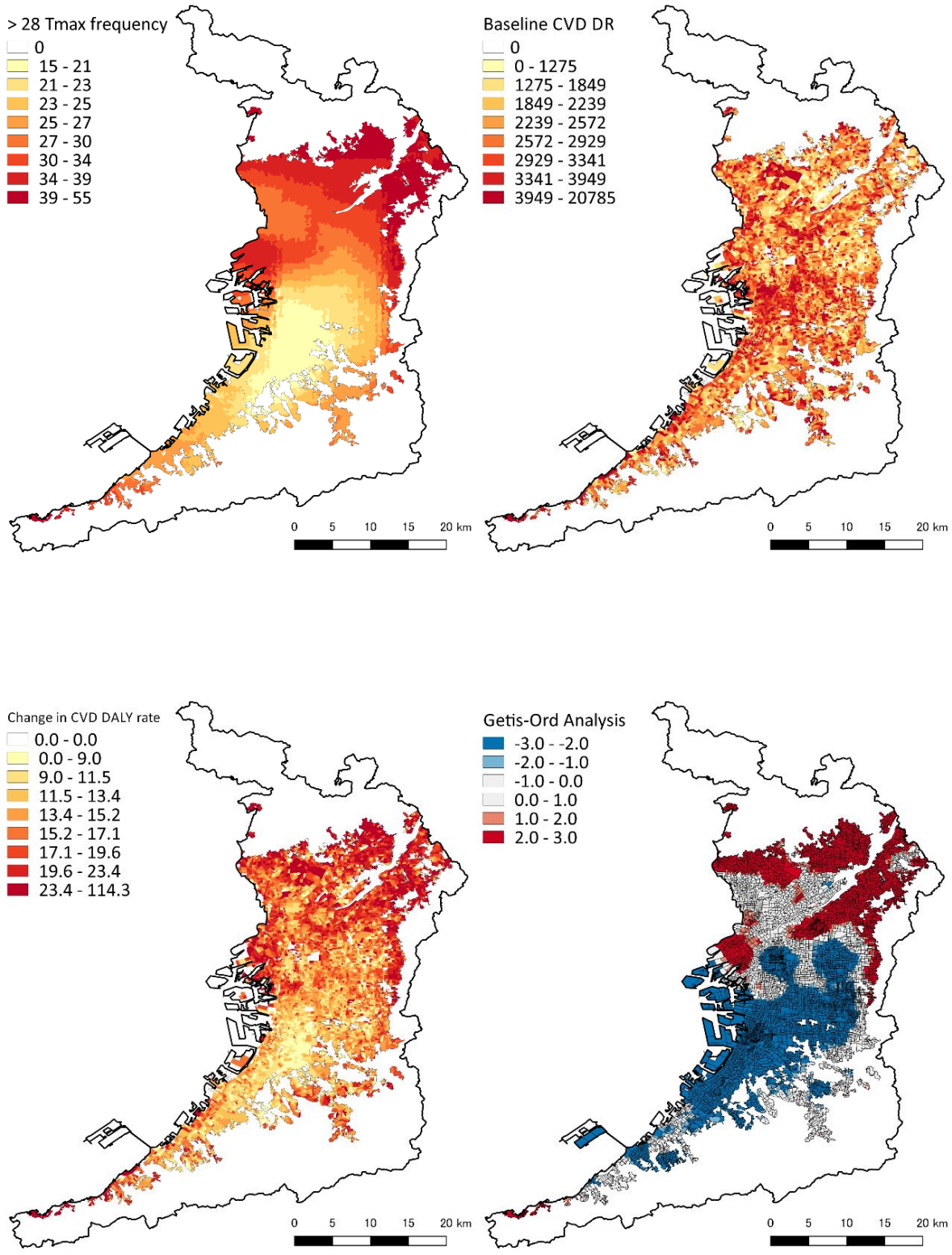

Figure 4.5.5: Urban area only visualisations of the degree of increased exposure to > 28 °C Tmax days (a), the baseline DALY rate of CVD (b). The projected change in DALY under climate change conditions (c) and a Getis-Ord cluster analysis of hot spots of high climate change impact (red) and low impact (Blue) areas within the Osaka Metropolitan Area (d).

4.6. Discussion

This study presents a methodology to calculate the impact of climate change on different human health outcomes. The study combines a method to calculate the relative risk of climate risk factors and the use of DALY, to provide an output on a common scale, which enables comparisons between risk factors and health outcomes and with other, non-climate related risks. The investigation into CVD risk due to climate change at a fine scale is a novel approach to assessing climate change health risks at a local level; combining demographics and climate outputs. The results indicate some of the uses and limitations of this approach.

4.6.1. Degree of exposure

The degree of exposure to the climatic risk factor influencing CVD prevalence (Tmax), is calculated based upon observations between average annual daily Tmax and the number of days above CVD Tmax risk thresholds (also based upon observations, in Takahashi et al. (2007)). The linear relationship is strong (R^2 = 0.74 for Tmax > 28ºC), but the robustness of this exposure is dependent on the accuracy of climate models and the continuation of such a trend. Currently the frequency of days at the high end of the scale (Tmax > 37ºC) is very low, so it is difficult to predict whether the increase will continue to be linear. The findings do, however, project an increasing trend in exposure to temperatures above the risk threshold for the region (Figure 4.5.1.2). The highest current and future exposures are situated in a low-lying, inland, urban areas, within the Osaka metropolitan area, which would indicate the influence of the Urban Heat Island (UHI) effect (Macnee and Tokai, 2016). The shift of the highest exposure to the North East, could be explained by changes in atmospheric circulation projected by the climate model. The temperature in Osaka City is influenced by sea-breezes (Masumoto, 2009), so a change in the pattern of these could cause a shift in the exposure to high temperatures.

A relationship between annual precipitation and the number of > 50 mm/hr events in Japan was identified (R^2 = 0.39), which was used as an extrapolation method for the projections. This method of predicting future extreme events from observed trends was proposed by Campbell-Lendrum et al. (2007). The difficulty in linking the physics of extreme precipitation events to climate change (Cutter et al. 2012) means that this statistical extrapolation method is applicable, as it is based on observed values. Data availability of extreme precipitation events for this study was limited to the whole of Japan (JMA, 2016b). Statistical downscaling of national values to Osaka Prefecture, therefore, increased the uncertainty of the exposure projection. The lack of data at a local level for extreme events has been listed as a major issue for climate change risk management (Cutter et al. 2012), and is further highlighted in this study.

4.6.2. Death rate projections

The death rate due to CVD in 2050 was projected based on the expected increase in the frequency days above two threshold Tmax values (28ºC and 32ºC). The relative risk (1.006) due to climate change between the baseline and future climate is comparable to previous studies that have been conducted at a larger scale (1.01 for developed countries: Campbell-Lendrum et al. 2007; McMichael et al. 2003). A caveat to the relative risk projection is that this study does not account for human adaptation to increasing temperatures. The fact that different regions are found to have different excess death thresholds (Campbell-Lendrum et al. 2007) and relative risk ratios (Basu et al. 2003), suggests that humans have an adaptive capacity to changing climates. However, this capacity has not been conclusively quantified, meaning further research is required to account for adaptation. One method is proposed by Honda et al. (2013), which suggests using the 84th percentile Tmax as the threshold above which excess deaths occur. This approach could be incorporated into the framework presented in this study to provide projections that account for natural adaptation to climate change.

The death rate due to CVD is slightly below the average CVD death rate for Japan (Table 4.5.2), which means that the death rate estimates for the combined total of the administrative zones in Osaka Prefecture is overestimated by a factor of 1.13. This is a limitation due to data availability of CVD deaths by age group and sex at the smallest scale. The assumption had to be made that the death rate by age group and sex was the same for Osaka Prefecture as Japan. The death rate of each zone is based on the demographics from which CVD mortality is calculated, so the resulting maps provide a visualisation of the relative vulnerability. Figure 4.5.3 indicates that the relative risk is higher in the North East of the prefecture. The distribution is different to the exposure distribution in Figure 4.5.2, because it accounts for the population demographics and estimated baseline death rate. The relative low risk area in the central southern area of the prefecture can be attributed to the shift, projected by the climate model, of the highest exposure areas to the north east. The low risk area, therefore, is projected to experience a smaller relative increase in exposure to Tmax values above current levels.

The relative risk of meteorological DRIs is estimated to be 1.263. This shows a larger relative increase than climate change associated CVD risk, although the actual death rate is much lower. This estimate falls within the range predicted for developed countries by McMichael et al. (2003). The caveat for this projection is that the death rate is statistically downscaled to Osaka Prefecture based upon the ratio of the number of DRI hospitilisations in 2002, 2005 and 2008 between Osaka Prefecture and Japan.

4.6.3. Burden of climate change

The burden of climate on CVD in 2050 (16.866 DALY/100,000) is projected to be much larger than that of meteorological DRIs (0.654 DALY/100,000), despite the relative risk being higher. This is due to the larger baseline impact (Table 4.5.4). Based on the projections made in this model, the impact of climate change on CVD will be very small compared to the current DALY rate. However, these

projections do not include changes in the population structure by 2050. The proportion of people > 65 years old is projected to continue increasing (NIPSSR, 2002), meaning that more people will be vulnerable to climate change induced CVD in the future (Campbell-Lendrum et al. 2007). The purpose of this study was solely to isolate the change in climate, however, projected changes in population could be incorporated into the methodology. The burden of climate on Meteorological DRIs is projected to remain small, but the relative risk is higher than that for CVD in Osaka Prefecture (Table 4.5.4). Assumptions had to be made, due to the lack of prefecture and sub-prefecture level data. Estimates of the impact of extreme events could be improved with continuous fine scale recording of event occurrence, severity and health impacts (Cutter et al. 2012).

Regarding the administrative zone projections of climate change related CVD risk, the projections indicate that in terms of DALY rate, the peripheral areas of the prefecture will experience the largest impact (Figure 4.5.4). It must be noted that these areas generally have a much lower actual burden of CVD than the central areas of the prefecture, due to their rural setting and much smaller population (E-Stat, 2016; Figure 4.5.4). These zones also have a higher percentage of elderly people (e-Stat, 2016), meaning that their vulnerability to CVD is higher than the more central, urban zones. Due to the low population of the peripheral areas, an analysis of the MLIT defined metropolitan area was conducted. When the results are mapped for the urban area of Osaka Prefecture only, the Getis-Ord cluster analysis identified hotspots with the strongest burden from climate change. These hotspots are concentrated towards the North East of the urban area, with smaller concentrations in the west and immediately south of the city centre (Figure 4.5.5). These areas generally correspond to the locations with the highest projected increase in exposure to temperatures above the risk thresholds (Figure 4.5.1; Figure 4.5.5). The differences in the distribution of the burden hotspots and the exposure maps indicate that although the exposure factor contributes highly to the spatial variation of the impact of climate change on CVD, the underlying vulnerability to CVD also influences the burden (Figure 4.5.5). For instance, the area to the south of the city centre (Nishinari Ward) is acknowledged as the most socially vulnerable area in Osaka Prefecture (Tabuchi et al. 2012). These results underline the comprehension that climate change impacts are dictated by both exposure and vulnerability (Field et al. 2014), as this particular area of the city is not projected to have a large increase in exposure compared to areas to the north and east of the urban area. It also highlights the requirement of impact assessments to be carried out at a high resolution, because these features, influencing distribution, only become apparent when analysed at a very small scale. This study is limited by data availability at the smallest scale. The accuracy of the results depends on assumptions made in downscaling data and in the calculation of the climate-response variables. Basing future estimates on robust observed relationships is important for applicability to real world situations.

4.7. Conclusion

This study proposes a novel approach to projecting the impact of climate change on health outcomes, by combining the relative risk of climate change with DALYs at a fine scale. The impact of climate change on two different health outcomes (CVD and meteorological DRIs) was assessed for Osaka Prefecture, with a finer scale assessment of CVD conducted. The burden of climate change in 2050 was calculated to be 16.866 DALY/100,000 population for CVD and 0.645 DALY/100,000 for meteorological DRIs. Therefore, the actual impact of climate change on CVD is judged to be higher, although the relative risk is lower (1.006, compared to 1.263 for meteorological DRIs). The mean impact of climate change on CVD for each administrative zone was calculated to be 16.10 DALY/100,000, with a maximum value of 114.29 DALY/100,000. The results were affected by a lack of data at the smallest scale, meaning that assumptions had to be made in downscaling data. The lack of any sub-prefectural level data about extreme precipitation events and meteorological DRIs also limited the local scale climate impact assessment to CVD. The results, therefore, provide an overview of the framework and highlight the relative risks of climate change on two health outcomes and of CVD at a very fine scale. The availability of continuous, accurate and fine scale data is important in generating robust results from this method. Acknowledging the caveat of data availability, the framework presented in this study is a logical and transferable approach to comparing climate change health impacts at a local level, on a common scale.

References

Basu, R. and Samet, J.M., 2002. Relation between elevated ambient temperature and mortality: a review of the epidemiologic evidence. *Epidemiologic reviews*, **24**(2), pp.190-202.

Cabinet Office, 2016. Government of Japan. *Available from: http://www.esri.cao.go.jp/jp/sna/menu.html (Japanese).*

Campbell-Lendrum, D., Woodruff, R., Prüss-Üstün, A. and Corvalán, C., 2007. Quantifying the health impact at national and local levels. *WHO Environmental Burden of Disease Series*, (14).

Cutter, S., Osman-Elasha, B., Campbell, J., Cheong, S.-M., McCormick, S., Pulwarty, R., Supratid, S. and Ziervogel, G., 2012. Managing the risks from climate extremes at the local level. In: Managing the Risks of Extreme Events and Disasters to Advance Climate Change Adaptation [Field, C.B., V. Barros, T.F. Stocker, D. Qin, D.J. Dokken, K.L. Ebi, M.D. Mastrandrea, K.J. Mach, G.-K. Plattner, S.K. Allen, M. Tignor, and P.M. Midgley (eds.)]. *A Special Report of Working Groups I and II of the Intergovernmental Panel on Climate Change (IPCC)*. Cambridge University Press, Cambridge, UK, and New York, NY, USA, pp. 291-338.

De Schryver, A.M., Brakkee, K.W., Goedkoop, M.J. and Huijbregts, M.A.J., 2008. Characterization Factors for Global Warming in Life Cycle Assessment Based on Damages to Humans and Ecosystems, *Environmental Science & Technology*, **43**(6), pp.1689-1695.

e-Stat, 2016. Portal Site of Official statistics of Japan. *Available from: http://e-stat.go.jp/SG2/eStatGIS/page/download.html (Japanese).*

Ezzati, M., Lopez, A.D., Rodgers, A., Vander Hoorn, S. and Murray, C.J.L., 2002. Selected major risk factors and global and regional burden of disease, *The Lancet*, **360**(9343), pp.1347–1360.

Field, C.B., Barros, V.R., Mach, K.J., Mastrandrea, M.D., van Aalst, M., Adger, W.N., Arent, D.J., Barnett, J., Betts, R., Bilir, T.E., Birkmann, J., Carmin, J., Chadee, D.D., Challinor, A.J., Chatterjee, M., Cramer, W., Davidson, D.J., Estrada, Y.O., Gattuso, J.-P., Hijioka, Y., Hoegh-Guldberg, O., Huang, H.Q., Insarov, G.E., Jones, R.N., Kovats, R.S., Romero-Lankao, P., Larsen, J.N., Losada, I.J., Marengo, J.A., McLean, R.F., Mearns, L.O., Mechler, R., Morton, J.F., Niang, I., Oki, T., Olwoch, J.M., Opondo, M., Poloczanska, E.S., Pörtner, H.-O., Redsteer, M.H., Reisinger, A., Revi, A., Schmidt, D.N., Shaw, M.R., Solecki, W., Stone, D.A., Stone, J.M.R., Strzepek, K.M., Suarez, A.G., Tschakert, P., Valentini, R., Vicuña, S., Villamizar, A., Vincent, K.E., Warren, R., White, L.L., Wilbanks, T.J., Wong, P.P. and Yohe, G.W., 2014 Technical summary. In: *Climate Change 2014: Impacts, Adaptation, and Vulnerability. Part A: Global and Sectoral Aspects. Contribution of Working Group II to the Fifth Assessment Report of the Intergovernmental Panel on Climate Change* [Field, C.B., V.R. Barros, D.J. Dokken, K.J. Mach,

M.D. Mastrandrea, T.E. Bilir, M. Chatterjee, K.L. Ebi, Y.O. Estrada, R.C. Genova, B. Girma, E.S. Kissel, A.N. Levy, S. MacCracken, P.R. Mastrandrea, and L.L.White (eds.)]. Cambridge University Press, Cambridge, United Kingdom and New York, NY, USA, pp. 35-94.

Fujibe, F., Yamazaki, N. and Kobayashi, K., 2006. Long-term changes of heavy precipitation and dry weather in Japan (1901-2004). *Journal of the Meteorological Society of Japan*, **84**(6), pp.1033-1046.

GBD, 2013a. Global, regional, and national incidence, prevalence, and years lived with disability for 301 acute and chronic diseases and injuries in 188 countries, 1990–2013: a systematic analysis for the Global Burden of Disease Study 2013 [Global Burden of Disease Study 2013 Collaborators, and others], *The Lancet*, **386**(9995), pp.743-800.

GBD, 2013b. Global Burden of Disease Study 2013 (GBD 2013) Results by Location, Cause, and Risk Factor. Seattle, United States: *Institute for Health Metrics and Evaluation (IHME)*, http://ghdx.healthdata.org/global-burden-disease-study-2013-gbd-2013-data-downloads-full-results.

GHDx, 2016. GBD Results Tool, *Global Health Data Exchange*. http://ghdx.healthdata.org/gbd-results-tool.

Haines, A., Kovats, R.S., Campbell-Lendrum, D. and Corvalán, C., 2006. Climate change and human health: impacts, vulnerability and public health. *Public health*, ***120***(7), pp.585-596.

Hijmans, R. J., Cameron, S.E., Parra, J.L., Jones, P.G. and Jarvis, A., (2005). Very high resolution interpolated climate surfaces for global land areas. *International journal of climatology*, **25**(15), pp.1965-1978.

Honda, Y., Kondo, M., McGregor, G., Kim, H., Guo, Y.-L., Hijioka, Y., Yoshikawa, M., Oka, K., Takano, S., Hales, S. and Kovats, R.S., 2014. Heat-related mortality risk model for climate change impact projection, *Environ Health Prev Med*, **19**, pp.56–63.

IPCC, 2012. Managing the Risks of Extreme Events and Disasters to Advance Climate Change Adaptation. *A Special Report of Working Groups I and II of the Intergovernmental Panel on Climate Change* [Field, C.B., V. Barros, T.F. Stocker, D. Qin, D.J. Dokken, K.L. Ebi, M.D. Mastrandrea, K.J. Mach, G.-K. Plattner, S.K. Allen, M. Tignor, and P.M. Midgley (eds.)]. Cambridge University Press, Cambridge, UK, and New York, NY, USA, 582 pp.

JMA, 2016a. Disaster Prevention Report, Japan Meteorological Agency. *Available from: http://www.data.jma.go.jp/obd/stats/data/bosai/report/index_1989.html (Japanese).*

JMA, 2016b. Heavy Rain Trend, Japan Meteorological Agency. *Available from: http://www.jma.go.jp/jma/kishou/info/heavyraintrend.html (Japanese).*

JMA, 2016c. Past weather data download, Japan Meteorological Agency. *Available from: http://www.data.jma.go.jp/gmd/risk/obsdl/index.php (Japanese).*

Knutson, T.R., McBride, J.L., Chan, J., Emanuel, K., Holland, G., Landsea, C., Held, I., Kossin, J.P., Srivastava, A.K. and Sugi, M., 2010. Tropical cyclones and climate change. *Nature Geoscience*, **3**(3), pp.157-163.

Lim, S.S., Vos, T., Flaxman, A.D., Danaei, G., Shibuya, K., Adair-Rohani, H., AlMazroa, M.A., Amann, M., Anderson, H.R., Andrews, K.G. and Aryee, M., 2013. A comparative risk assessment of burden of disease and injury attributable to 67 risk factors and risk factor clusters in 21 regions, 1990–2010: a systematic analysis for the Global Burden of Disease Study 2010. *The lancet*, **380**(9859), pp.2224-2260.

Macnee, R.G.D., Tokai, A., 2016. Heat wave vulnerability and exposure mapping for Osaka City, Japan, *Environment Systems & Decisions*. doi:10.1007/s10669-016-9607-4.

Masumoto, K., 2009. Urban heat island in Osaka city distribution of air temperature and west bulb globe temperature. *In The Seventh International Conference on Urban Climate, 29 June-3 July 2009.*

McMichael, A. J., Campbell-Lendrum, D. H., Corvalán C. F., Ebi, K. L., Githeko, A. K., Scheraga, J. D. and Woodward, A., 2003. *Climate change and human health: risks and responses*, World Health Organisation, Geneva.

McMichael, A. J., Woodruff, R. E. and Hales, S., 2006. Climate change and human health: present and future risks, *The Lancet*, **367**(9513), pp.859-869.

Murray, C.J., Vos, T., Lozano, R., Naghavi, M., Flaxman, A.D., Michaud, C., Ezzati, M., Shibuya, K., Salomon, J.A., Abdalla, S. and Aboyans, V., 2013. Disability-adjusted life years (DALYs) for 291 diseases and injuries in 21 regions, 1990–2010: a systematic analysis for the Global Burden of Disease Study 2010. *The lancet*, **380**(9859), pp.2197-2223.

NIPSSR, 2002. Population Projections for Japan: 2001-2050 With Long-range Population Projections: 2051 - 2100 January, 2002 National Institute of Population and Social Security Research. *Available from: http://www.ipss.go.jp/pp-newest/e/ppfj02/ppfj02.pdf.*

NLNI, 2016. National Land Numerical Information download service. *Available from: http://nlftp.mlit.go.jp/ksj/jpgis/jpgis_datalist.html (Japanese).*

OPG, 2016. Osaka Prefectural Government. *Available from: http://www.pref.osaka.lg.jp/toukei/d-osaka/index.html (Japanese).*

Patz, J. A., Campbell-Lendrum, D., Holloway, T. and Foley, J.A., 2005. Impact of regional climate change on human health, *Nature,* **438**, pp.310-317.

Salomon, J.A., Vos, T., Hogan, D.R., Gagnon, M., Naghavi, M., Mokdad, A., Begum, N., Shah, R., Karyana, M., Kosen, S. and Farje, M.R., 2013. Common values in assessing health outcomes from disease and injury: disability weights measurement study for the Global Burden of Disease Study 2010. *The Lancet*, **380**(9859), pp.2129-2143.

Sugimoto, S. and Ueno, K., 2012. Role of Mesoscale Convective Systems Developed around the Eastern Tibetan Plateau in the Eastward Expansion of an Upper Tropospheric High during the Monsoon Season, *Journal of the Meteorological Society of Japan*, **90**(2), pp.297–310, DOI:10.2151/jmsj.2012-209.

Tabuchi, T., Fukuhara, H. and Iso, H., 2012. Geographically-based discrimination is a social determinant of mental health in a deprived or stigmatized area in Japan: A cross-sectional study. *Social Science & Medicine*, **75**(6), pp.1015-1021.

Takahashi, K., Honda, Y. and Emori, S., 2007. Mortality Risk from Heat Stress due to Global Warming, *Journal of Risk Research*, **10**(3), pp.339-354.

Van Vuuren, D.P., Edmonds, J., Kainuma, M., Riahi, K., Thomson, A., Hibbard, K., Hurtt, G.C., Kram, T., Krey, V., Lamarque, J.F. and Masui, T., 2011. The representative concentration pathways: an overview. *Climatic change*, **109**, pp.5-31.

VSJ, 2016. Portal Site of Official Statistics of Japan. *Available from: http://www.e-stat.go.jp/SG1/estat/NewListE.do?tid=000001028897.*

World Health Organisation, 2012. *Atlas of health and climate*. World Health Organisation.

Chapter 5. Conclusion and future recommendations

Quantification of climate change impacts on human health is an important assessment method that enables the identification of key risks and conclusions to be drawn on the effectiveness of different responses (Campbell-Lendrum et al. 2007). The global span of climate change and the large variety of risk factors that is possesses makes quantification extremely important, but also poses difficulties. This study was designed to investigate current issues, propose solutions to these issues and develop a framework to quantify climate change impacts on health at a local scale, using a common unit.

At the beginning of this thesis, four key objectives were formulated to address the research question surrounding quantification of climate change on human health: (1) understand the impact of climate on infectious disease prevalence in two East Asian countries: Japan and the Republic of Korea; (2) determine the variables affecting vulnerability to heat waves and map these at a local level; (3) develop a transferrable framework to quantify the impact of climate change on health outcomes at a local and regional scale, using a common unit; (4) provide recommendations for policy makers and researchers in this field and suggest future research advancement requirements and direction. The thesis structure is formulated around these objectives with each one forming a chapter, following on from the introductory Chapter 1.

Chapter 1 reviews the impacts of climate change on human health and the pathways that these impacts follow. An overview of climate change on a global scale is provided, followed by a more specific review of the potential impacts faced by Japan. This overview chapter provides basis for the requirements of this research and introduces the structure of the study. Chapter 2 explores the impact pathway from anthropogenic induced climate change to an infectious disease outcome (malaria). This chapter provides information on the issues with modelling the impact of climate change on infectious diseases and provides a quantification method to analyse comparative risk between regions. Chapter 3 introduces a methodology to assess human health risk from heat waves at a local scale, combining vulnerability and exposure. The results produced a quantified risk ranking specific to the study region, using a transferrable methodology. Chapter 4 provides a framework for quantifying local and regional scale human health impacts of climate change, using a common unit (DALY). This chapter will discuss the contributions of the whole study to the scientific and policy making sectors and outline the current limitations to quantification at a local scale. The three chapters that form the body of this research aim to provide risk assessment frameworks for different risk factors relating to climate change. The limitations and difficulties identified in Chapters 2 and 3 are somewhat addressed in Chapter 4. The final chapter, Chapter 5, coalesces the findings of the previous chapters and draws conclusions from

each chapter and the combined findings of the three study chapters. Research and policy recommendations are discussed as a final conclusion to the study.

5.1. Quantification of climate change impacts on infectious diseases

5.1.1. Climate as a driver of malaria transmission in a re-emerging risk area

A comprehensive assessment of malaria transmission and climatic factors was conducted in the Republic of Korea, a country where malaria has re-emerged in the past 25 years. No significant trend was found between the climate and malaria prevalence at an annual level. However, when investigated at a country-wide monthly scale, minimum and maximum temperature, precipitation and relative humidity combined described 11.1% of the variance in malaria transmission. This trend became more pronounced at a regional scale, ranging from 35.5-76.2%. This study therefore indicates that currently annual climate is not a limiting factor of malaria transmission in the region. It did, however, highlight the highly seasonal nature of malaria transmission, meaning that the region is climatically vulnerable to a climate induced extension of the transmission season. Differences in transmission between the Republic of Korea, Democratic Republic of Korea and Japan identified health care and proximity to endemic regions as the main limiting factors of malaria transmission in the region

5.1.2. Base reproduction rate model

Based upon the identified risk of increased malaria transmission in a warmer climate, but a lack of data at an annual level, this study proposed the use of a biological model to predict the change in the length of the transmission season in the study region. The model projected an increase in the number of months that the climate was suitable for malaria transmission in all areas. When added to the findings of the quantitative study, this provides an insight into the potential for malaria transmission under climate change scenarios. This model provides a cost effective tool to comparatively assess the climatic suitability of an area for malaria transmission.

5.1.3. Limitations and applicability

The model proposed in this study should be considered as the first step towards assessing malaria risk due to climate change. The output is an indicator of the climatic suitability of an area to malaria transmission, but it is not equitable to a real world quantified risk. Other factors, such as the population density of vectors and susceptibility of the human population to transmission must be considered to develop a physical quantification of risk. Currently, information concerning vector density is not available in most regions, which suggests that this should be considered as a future direction of study. The model does, however, have two useful outcomes. Firstly, it provides an overview of climatic suitability for malaria transmission, which can be used to identify how the risk season from imported

cases of malaria may be extended. Secondly, the uncertainty identified in the model gives us a clear idea of which factors in the model are the most influential. This helps guide the direction of future study towards developing modelling techniques that enable the uncertain variables to be quantified more robustly.

5.1.4. Recommendations

This study highlighted the requirement for two key areas of further study. The first is in improving the accuracy of the biting rate of malaria vectors (ma) in the base reproduction rate model. This can be done by researching vector population density, specifically for different habitats. This would enable population, habitat and climate to be combined, to produce a more comprehensive risk projection. The second area is into the other risk factors associated with malaria. This includes vector habitat (as mentioned above) and health care risk factors. Addressing these two areas would greatly advance understanding in this topic. As is, the model could be recommended for use by authorities concerned about re-emerging malaria (incidences of which have occurred in several countries). It quickly and easily identifies the most climatically suitable areas for transmission, which can provide the basis for a full investigation that includes the other risk factors.

5.2. Human vulnerability and exposure to heat waves

5.2.1. Applicability of a heat wave vulnerability index to Japan

This was the first study to investigate vulnerability to heat waves in Japan at a local scale. The composition of such an index was adjusted to account for unique demographic characteristics of Japan. The methodology, adapted to Osaka City, Japan, identified three key indicators of heat wave vulnerability: (1) socioeconomic – age, employment and education; (2) social isolation – percentage of people living alone and percentage of > 65-year-old people living alone; (3) physical conditions – population density and lack of green space. The inclusion of density and lack of green space as indicators contributes to the usefulness of the output, as these specific vulnerability factors require different counteractions to the other two indicators (urban planning as opposed to public health measures). Mapping this indicator separately provides a clear indication of where urban planning initiatives could be targeted to counteract the impact of heat waves (Chapter 3: Figure 3.1.4.1) The result is useful in comparing vulnerability distribution in a Japanese city (Osaka City) to cities in other countries. A low risk area identified in the CBD area is a unique feature of the vulnerability distribution of Osaka City compared to previous vulnerability studies, which highlights the requirement for location specific studies to be conducted.

5.2.2. Fine scale heat exposure assessment

An assessment of heat exposure for an entire summer season at a local scale was conducted. Previous heat wave studies have utilised satellite derived land surface temperatures or monthly level temperature assessments. This study used daily and hourly recordings to map the level of exposure to extreme temperatures at a very fine temporal scale. The benefit of this method is that the actual time that a particular area is exposed to temperatures above a heat wave threshold can be identified accurately. It also enables the diurnal pattern of exposure distribution to be mapped. The key contribution of this assessment is that it highlights the shift in exposure to heat between daylight hours and night-time. Studies using Monthly totals and satellite images fail to identify this change. This study identified a pronounced diurnal shift in exposure in the study area, which highlights the need for fine temporal scale assessments to be conducted to maximise heat wave risk assessments.

5.2.3. Combined exposure and vulnerability analysis

This assessment indicated that in the study region, the most vulnerable area was located in an area of high night time exposure to ambient heat. This finding became apparent after combining the vulnerability distribution with the exposure distribution. The apparent risk hot-spot would not have been as clearly identified had a courser (temporal or spatial) assessment been conducted. This emphasises the usefulness of conducting vulnerability and exposure assessments at a fine scale. As vulnerability and exposure to heat waves have different countermeasure approaches (public health measures and urban planning respectively; Milan and Creuzig, 2015), a combined study provides information that can help to identify which type of countermeasure would be most effective in each area.

5.2.4. Limitations and recommendations

This study is limited by the availability of health information at the smallest scale. Records of hospitilisations and underlying health incidences at a neighbourhood scale would add to the vulnerability index applicability and enable it to be more robustly verified. Data such as ambulance call-outs and mortality could be used in future studies to strengthen the vulnerability index (Wolf and McGregor, 2013). A further limitation of this study is that it focuses on a risk factor rather than specific health outcomes. This makes it difficult to compare the results to other health end points. This limitation is in part due to the difficulty of attributing many specific deaths to heat waves, as there are a number of end point deaths that may be triggered by heat waves (Reid et al. 2009). This limitation is in part addressed in Chapter 4, by providing a method to calculate the impact of hot days on a specific health outcome.

Utilising this method of combining vulnerability assessments and exposure assessments would be recommended to policy makers, as it is a cost effective method of clearly identifying risk areas and exposure hot spots. The output can be used in conjunction with field studies to determine the most

effective control measures against heat wave risks to pursue. Recommendations for further study are to include fine scale health data in the vulnerability assessment, which will also enable full validation. It will also be useful to quantify the impact of heat waves in climate change scenarios, by investigating the impact pathways from climate to heat waves and specific health outcomes. One particular methodology is proposed in Chapter 4.

5.3. Determining the burden of climate change on human health at a local scale

5.3.1. A framework for quantifying the impact of climate change on health outcomes using a common unit.

This study presents a worked framework for quantifying the impact of climate change on different health outcomes at different scales, using DALY as a common unit. The whole world is exposed to climate change; however, the level of exposure to different climate related risk factors and the underlying vulnerability of a population is determined by various local and regional scale factors (McMichael et al. 2006). For this reason, there is a requirement for frameworks to be developed to provide a methodology for quantifying human health impacts at a local scale, but with the possibility to directly compare the results. This study developed a framework for local scale quantification of health impacts by building on previous work (Campbell-Lendrum et al. 2007) and adding further steps to produce an output that quantifies different health risks in DALYs, a common unit. The importance of such a unit is paramount to effective climate change risk analysis, due to the complex impact pathways, different risk factors and varied underlying vulnerability. Decision makers are required to prioritise adaptation to and mitigation of health outcomes, such as cardiovascular disease and infectious disease. They may also be required to prioritise specific risk factors. The framework presented in this study enables risk factors and health outcomes to be assessed together as well as independently, providing a methodology that suits the requirements of two different approaches to risk assessment using the same methodology.

This study takes assessment of the impact of climate change to human health end points and considers the total baseline impact of each health impact from all risk factors. The additional benefit of this is that the portion of each health impact that is attributable to climatic factors and climate change is quantified in the context of the total risk. Not only can the impact of climate change be attributed, but this impact can be directly compared to all other risk factors contributing to certain health outcomes. Contextualising the risks of climate change is vital in informing policy decisions and also the perception of risk. Producing outputs that are directly comparable to other risk factors improves understanding of climate change risk in the context of general risk assessment. All policy decisions require justification.

Producing quantified values of risk in context provides clear justification for action and improves transparency in the decision making process.

5.3.2. Consideration of vulnerability

The framework developed in Chapter 4 is important in that it considers population vulnerability in addition to exposure. Let us consider heat related morbidity and mortality as an example. When considering future risk under climate change scenarios, it is important that the change in the frequency of high temperature days is projected. This provides us with information about how the exposure to potentially dangerous temperatures will change. However, unless we consider vulnerability, this information is limited in value. Different populations are adapted at different levels to heat (Campbell-Lendrum et al. 2007; Ezzati et al. 2002; Honda et al. 2014). The vulnerability of a population also depends on the demographics. For instance, people over the age of 65 are at greater risk to extreme heat than other age groups (Wolf and McGregor, 2013). Therefore, to calculate the actual health endpoint impact of climate change on heat related illness, such as cardiovascular disease, we need to know the baseline vulnerability. This study provides a method of including vulnerability in the form of an empirically identified threshold temperature, above which, heat related deaths increase. Underlying vulnerability is also included by considering the baseline death rate (specifically for this study, of cardiovascular disease deaths). By including these two factors affecting vulnerability, we can then project how future changes in exposure to climate risk factors will impact the population in a specific region. Continuing the example of heat related illness; by considering local scale vulnerability, we can project the actual impact of a climate change scenario on health. Furthermore, as vulnerability and exposure often have different adaptation approaches, including both in a quantified risk assessment can give indications as to which approach is likely to me more effective in each area of concern.

5.3.3. Local scale spatial analysis of climate change impacts

Impacts from climate change are felt most strongly at a local level (Tran et al. 2009). Despite this, the perception of climate change risk held by most lay people is that it is a global risk that will affect distant populations more than themselves (Leiserowitz, 2006). Risk mapping of climate change impacts is a useful tool for providing information about the spatial distribution of the impacts of climate change on people at a local level, that can help alter peoples' perception of the risk and encourage proactive countermeasures to the health risks. The complexity of climate related risks also requires spatial and local knowledge to be incorporated into climate change health risk assessments (Aalst and Burton, 2002). Attempts to map climate change impacts have been made at a local scale (McMichael et al. 2006; Tran et al. 2009). However, the human health impact of specific outcomes at a local scale has not been mapped. Chapter 4 demonstrates a method of using GIS to map climate change impacts on a specific health outcome (cardiovascular disease), using DALYs as a unit of measurement. This mapping technique provides valuable spatial information about climate change risk, and highlights the variations

in vulnerability, exposure and overall risk. Mapping climate change risks enables quick and easily identification of risk areas, and the integration of local knowledge to greater understand the nature of the risk. This provides an additional aspect to risk assessment and means that decision makers can investigate risks quantitatively and integrate this with their knowledge of local areas, by pinpointing risk hot spots (Tran et al. 2009). Chapter 4 Demonstrates how even the risk of chronic illnesses impacted by climate change is highly spatially variable at a local level. This has implications for the application of control measures at a local scale, as spatial variety suggests that targeted action will likely be an efficient form of countermeasure. As this is the first study to map the impact of climate change on cardiovascular disease at this scale, it is not currently possible to draw comparative conclusions from other studies about the distribution of impacts in an urban area. After future studies on this scale are conducted, direct comparisons in both the overall projected impact and the local level spatial distribution will shed light upon the local scale variations between locations in different climatic and topographical zones, which will provide insights into which countermeasures will be most effective in different regions.

5.3.4. Applicability of DALY to adaptation planning

The concept of DALY is highly applicable to climate change adaptation planning, because it has the capacity to calculate minor and major individual health impacts, using the same unit. Many of the impacts felt by humans are negative, but not fatal. For instance, an increase in the spread of infectious disease will impact human health, but not all cases result in deaths. DALY also enables different risk factors to be compared. Extreme events such as storms and floods cause sometimes fatal human health impacts on a large scale, however, they are relatively infrequent. Rising average summer temperatures have initially less obvious health impacts, however, evidence exists of the large impact on health that rising summer temperatures has (Ezzati et al. 2002; Honda et al. 2013; Takahashi et al. 2007). In terms of adaptation planning, DALY enables local, national or regional authorities to calculate the current and projected impact of climate on human health of fundamentally different risk factors such as extreme events and rising summer temperatures in a comparative context (McMichael et al. 2006). This comparative aspect is important in enabling authorities to designate resources to adaptive measures that are appropriate for each individual area. A further benefit of using DALY is the fact that it can be used to compare climate specific risk factor impacts on human health with risk factors from other sources, such as chemical exposure, lifestyle, physiology and other environmental impacts. Therefore, DALY provides a tool to not only prioritise adaptation planning within the sphere of climate change research, but in the context of risk research in general. If applied correctly, with robust data, DALY can provide a unit by which climate change adaptation planning measures can be prioritised internally (i.e. which climate change adaptation measures are the most important for a specific region or locality) and externally (i.e. how important are climate change adaptation measures compared to other risk management measures).

As identified by the research conducted in Chapter 4, there are limitations of the application of DALY to adaptation planning, particularly regarding data availability and collation. The limitations are centred around the requirement for assumptions to be made, when calculating DALY. The largest area of uncertainty in the method is currently in the determination of disability weights for the calculation of Years Lost due to Disability (YLD). Disability weights were initially calculated from value judgements of medical professionals on the comparative severity of individual diseases or injuries, with values ranging from 0 (no negative impact) to 1 (equivalent to death). This leaves some degree of subjectivity to the weightings, although the WHO conducted a large scale empirical study in 2010 to further quantify the weightings (Solomon et al. 2013). Future research in this area will continue to quantify the disability weightings and remove subjectivity, but it is an ongoing process, and one that should be acknowledged when using DALY. Another limitation of DALY in climate change studies is the calculation of relative risk ratios for climate scenarios and health impacts. Data availability limits the number of empirical studies into climate change and human health impacts (Campbell-Lendrum et al. 2007). Furthermore, relative risk ratios calculated from past data generally produce linear or simplistic relationships between climate and health outcomes. As climate change progresses, there is the possibility of currently unknown thresholds being reached, which may undermine relative risk ratios calculated from past data (Costello et al. 2009). The uncertainty around future climate projections can be somewhat mitigated by the IPCC approved RCP scenarios and by using ensemble modelling, but no objective threshold has been defined as when a dangerous global climate change threshold will be reached (Collins et al. 2013). Therefore, research in this area is limited to the current capabilities of climate modelling. This caveat, however, applies to all climate change impact research, not just that involving DALY.

5.3.5. Limitations and recommendations

The key limitation of the method of climate change human health impact quantification proposed in Chapter 4 is the availability of data at the smallest scale. The method for calculating the climate-response values is based upon observed values. Thus, any data gaps influence the reliability of the climate-response value. In addition to this, data on incidence of climate related diseases at a baseline level and suitable spatial scale is required to build an accurate understanding of the current risks. The accuracy of current risk assessments also influences the uncertainty surrounding future impact projections (Campbell-Lendrum et al. 2007). Currently, the application of such a methodology to policy making should be advisory, due to the data gaps and uncertainties. However, the framework itself enables policy makers and researchers to build up an inventory of the relevant available data. This is useful, as data gaps are identified and can be incorporated into the methodology as explicitly quantified uncertainties, as recommended by Smith et al. (2014).

Specifically, for the case examples used in Chapter 4, data at the smallest administrative level for cardiovascular disease incidence and mortality would greatly improve the applicability of the fine scale

spatial analysis to formal policy making practice. To address the issue with uncertainty about the level of adaptation that a population will undergo to warmer temperatures, different adaptation scenarios can be developed. An example that can be easily added to the model framework is suggested by Honda et al. (2014), where percentage adaptation to climate change scenario temperatures is used as a base for adaptation scenarios. For example, Honda et al. suggested 0%, 50% and 100% adaptation as scenarios to account for uncertainty. A further, more detailed assessment of the risk of disaster related injuries related to flooding events could be conducted by utilising GIS flood risk mapping to identify zones at risk of flooding from specific rainfall events (Appendix 3.12). This, in addition to higher resolution data on the location of injuries from flooding would improve the local level applicability of the assessment.

For all projects utilising this method, it is recommended that the maximum amount of available data at the smallest available scale be used to calculate the climate-response function and the baseline impact value. The climate-response function is highly dependent on local vulnerability and exposure. For example, Basu and Samet (2002) reviewed the literature on heat related mortality and found 98 separate studies (1970-2002) with a range of different exposure-response functions, in different locations around the world. For this reason, it is imperative that the climate-response function for a particular area be based on observed data in that specific region. The framework presented in Chapter 4 outlines the structure that studies should follow, but recommends that the values used must be specific to the study region. Another finding from Basu and Samet (2002), that this study addressed is that the endpoint that previous studies used and the specific risk factor analysed was not uniform, so comparisons between studies are difficult. This method proposes daily maximum temperature as the most applicable method in terms of determining an exposure-response function and converting climate model outputs into a useable output. It is a straightforward process to convert future mean temperature outputs into daily frequency based on present day observations. Additionally, the availability of daily maximum temperature values is widely available in most populated areas, meaning that it is likely that an exposure-response variable can be established in more areas. For studies that aim to project the impact of climate change on health impacts for a time period beyond 2050, it is strongly recommended to run the future projections using different RCP scenarios, to account for the increased uncertainty in climate model projections and divergence in the scenarios beyond this time period (van Vuuren et al. 2011).

Regarding disaster related injuries, it would be beneficial to have a standardised approach to recording the event type, location, cause of death/injury and age/sex of victims of meteorological disasters. This would improve understanding of how and when disaster related injuries occur and may shed some light on the characteristics of more vulnerable population types and locations. The assessment in Chapter 4 relied solely on the number of deaths and injuries per event in Japan. More information about the circumstances and location of each event would enable more detailed projections about the climate-event-health impact relationship and would help to reduce uncertainty.

5.4. Concluding remarks and recommendations

This research pursued a case based assessment of methods for quantifying the impact of climate change on human health at a local and regional scale. The major research problem that it combatted was the lack of a transferrable framework for assessing human health impacts of climate change at a local scale, allowing for comparisons between risk factors and health outcomes. The research also sought to produce a quantified output of risk that could be placed in the context of risk assessment in general. Two methodologies for assessing widely different climate change risk factors were proposed, enacted and reviewed. The findings of these two methodologies were considered and an additional methodology, that tackled the full research question, was presented. Worked examples of two different health outcomes from two separate climate risk factors were used to demonstrate the methodology and a standard, transferrable, framework was proposed. The findings of the studies produced two concurrent categories of findings. The first category of findings related to the applicability of each method to real world scenarios and provided insight into the limitations. The second category of findings was based on the outputs of the three methods proposed and drew localised conclusions about what the results showed for each projection. The concurrent findings demonstrate the flexibility of the approaches proposed, as they provide insight into the implications of the outputs as well as reviewing the methods employed.

The process of determining a framework to quantify climate change health impacts at a local level on a common scale was evolutionary, with each research chapter building on discoveries and limitations from the previous ones. This approach leaves several pathways open for further research to improve the methodologies presented in this research (Figure 5.4). These pathways have been opened up in equal part due to findings from the studies and limitations with the approaches used. The recommended further research pathways identified in Figure 5.4 are not exclusive, but they encompass three major areas that the author sees as open to further study that would address the limitations of this research and also develop the findings further into aiding and informing policy decisions and academic research. The recommendations of future research direction are addressed below. The first selection of recommendations are derived from the limitations of the research and aim to combat these. Specific reference is made to a number of recommendations that apply specifically to Japan, based upon the findings of the three studies conducted in this region. The recommendations provide guidance on how to reduce uncertainty and improve empirical based studies into climate change impacts on human health. The second group of recommendations build upon the findings of the research and detail new areas that this research exposes in the context of climate change risk assessment. The aim of these recommendations is to direct future study with the aim of advancing understanding in this field and developing highly applicable methodologies for climate change risk assessment.

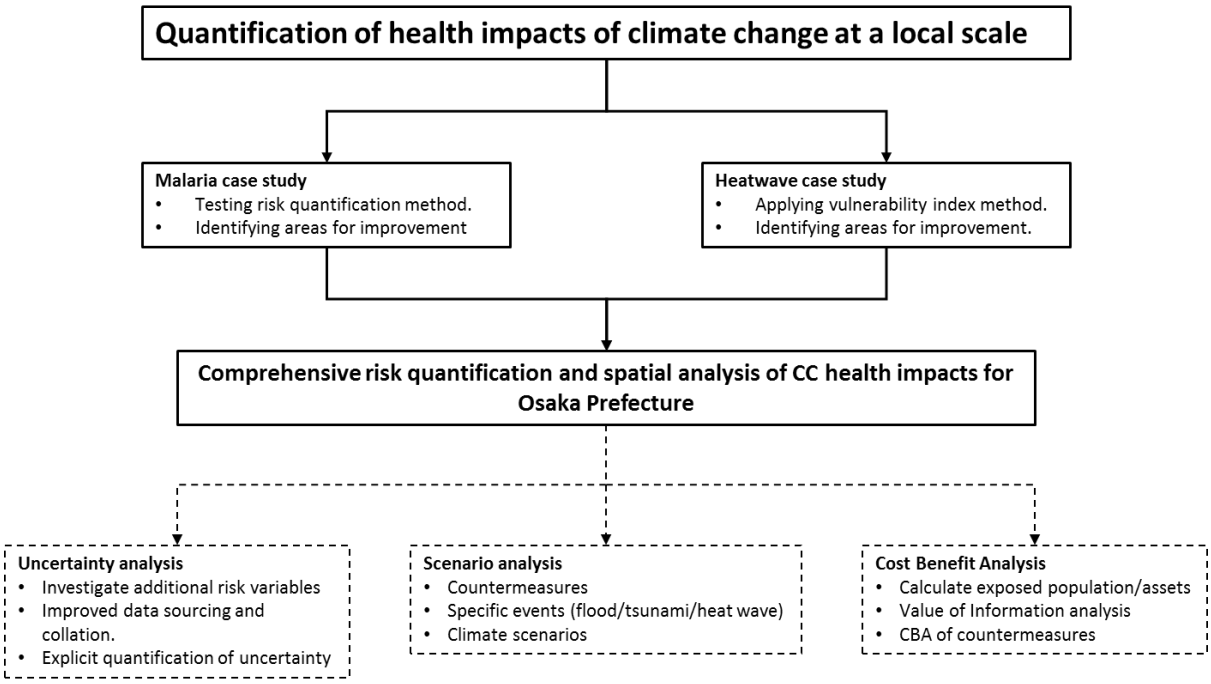

Figure 5.4.1: Schematic of the research flow and further areas of study that can build on the findings of this project (dashed boxes).

5.4.1. Recommendations to address limitations at the current stage of research

A key issue with all risk research is uncertainty, and how it is addressed (Morgan and Henrion, 1990). In order to be fully incorporated into effective risk policy, assessments should explicitly acknowledge uncertainty, and quantify it where possible. The studies in this research are exposed to uncertainty, and while this has been acknowledged and addressed in most cases, there is room for improvement. The following, are recommended areas for future research to tackle the remaining areas of uncertainty:

- The function determining vector biting rate in the malaria base reproduction rate model needs to be more explicitly linked to external factors, including land use, vector and human population density and health care capacity. Addressing this will enable the projection of the actual number of cases of malaria in a study area to be calculated (rather than the climatic suitability alone). Such a projection can then be verified against observed values, to produce a quantification of uncertainty.
- Vulnerability areas identified in the heat wave vulnerability study can be verified against incidences of heat related illness and mortality at a local scale. This requires access to daily medical/hospital data at a local level. Alternatively, data from ambulance callouts can be used to calculate the number of excess call outs on specific heat wave days.
- Development of a unified system of recording and storing health data at a local level, specifically relating to natural disasters would enable more detailed exposure-response functions to be developed. The more data that is available at the highest resolution and detail,

the easier it is to analyse and identify response variables. Some of the most difficult aspects of this study were presented by a lack of data, meaning more difficult methodological solutions had to be sought and larger assumptions made. Exposure-response variables are currently the most uncertain aspect of climate change health impact studies, so an increase in the availability of detailed standardised data will greatly advance the development of these key variables.

- Specifically, for Japan, steps should be made to record deaths and mortality linked to climatic factors in a single database at the finest scale possible. This should relate to all health endpoints that are affected by the climate, even if the link for a specific case cannot be identified. Information regarding the patient cause of death or diagnosis should be clearly documented alongside the categorised data to enable in depth investigations into climatic risk factors and health to be conducted. Such a database would provide an invaluable tool for conducting future climate change health impact studies. Ideally, all climate change health impact studies require accurate health and climate data on the same scale so that links via observed data can be established with the maximum robustness. A specific database storing information on mortality, morbidity, location, date and patient demographic data would be a major advancement in terms of how climate change and health is analysed in Japan and would enable it to be established as a world leader in this field of research. An amalgamated database, detailing census data down to the smallest administrative level, currently exists in Japan; organised by the Statistics Bureau, Ministry of Internal Affairs and Communication. This database is accessed through a portal site (E-Stat, 2016), which acts as a central access point for census and GIS data. This portal site could be used as a model for development of a similar system relating to climate change impacts and human health risks. The existence of a database and portal for climate change human health risks would advance research capabilities and greatly improve the communication of risks posed by climate change. Research and communication are key aspects of risk management, so investment in such a facility would prove invaluable to improving knowledge about climate change and human health impacts.
- Further to recordings of mortality and morbidity from climate change influenced health outcomes in Japan, additional investigations should be conducted into the climatic risk factors themselves. For example, the density of infectious disease vectors (namely dengue fever and malaria transmitting mosquitos) in different regions and habitats should be analysed. For instance, studies have discovered the existence of the malaria vector, *Anopheles sinensis*, in all prefectures of Japan (Rueda et al. 2005). However, these studies were conducted at point locations and a full picture of the density of vectors in different locations and habitats is not fully known. This would help to build up knowledge of areas at risk of imported disease transmission and could be combined with climate projections and observations to identify areas that are a priority for targeted countermeasure action such as vector control or disease control.

- Currently, in Japan recordings of extreme events are controlled by disparate agencies in different regions, meaning that there is a lack of coordination in past observed events. There needs to be a greater integration of data regarding extreme events such as storms, typhoons and heat waves. This study recommends a centrally controlled database, where all reports of extreme events and the impact on structural, human and environmental aspects can be recorded and collated into a unified directory. The intensity, scale and location of extreme events should be recorded at a prefectural and even city level and stored in one database. The creation of such a database would allow for detailed empirical studies to be conducted at a much smaller scale than is currently possible. As demonstrated by this Study, particularly in Chapter 4, the importance of studying climate change impacts at a very small scale cannot be underestimated and should provide the basis for future impact studies. A single database of all extreme events and their impacts in Japan would enable studies at the most appropriate scale to be conducted and would further improve understanding of the spatial variations in risk throughout Japan. An emerging solution to the lack of detailed data at a local level is the concept of Big Data. This would provide up to date and extremely fine scale data of underlying health issues, which could be used to identify spatial vulnerability, as well as enabling real time monitoring of health during particular climate events such as heat waves and tropical storms. Incorporating big data into methodologies such as this would greatly reduce the limitations imposed by access to traditional data sources (Jee and Kim, 2013). The framework in this paper enables the use of Big Data to be included in the methodology, so future studies should look to utilise available Big Data sources where they exist.
- There are uncertainties with all climate models, and these uncertainties increase and diverge after 2050. When considering climate change health risks after this time, it is advisable to run risk simulations using different climate scenarios to account for uncertainties in the general science behind climate models. Standardised emissions scenarios are provided by the Intergovernmental Panel on Climate Change (IPCC) in the form of the Representative Concentration Pathways (RCP). In the interests of standardised research practice, it is recommended that these scenario outputs are used to account for emissions scenario uncertainty.
- This research provides quantification of human health impacts of climate change. There are, however, other types of impacts to consider. Ecosystem damage and financial costs, for example, are two examples of different endpoint losses due to climate change (de Schryver et al. 2008). The framework from this study provides an output detailing the human health risks from climate change, but a truly comprehensive climate impact study should also include outputs for alternative types of impact. Ecosystem health can be quantified in terms of the Potentially Disappeared Fraction (PDF; de Schryver et al. 2008), whereas financial damage due to crop viability change and extreme events can be quantified in monetary values. Of the three

facets of climate change impacts, only monetary values have the potential to be transferrable across all impacts, although the moral consequences of monetising human health and ecosystem damage leave the appropriateness of such an approach ambiguous. Perhaps the most appropriate course of action based on our current knowledge is to investigate the three impact types using individual quantification scales. The result of such an assessment will provide decision makers with quantified impact values in each sector, from which prioritisations can be made using the empirical data and expert judgement.

5.4.2. Recommendations to expand the scope of this research

This research presents a method to evaluate climate change impacts on human health using a common unit, which enables the risk of climate change on health outcomes to be placed in the context of the wider field of risk research. With this in mind, several recommendations are made regarding the future direction of study that can build on the findings of this research:

- Regarding the use of the methodologies and key framework produced by this research, it is recommended that policy makers and researchers consider communication of risk as a central theme for their work and research. This research provides a framework and an output unit that is transferrable, transparent and contextual. These three attributes are important for all aspects of risk assessment as they greatly improve risk communication. Improved communication, based upon transparent studies, encourages greater cooperation between stakeholders and policy makers, which in turn aids effective implementation of risk reduction measures. This study provided evidence that it is possible to model climate change risk on intrinsically different human health outcomes at a local scale, using a common unit. If the limitations of the methodology are addressed, then this could provide a useful framework that could improve understanding within policy making sectors and improve communication of risk to the public from these sectors.
- Although out of the scope of this research, the studies shed some light on countermeasure options for the topics covered. The resulting outputs also provide a strong basis for investigating the potential impact of different countermeasure approaches. The topic in Chapter 4, in particular, provides this option. It describes a method of projecting climate change health impacts at a local scale, using DALY. Future research could run the projections while accounting for different adaptation and countermeasure options. If we take the projection of the impact of climate change on cardiovascular disease as an example, the case study output in Chapter 4 can be used as a Business as Usual (BAU) scenario. Countermeasure options, such as reducing vulnerability through public health measures or reducing exposure through urban planning can then be tested against the BAU scenario and compared with each other for

effectiveness. This is a particularly important area of expansion for local level policymakers, who have to prioritise risk reduction actions.

- Following on from the previous recommendation, the effectiveness of potential countermeasures can be assessed and combined with a Cost Benefit Analysis (CBA). Again, the method presented in this research can be used as a BAU scenario. The effectiveness of the target countermeasures can then be offset against their costs and trade-offs, to incorporate economics and finances into climate change health impact assessments. All authorities have finite resources, so combining the framework in this research with economic considerations would provide invaluable information to policy makers. The framework presented in this study is designed to facilitate CBA studies by providing authorities and decision makers with a foundation from which they can develop regional and locally applicable scenarios.
- Climate change risk research must be contextual. Decision makers need to prioritise both countermeasures and risks (Laboy-Nieves et al. 2010). The fact that the output from Chapter 4 is in a unit that can be used to determine human health risk from various health outcomes and risk factors, means that risks from different sources can be compared on the same scale. It also enables the impact of climate risk factors on a particular health outcome to be isolated and therefore compared to the impact of other risk factors on the same health outcome. Cross-sector and even cross-field (scientific) studies can therefore be conducted to determine the most important risk factors to different health outcomes. The total impact of specific risk factors can also be calculated and compared. The benefit of pursuing research in this direction is that risks can be prioritised based upon assessments placing them in a multi-criteria risk context.
- The final recommendation from this study is that future research could investigate the value of information related to determining the risk of climate change on human health. This concept enables quantification of the importance of information relating to a decision (Morgan and Henrion, 1990). In the context of climate change health impact research, this means identifying which pieces of information are the most important to know in order to make an effective decision, such as implementing a countermeasure. The frameworks developed in this research provide a platform for such research to be conducted, which would benefit prioritisation of measures to reduce risks to human health.

References

Aalst, M. and Burton I., 2002. The Last Straw: Integrating Natural Disaster Mitigation with Environmental Management. *Disaster Risk Management Working Paper No. 5*. The World Bank, Washington, DC.

Campbell-Lendrum, D., Woodruff, R., Prüss-Üstün, A. and Corvalán, C., 2007. Quantifying the health impact at national and local levels. *WHO Environmental Burden of Disease Series*, (14).

Collins, M., R. Knutti, J. Arblaster, J.-L. Dufresne, T. Fichefet, P. Friedlingstein, X. Gao, W.J. Gutowski, T. Johns, G. Krinner, M. Shongwe, C. Tebaldi, A.J. Weaver and M. Wehner, 2013. Long-term Climate Change: Projections, Commitments and Irreversibility. In: *Climate Change 2013: The Physical Science Basis. Contribution of Working Group I to the Fifth Assessment Report of the Intergovernmental Panel on Climate Change* [Stocker, T.F., D. Qin, G.-K. Plattner, M. Tignor, S.K. Allen, J. Boschung, A. Nauels, Y. Xia, V. Bex and P.M. Midgley (eds.)]. Cambridge University Press, Cambridge, United Kingdom and New York, NY, USA.

Costello, A., Abbas, M., Allen, A., Ball, S., Bell, S., Bellamy, R., Friel, S., Groce, N., Johnson, A., Kett, M. and Lee, M., 2009. Managing the health effects of climate change. *The Lancet*, **373**(9676), pp.1693-1733.

De Schryver, A.M., Brakkee, K.W., Goedkoop, M.J. and Huijbregts, M.A.J., 2008. Characterization Factors for Global Warming in Life Cycle Assessment Based on Damages to Humans and Ecosystems, *Environmental Science & Technology*, **43**(6), pp.1689-1695.

E-Stat, 2016. Portal site of Official Statistics of Japan. Available online at https://www.e-stat.go.jp/SG1/estat/eStatTopPortal.do **(Japanese)**

Ezzati, M., Lopez, A.D., Rodgers, A., Vander Hoorn, S. and Murray, C.J.L., 2002. Selected major risk factors and global and regional burden of disease, *The Lancet*, **360**(9343), pp.1347–1360.

Jee, K. and Kim, G.H., 2013. Potentiality of big data in the medical sector: focus on how to reshape the healthcare system. *Healthcare informatics research*, **19**(2), pp.79-85.

Laboy-Nieves, E.N., Goosen, M.F.A. and Emmanuel, E., 2010. *Environmental and Human Health: Risk Management in Developing Countries*, CRC Press, The Netherlands, pp. 271.

Leiserowitz, A., 2006. Climate Change Risk Perception and Policy Preferences: The Role of Affect, Imagery, and Values, *Climatic Change*, **77**(1), pp.45-72.

McMichael, A. J., Woodruff, R. E. and Hales, S., 2006. Climate change and human health: present and future risks, *The Lancet*, **367**(9513), pp.859-869.

Milan, B. and Creuzig, F., 2015. Reducing urban heat wave risk in the 21st century, *Current Opinion in Environmental Sustainability*, **14**, pp.221-231.

Morgan, M.G., Henrion, M. (1990) *Uncertainty: A Guide to Dealing with Uncertainty in Quantitative Risk and Policy Analysis*, Cambridge University Press, Cambridge, U.K.

Reid, C.E., O'Neill, M.S., Gronlund, C.J., Brines, S.J., Brown, D.G., Diez-Roux, A.V. and Schwartz, J., 2009. Mapping community determinants of heat vulnerability. *Environmental Health Perspectives* **117**(11), pp.1730-1736.

Rueda, L.M., Iwakami, M., O'Guinn, M., Mogi, M., Prendergast, B.F., Miyagi, I., Toma, T., Pecor, J.E. and Wilkerson, R.C., 2005. Habitats and distribution of Anopheles sinensis and associated Anopheles hyrcanus group in Japan. *Journal of the American Mosquito Control Association*, **21**(4), pp.458-463.

Smith, K.R., Woodward, A., Campbell-Lendrum, D., Chadee, D.D., Honda, Y., Liu, Q., Olwoch, J.M., Revich, B. and Sauerborn. R., 2014. Human health: impacts, adaptation, and co-benefits. In: *Climate Change 2014: Impacts, Adaptation, and Vulnerability. Part A: Global and Sectoral Aspects. Contribution of Working Group II to the Fifth Assessment Report of the Intergovernmental Panel on Climate Change* [Field, C.B., V.R. Barros, D.J. Dokken, K.J. Mach, M.D. Mastrandrea, T.E. Bilir, M. Chatterjee, K.L. Ebi, Y.O. Estrada, R.C. Genova, B. Girma, E.S. Kissel,A.N. Levy, S. MacCracken, P.R. Mastrandrea, and L.L.White (eds.)]. Cambridge University Press, Cambridge, United Kingdom and New York, NY, USA, pp. 709-754.

Salomon, J.A., Vos, T., Hogan, D.R., Gagnon, M., Naghavi, M., Mokdad, A., Begum, N., Shah, R., Karyana, M., Kosen, S. and Farje, M.R., 2013. Common values in assessing health outcomes from disease and injury: disability weights measurement study for the Global Burden of Disease Study 2010. *The Lancet*, **380**(9859), pp.2129-2143.

Tran, P., Shaw, R., Chantry, G., and Norton, J., 2009. GIS and local knowledge in disaster management: a case study of flood risk mapping in Viet Nam, *Disasters*, **33**(1), pp.152–169.

Van Vuuren, D.P., Edmonds, J., Kainuma, M., Riahi, K., Thomson, A., Hibbard, K., Hurtt, G.C., Kram, T., Krey, V., Lamarque, J.F. and Masui, T., 2011. The representative concentration pathways: an overview. *Climatic change*, **109**, pp.5-31.

Wolf, T. and McGregor, G., 2013. The development of a heat wave vulnerability index for London, United Kingdom, *Weather and Climate Extremes*, **1**, pp.59–68.

Appendix

Appendix 1.1. Average number of monthly malaria cases and average monthly climatic variables for each region in South Korea (2001-2011)

		Jan	Feb	Mar	Apr	May	Jun	Jul	Aug	Sep	Oct	Nov	Dec
Seoul	Malaria	1.8	1.4	2.2	3.8	10.5	26.2	56.4	56.2	37.9	17.7	6.4	2.5
	Daily min	-5.7	-2.4	1.7	8.1	13.7	18.6	22.0	22.7	17.9	11.0	3.6	-3.3
	Daily max	1.4	5.5	10.1	17.4	23.4	27.0	28.2	29.5	26.1	20.1	11.7	4.0
	Precip	20.2	29.5	42.6	77.0	101.2	157.6	545.4	342.1	181.3	40.9	37.6	16.9
	Humidity	57.1	54.8	54.1	53.4	59.7	65.6	76.9	73.2	66.1	60.8	59.0	56.6
Busan	Malaria	0.6	0.0	0.4	0.4	1.8	5.2	10.6	10.6	5.6	1.8	0.9	0.3
	Daily min	-0.4	2.1	5.0	10.0	14.3	18.2	21.6	23.4	20.0	14.6	8.1	2.0
	Daily max	7.6	10.5	13.5	18.1	21.6	24.6	27.1	29.2	26.4	22.5	16.3	10.1
	Precip	27.7	58.4	72.9	149.7	188.5	183.8	385.1	227.6	124.2	68.5	26.8	26.7
	Humidity	45.4	49.6	54.0	60.3	69.2	74.7	83.0	77.3	71.7	61.3	52.8	46.1
Daegu	Malaria	0.0	0.0	0.0	0.3	0.8	3.0	5.7	7.1	2.6	1.1	0.5	0.0
	Daily min	-3.1	-0.7	3.3	8.9	14.2	18.9	22.6	23.1	18.3	11.5	4.5	-1.2
	Daily max	5.5	9.2	13.9	20.6	25.2	28.7	30.3	30.9	27.0	22.0	14.7	7.7
	Precip	17.4	32.7	33.8	63.3	100.9	142.5	265.8	260.0	125.5	34.7	19.5	19.3
	Humidity	48.5	48.3	46.2	47.6	55.4	61.2	72.6	71.0	69.0	61.0	54.4	50.7
Inchon	Malaria	1.7	0.6	1.5	3.7	12.8	30.4	57.4	62.3	46.2	22.5	4.5	1.8

	Daily min	-5.0	-2.0	2.1	8.1	13.3	17.9	21.5	22.6	18.2	11.8	4.4	-2.5
	Daily max	2.2	5.7	10.1	16.4	22.1	25.5	27.3	28.8	26.0	20.2	12.3	4.9
	Precip	18.1	24.9	35.9	68.4	100.5	135.0	447.6	266.4	149.4	43.2	38.5	15.5
	Humidity	60.4	61.1	61.1	61.9	68.2	74.1	82.9	78.3	70.5	64.5	61.6	59.3
Gwangju	**Malaria**	0.1	0.2	0.1	0.0	0.5	2.6	3.6	3.4	1.7	0.6	0.3	0.1
	Daily min	-3.1	-1.1	2.3	7.7	13.7	18.8	22.7	23.0	18.5	11.4	4.7	-0.7
	Daily max	4.7	8.8	13.3	19.7	24.7	27.9	29.6	30.5	27.4	22.1	14.8	7.8
	Precip	34.7	60.1	49.3	92.2	115.1	160.6	353.3	341.6	143.0	35.7	31.2	42.0
	Humidity	65.6	61.3	58.2	58.6	64.2	69.9	79.0	77.1	72.2	65.7	64.2	66.3
Daejon	**Malaria**	0.0	0.2	0.1	0.2	1.0	2.2	4.2	4.7	1.8	1.4	0.2	0.0
	Daily min	-5.6	-2.9	1.0	7.0	12.9	18.0	22.0	22.3	17.3	9.6	2.6	-3.3
	Daily max	3.6	7.2	12.2	19.1	24.2	27.6	28.7	29.6	26.2	20.8	13.3	6.0
	Precip	30.7	40.9	50.0	78.7	105.7	184.2	368.2	302.4	156.2	34.7	27.8	28.4
	Humidity	63.5	59.0	55.1	53.7	60.9	66.2	77.6	76.3	72.9	69.0	65.2	65.8
Ulsan	**Malaria**	0.2	0.2	0.2	0.3	0.3	2.5	3.5	5.1	1.7	0.6	0.3	0.1
	Daily min	-1.9	0.2	3.4	8.5	13.4	17.8	21.8	22.6	18.3	12.2	5.5	0.2
	Daily max	7.2	10.0	13.7	19.5	23.3	26.7	29.0	30.0	26.1	22.1	16.0	9.6
	Precip	29.9	47.7	51.2	86.5	130.5	159.2	287.6	201.4	160.2	47.0	30.7	23.1
	Humidity	46.8	51.0	53.5	57.1	65.5	70.4	77.7	75.5	74.6	65.9	56.1	48.7
Gyeonggi	**Malaria**	2.8	3.2	4.3	13.5	48.2	100.8	157.5	168.0	101.8	59.2	14.4	2.7
	Daily min	-7.1	-4.1	0.3	6.4	12.4	17.8	21.8	22.5	17.4	9.8	2.3	-4.4
	Daily max	2.0	5.7	10.6	17.7	23.3	27.0	28.7	29.9	26.4	20.4	12.0	4.7

	Precip	19.6	30.1	43.5	83.0	94.6	162.3	457.8	264.9	151.9	40.0	40.8	18.5
	Humidity	62.1	61.5	60.4	60.0	64.3	70.0	80.4	77.1	71.3	67.6	64.5	61.4
Gangwon	**Malaria**	0.6	0.5	1.4	6.3	20.5	31.7	40.2	36.1	19.8	7.1	1.9	0.2
	Daily min	-10.1	-6.1	-1.3	4.6	11.4	16.8	21.2	21.1	15.5	7.7	0.1	-6.7
	Daily max	1.4	6.1	11.2	18.7	24.3	27.7	28.8	29.7	25.7	19.9	11.3	3.6
	Precip	20.5	26.6	40.0	77.6	99.7	155.1	494.1	325.8	155.2	40.3	34.6	19.8
	Humidity	45.3	50.1	53.1	56.7	67.5	75.0	81.8	79.9	76.1	62.6	50.9	43.5
North ChungChong	**Malaria**	0.2	0.1	0.2	0.5	0.8	1.8	5.4	4.2	3.4	0.7	0.5	0.2
	Daily min	-6.2	-3.2	0.8	7.0	13.3	18.4	22.2	22.5	17.3	9.6	2.3	-3.8
	Daily max	3.0	6.9	12.2	19.4	24.6	27.9	29.4	30.1	26.5	20.9	12.9	5.4
	Precip	24.5	32.3	45.4	75.3	97.5	167.5	336.0	276.0	154.6	36.5	27.9	24.7
	Humidity	62.9	58.2	53.7	50.8	57.1	63.8	75.2	73.8	70.4	66.2	62.8	63.9
South ChungChong	**Malaria**	0.2	0.1	0.1	0.4	0.7	2.4	5.9	5.7	2.4	2.1	0.1	0.6
	Daily min	-8.2	-4.8	-1.0	4.8	11.9	17.0	21.2	21.2	15.5	7.3	0.5	-5.2
	Daily max	2.5	6.2	11.4	18.6	24.0	27.3	28.9	29.8	26.2	20.7	12.7	5.1
	Precip	21.8	27.9	40.5	73.9	88.0	154.4	332.5	280.1	169.6	37.8	31.3	27.0
	Humidity	69.8	66.2	61.4	58.3	63.5	69.2	78.5	77.9	75.2	71.8	69.1	69.8
North Jeolla	**Malaria**	0.0	0.1	0.4	0.2	0.8	3.4	5.3	6.2	4.5	0.9	0.1	0.1
	Daily min	-4.5	-2.3	1.1	6.8	12.9	18.2	22.6	22.8	17.9	10.2	3.7	-2.1
	Daily max	4.5	7.9	12.7	19.6	24.9	28.6	30.2	31.0	27.7	21.9	14.3	7.0
	Precip	28.9	43.1	45.7	80.0	94.9	145.4	353.5	325.5	118.3	36.2	28.8	36.0
	Humidity	66.0	62.7	59.0	56.8	62.5	67.4	76.2	75.1	71.6	67.1	64.0	66.0

South Jeolla	**Malaria**	0.2	0.1	0.1	0.3	0.6	2.4	4.8	5.9	3.4	0.8	0.2	0.4
	Daily min	-1.7	-0.5	2.6	8.0	13.7	18.4	22.4	23.3	19.1	12.7	6.3	0.7
	Daily max	5.0	7.5	11.3	17.0	22.1	25.6	28.0	29.5	26.4	21.3	14.4	7.8
	Precip	30.1	46.6	50.6	82.9	113.0	159.8	267.5	220.4	120.4	40.7	30.4	36.7
	Humidity	72.8	72.0	69.7	70.6	76.3	80.8	87.2	83.2	77.8	70.8	69.7	72.0
North Gyeongsang	**Malaria**	0.3	0.4	0.2	0.6	5.9	3.9	5.6	7.7	2.7	1.9	0.8	0.5
	Daily min	-7.7	-4.8	-0.5	5.1	11.2	16.3	20.8	20.9	15.7	8.1	0.5	-5.3
	Daily max	6.2	9.3	13.1	19.1	22.8	26.2	28.5	29.4	25.5	21.5	15.3	8.7
	Precip	36.8	42.5	45.0	72.9	117.1	145.9	239.7	218.5	183.8	46.8	35.5	24.9
	Humidity	48.1	50.9	52.8	55.6	66.2	72.4	79.5	78.7	76.3	65.1	55.1	48.8
South Gyeongsang	**Malaria**	0.4	0.2	0.2	0.3	0.9	3.2	7.9	7.7	4.6	1.6	0.9	0.2
	Daily min	-6.0	-3.4	0.4	5.9	12.0	17.3	22.0	22.3	17.3	9.0	1.5	-3.8
	Daily max	6.8	10.1	14.1	20.0	24.6	27.8	29.6	30.7	27.5	22.7	15.8	9.3
	Precip	69.7	65.5	76.3	82.4	110.0	184.9	217.6	262.7	231.7	71.6	59.3	65.8
	Humidity	56.9	57.5	56.1	60.6	67.4	72.4	80.3	78.3	75.4	70.5	66.2	60.9
Jeju	**Malaria**	0.1	0.0	0.0	0.1	0.3	0.3	0.7	2.9	0.4	0.4	0.0	0.1
	Daily min	3.5	4.2	6.3	10.4	14.8	19.1	23.5	24.5	21.1	15.7	10.0	5.5
	Daily max	7.8	10.3	13.2	17.8	21.7	24.9	29.2	29.9	26.1	21.7	16.1	10.8
	Precip	69.7	65.5	76.3	82.4	110.0	184.9	217.6	262.7	231.7	71.6	59.3	65.8
	Humidity	61.8	61.1	58.4	60.4	66.7	73.9	75.0	73.3	72.0	62.9	59.9	61.7

Appendix 1.2. Annual malaria cases per region in the Republic of Korea 2001-2011

	2001	2002	2003	2004	2005	2006	2007	2008	2009	2010	2011
Busan	68	49	27	16	28	62	41	27	33	43	26
Daegu	30	25	13	13	16	25	36	15	25	19	16
Daejon	32	18	9	12	12	14	23	10	21	15	9
Gangwon	545	216	132	65	78	123	125	109	154	184	96
Gwangju	32	17	17	16	8	15	7	8	10	9	6
Gyeonggi	909	756	518	399	660	869	1,007	490	611	818	387
Inchon	275	267	166	107	222	465	484	164	164	256	123
Jeju	7	2	2	1	4	4	2	5	1	7	4
North ChungChong	25	22	9	12	10	25	30	11	18	23	11
North Gyeongsang	43	29	24	16	26	32	35	17	32	19	12
North Jeolla	40	27	12	17	25	30	23	14	18	22	12
Seoul	370	285	170	136	213	272	314	126	178	289	93
South ChungChong	35	22	16	17	11	23	23	21	27	14	12
South Gyeongsang	64	32	13	12	22	40	41	17	26	24	13
South Jeolla	37	19	20	11	20	29	20	11	11	21	11
Ulsan	32	10	18	13	13	23	16	7	16	8	7
Other	12	3	5	1	1	0	0	0	0	0	0
TOTAL	2,556	1,799	1,171	864	1,369	2,051	2,227	1,052	1,345	1,771	838

Appendix 1.3. Annual malaria cases in the Republic of Korea 2001-2011

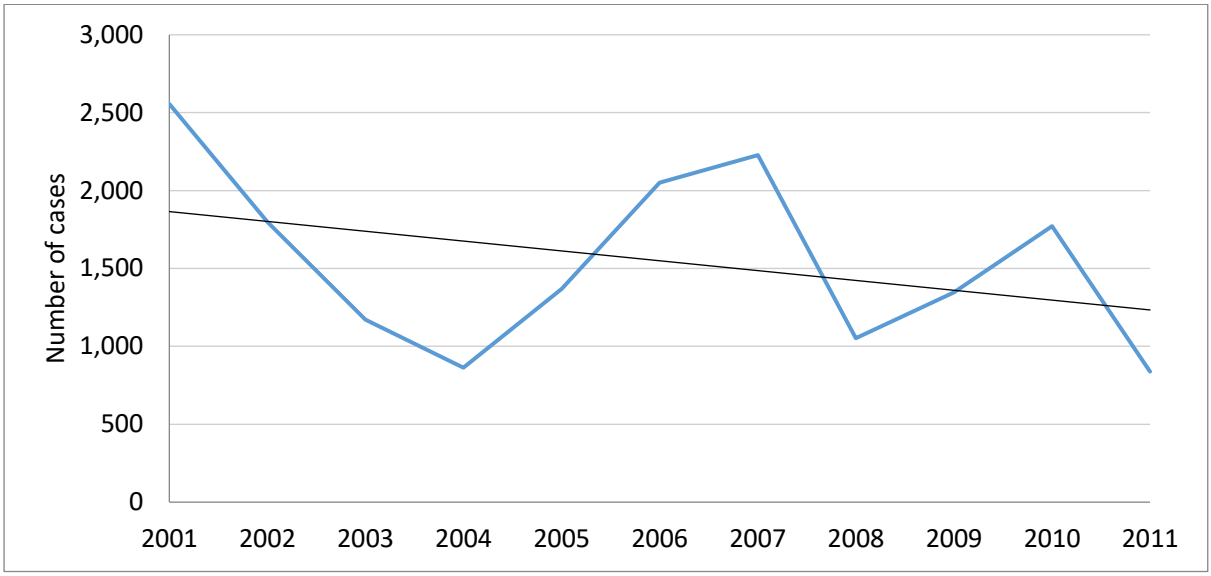

Appendix 1.4. Monthly maximum temperature and malaria cases for all regions in the Republic of Korea (2001-2011)

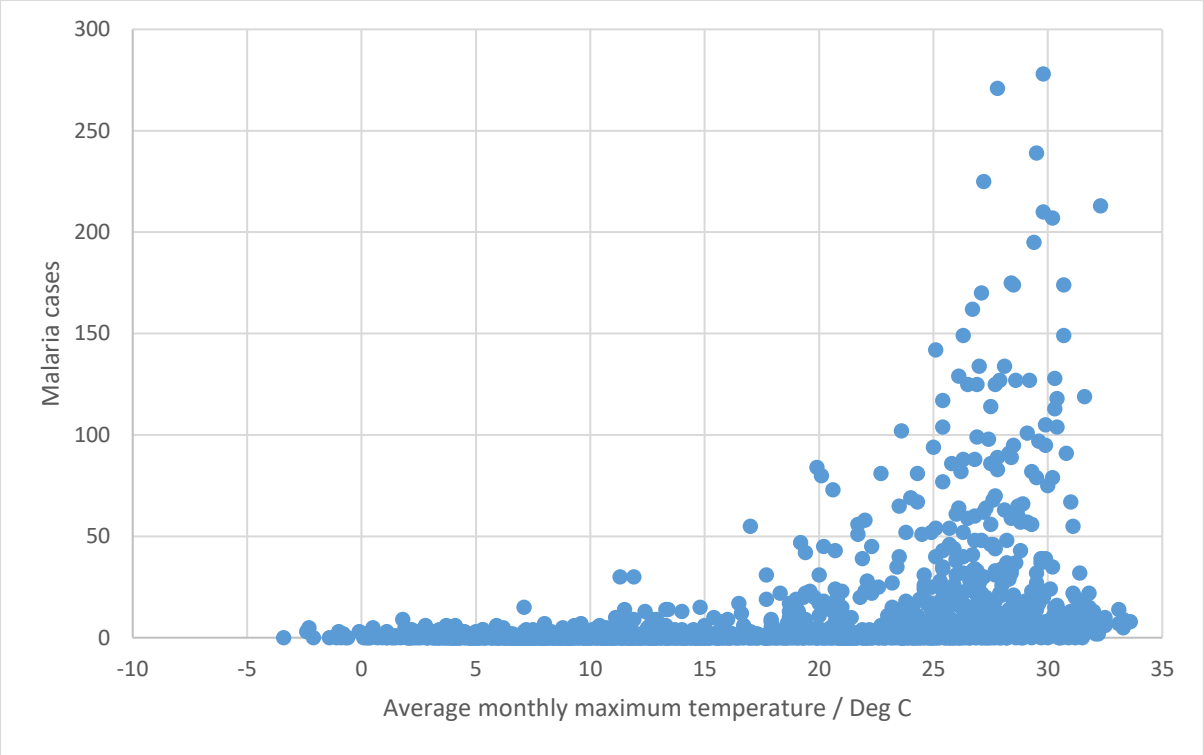

Appendix 1.5. Monthly minimum temperature and malaria cases for all regions in the Republic of Korea (2001-2011)

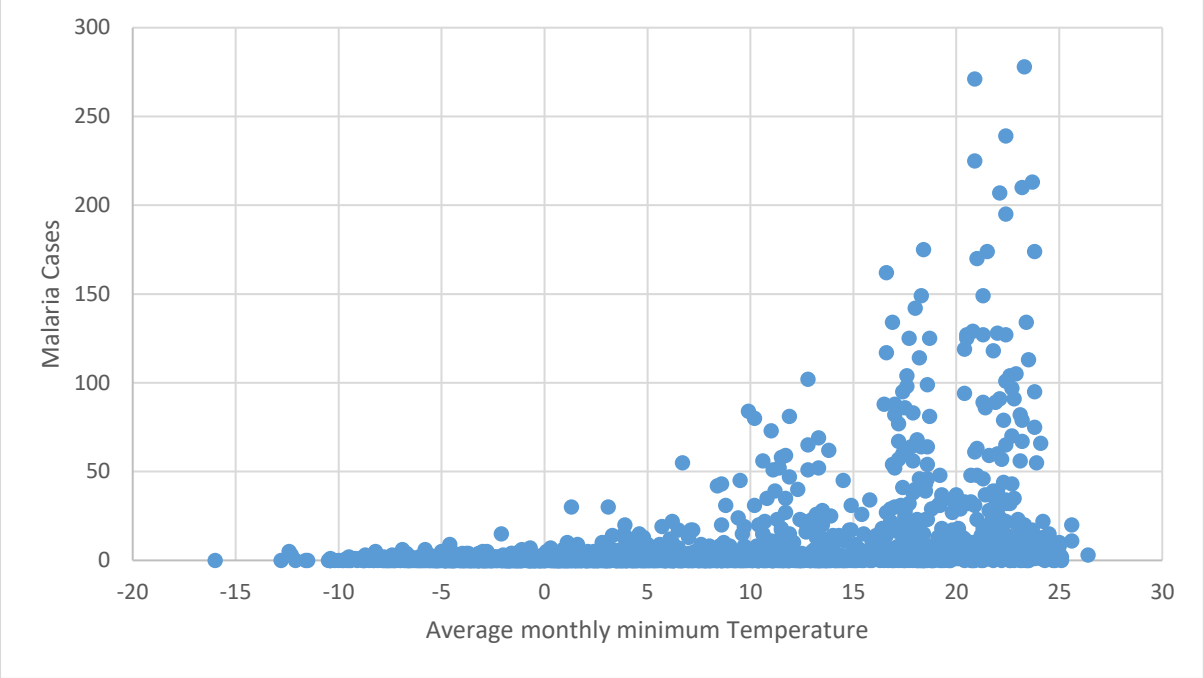

Appendix 1.6. Monthly precipitation and malaria cases for all regions in the Republic of Korea (2001-2011)

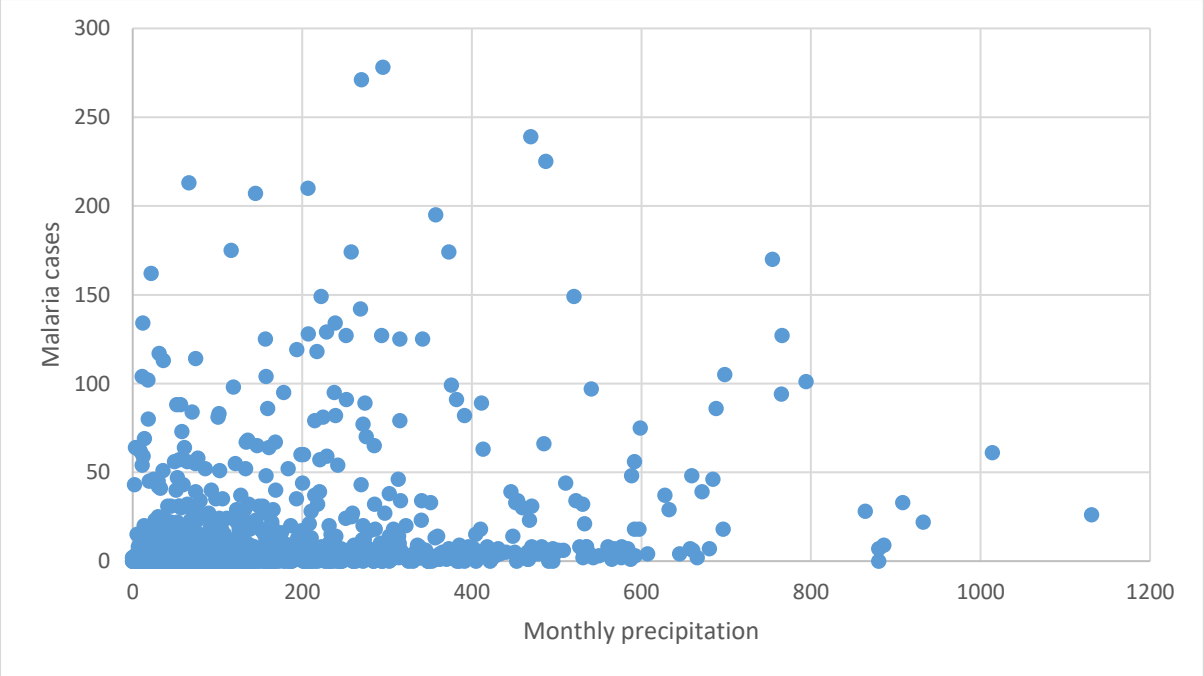

Appendix 1.6. Monthly relative humidity and malaria cases for all regions in the Republic of Korea (2001-2011)

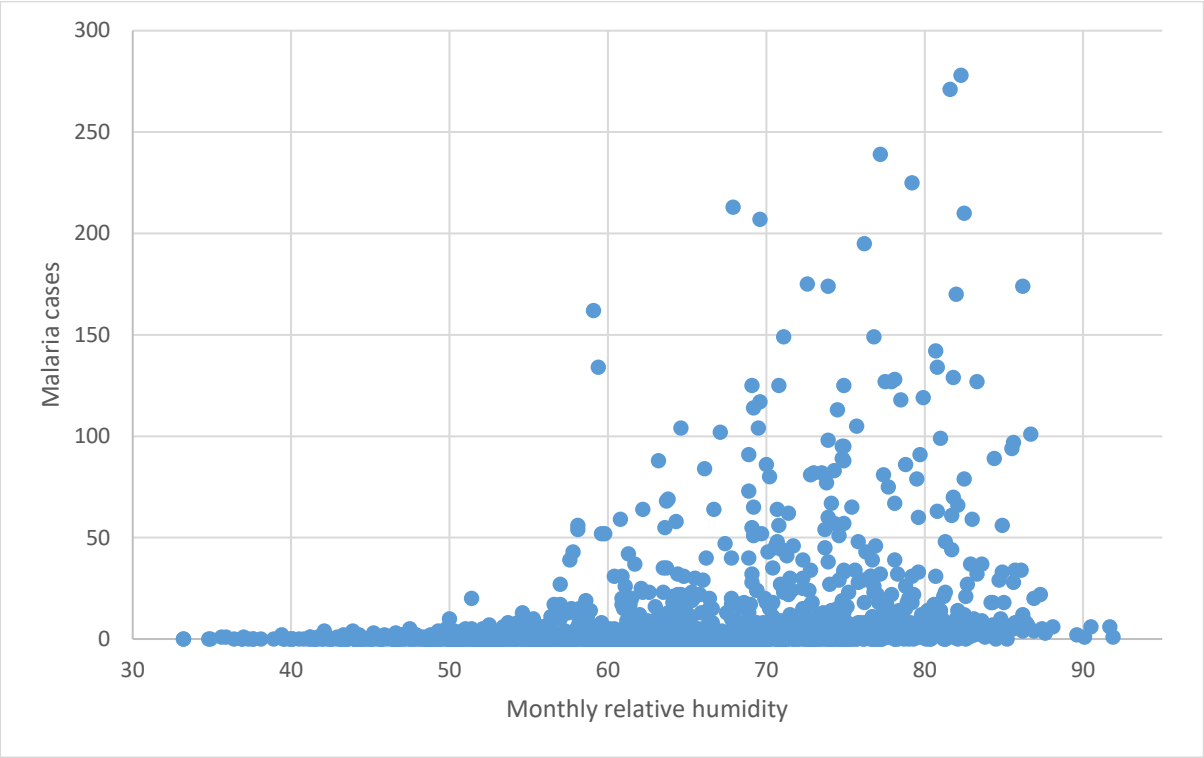

Appendix 2.1. Heat wave vulnerability index scores and vulnerability information for Chuo Ward, Osaka City, Japan

KEY_CODE	Ku	Ward	Chome	Households	Population	DENSITY /he	pop >65	% >65	Pop living alone	% living alone	Employed	% not in work	lone >65	% lone >65	% built up	HVI score
27128002001	中央区	Chuo	上本町西１丁目	435	742	21.64	86	11.59	276	63.45	384	48.25	34	39.53	100.00	58.90
27128002002	中央区	Chuo	上本町西２丁目	616	1021	26.57	235	23.02	396	64.29	534	47.7	91	38.72	100.00	63.63
27128002003	中央区	Chuo	上本町西３丁目	338	694	20.21	164	23.63	151	44.67	350	49.57	31	18.90	70.88	49.04
27128002004	中央区	Chuo	上本町西４丁目	202	426	22.19	50	11.74	82	40.59	213	50	14	28.00	100.00	51.50
27128002005	中央区	Chuo	上本町西５丁目	395	755	26.55	79	10.46	190	48.1	387	48.74	34	43.04	100.00	56.81
27128004001	中央区	Chuo	上汐１丁目	231	425	19.65	82	19.29	129	55.84	218	48.71	20	24.39	100.00	56.46
27128004002	中央区	Chuo	上汐２丁目	387	608	19.56	152	25	246	63.57	314	48.36	51	33.55	100.00	61.81
271280610	中央区	Chuo	上町	217	289	15.39	48	16.61	172	79.26	161	44.29	19	39.58	46.74	53.59
271280710	中央区	Chuo	上町１丁目	1150	2167	14.16	496	22.89	613	53.3	1029	52.51	188	37.90	80.40	55.71
27128005001	中央区	Chuo	中寺１丁目	174	388	10.19	45	11.6	71	40.8	199	48.71	13	28.89	100.00	49.62
27128005002	中央区	Chuo	中寺２丁目	173	266	7.40	62	23.31	128	73.99	132	50.38	32	51.61	100.00	66.52
27128033001	中央区	Chuo	久太郎町１丁目	350	417	7.33	12	2.88	306	87.43	213	48.92	6	50.00	100.00	62.43
27128033002	中央区	Chuo	久太郎町２丁目	52	64	1.72	12	18.75	44	84.62	25	60.94	6	50.00	100.00	67.09
27128033003	中央区	Chuo	久太郎町３丁目	40	45	1.19	8	17.78	34	85	29	35.56	2	25.00	100.00	55.60
27128033004	中央区	Chuo	久太郎町４丁目	9	15	0.40	9	60	5	55.56	9	40	1	11.11	100.00	60.83
27128021001	中央区	Chuo	今橋１丁目	139	219	10.04	33	15.07	90	64.75	125	42.92	5	15.15	100.00	50.81
27128021002	中央区	Chuo	今橋２丁目	0	0	0.00	0	0	0	0	0	0	0	0.00	100.00	16.69
27128021003	中央区	Chuo	今橋３丁目	0	0	0.00	0	0	0	0	0	0	0	0.00	100.00	16.69
27128021004	中央区	Chuo	今橋４丁目	0	0	0.00	0	0	0	0	0	0	0	0.00	100.00	16.69
27128023001	中央区	Chuo	伏見町１丁目	0	0	0.00	0	0	0	0	0	0	0	0.00	100.00	16.69
27128023002	中央区	Chuo	伏見町２丁目	12	16	1.31	4	25	8	66.67	6	62.5	2	50.00	100.00	64.64
27128023003	中央区	Chuo	伏見町３丁目	184	278	15.43	36	12.95	115	62.5	149	46.4	14	38.89	100.00	57.37
27128023004	中央区	Chuo	伏見町４丁目	0	0	0.00	0	0	0	0	0	0	0	0.00	100.00	16.69
27128028001	中央区	Chuo	備後町１丁目	152	226	8.74	14	6.19	110	72.37	103	54.42	3	21.43	100.00	54.26

27128028002	中央区	Chuo	備後町２丁目	0	0	0.00	0	0	0	0	0	0	0	0.00	100.00	16.69
27128028003	中央区	Chuo	備後町３丁目	0	0	0.00	0	0	0	0	0	0	0	0.00	100.00	16.69
27128028004	中央区	Chuo	備後町４丁目	0	0	0.00	0	0	0	0	0	0	0	0.00	100.00	16.69
27128059001	中央区	Chuo	内久宝寺町１丁目	0	0	0.00	0	0	0	0	0	0	0	0.00	100.00	16.69
27128059002	中央区	Chuo	内久宝寺町２丁目	388	744	24.69	103	13.84	188	48.45	406	45.43	24	23.30	100.00	52.22
27128059003	中央区	Chuo	内久宝寺町３丁目	286	373	21.27	25	6.7	232	81.12	226	39.41	4	16.00	100.00	54.04
27128059004	中央区	Chuo	内久宝寺町４丁目	275	382	23.02	54	14.14	213	77.45	221	42.15	21	38.89	100.00	61.87
27128044001	中央区	Chuo	内平野町１丁目	202	296	26.12	38	12.84	144	71.29	163	44.93	17	44.74	100.00	61.96
27128044002	中央区	Chuo	内平野町２丁目	327	486	31.16	47	9.67	238	72.78	291	40.12	16	34.04	100.00	59.23
27128044003	中央区	Chuo	内平野町３丁目	39	53	6.01	4	7.55	32	82.05	40	24.53	0	0.00	100.00	45.33
27128051001	中央区	Chuo	内本町１丁目	290	516	25.67	72	13.95	160	55.17	268	48.06	19	26.39	100.00	55.14
27128051002	中央区	Chuo	内本町２丁目	216	322	13.30	62	19.25	148	68.52	172	46.58	31	50.00	100.00	63.95
27128045001	中央区	Chuo	内淡路町１丁目	267	356	29.59	44	12.36	213	79.78	212	40.45	15	34.09	100.00	61.52
27128045002	中央区	Chuo	内淡路町２丁目	200	338	21.05	46	13.61	115	57.5	187	44.67	8	17.39	100.00	51.92
27128045003	中央区	Chuo	内淡路町３丁目	111	167	16.49	14	8.38	85	76.58	98	41.32	4	28.57	100.00	56.16
27128034001	中央区	Chuo	北久宝寺町１丁目	231	293	8.94	37	12.63	192	83.12	152	48.12	16	43.24	100.00	62.97
27128034002	中央区	Chuo	北久宝寺町２丁目	38	51	2.14	7	13.73	31	81.58	23	54.9	4	57.14	100.00	66.07
27128034003	中央区	Chuo	北久宝寺町３丁目	29	44	1.96	10	22.73	20	68.97	18	59.09	3	30.00	100.00	59.30
27128034004	中央区	Chuo	北久宝寺町４丁目	24	32	2.22	7	21.88	18	75	14	56.25	2	28.57	100.00	62.23
271280480	中央区	Chuo	北新町	70	136	15.72	25	18.38	29	41.43	56	58.82	8	32.00	100.00	54.13
27128020001	中央区	Chuo	北浜１丁目	7	13	0.33	3	23.08	4	57.14	6	53.85	2	66.67	0.00	47.05
27128020002	中央区	Chuo	北浜２丁目	73	83	1.76	12	14.46	67	91.78	53	36.14	7	58.33	0.00	48.05
27128020003	中央区	Chuo	北浜３丁目	23	47	0.93	18	38.3	12	52.17	21	55.32	8	44.44	21.03	51.70
27128020004	中央区	Chuo	北浜４丁目	0	0	0.00	0	0	0	0	0	0	0	0.00	41.33	6.90
271280380	中央区	Chuo	北浜東	21	27	0.37	5	18.52	16	76.19	18	33.33	1	20.00	0.00	36.21
271280630	中央区	Chuo	十二軒町	482	792	27.99	129	16.29	295	61.2	411	48.11	46	35.66	100.00	60.13
27128012001	中央区	Chuo	千日前１丁目	173	241	6.72	75	31.12	138	79.77	116	51.87	38	50.67	100.00	70.58
27128012002	中央区	Chuo	千日前２丁目	117	175	3.89	50	28.57	81	69.23	71	59.43	23	46.00	100.00	67.05
27128035001	中央区	Chuo	南久宝寺町１丁目	429	509	14.31	41	8.06	380	88.58	302	40.67	11	26.83	100.00	58.00
27128035002	中央区	Chuo	南久宝寺町２丁目	229	318	13.35	26	8.18	175	76.42	179	43.71	13	50.00	100.00	60.84

27128035003	中央区	Chuo	南久宝寺町３丁目	26	40	1.50	13	32.5	18	69.23	22	45	3	23.08	100.00	58.64
27128035004	中央区	Chuo	南久宝寺町４丁目	140	203	8.56	21	10.34	103	73.57	90	55.67	6	28.57	100.00	57.77
27128049001	中央区	Chuo	南新町１丁目	76	110	9.59	11	10	55	72.37	66	40	3	27.27	100.00	53.33
27128049002	中央区	Chuo	南新町２丁目	123	180	11.97	20	11.11	92	74.8	115	36.11	8	40.00	100.00	57.73
27128031001	中央区	Chuo	南本町１丁目	84	100	2.72	12	12	75	89.29	69	31	7	58.33	100.00	62.49
27128031002	中央区	Chuo	南本町２丁目	0	0	0.00	0	0	0	0	0	0	0	0.00	100.00	16.69
27128031003	中央区	Chuo	南本町３丁目	105	143	4.73	18	12.59	76	72.38	64	55.24	11	61.11	100.00	65.17
27128031004	中央区	Chuo	南本町４丁目	0	0	0.00	0	0	0	0	0	0	0	0.00	100.00	16.69
27128009001	中央区	Chuo	南船場１丁目	1297	1928	14.01	216	11.2	888	68.47	963	50.05	60	27.78	100.00	56.51
27128009002	中央区	Chuo	南船場２丁目	293	415	4.57	67	16.14	215	73.38	198	52.29	27	40.30	100.00	60.66
27128009003	中央区	Chuo	南船場３丁目	97	133	1.40	31	23.31	72	74.23	72	45.86	8	25.81	100.00	57.69
27128009004	中央区	Chuo	南船場４丁目	134	201	2.52	43	21.39	95	70.9	94	53.23	16	37.21	100.00	60.67
27128036001	中央区	Chuo	博労町１丁目	251	319	8.93	33	10.34	205	81.67	158	50.47	10	30.30	100.00	59.12
27128036002	中央区	Chuo	博労町２丁目	145	168	6.98	9	5.36	128	88.28	96	42.86	6	66.67	100.00	66.05
27128036003	中央区	Chuo	博労町３丁目	118	154	6.89	11	7.14	96	81.36	81	47.4	2	18.18	100.00	54.31
27128036004	中央区	Chuo	博労町４丁目	64	82	3.65	11	13.41	53	82.81	40	51.22	5	45.45	100.00	62.77
27128058001	中央区	Chuo	和泉町１丁目	132	188	9.96	24	12.77	97	73.48	94	50	5	20.83	100.00	55.47
27128058002	中央区	Chuo	和泉町２丁目	112	188	10.87	21	11.17	68	60.71	91	51.6	6	28.57	100.00	54.26
27128067001	中央区	Chuo	城見１丁目	0	0	0.00	0	0	0	0	0	0	0	0.00	19.33	3.22
27128067002	中央区	Chuo	城見２丁目	0	0	0.00	0	0	0	0	0	0	0	0.00	29.16	4.87
27128056001	中央区	Chuo	大手前１丁目	129	197	1.46	44	22.34	79	61.24	115	41.62	9	20.45	18.68	38.73
27128056002	中央区	Chuo	大手前２丁目	0	0	0.00	0	0	0	0	0	0	0	0.00	46.22	7.71
27128056003	中央区	Chuo	大手前３丁目	0	0	0.00	0	0	0	0	0	0	0	0.00	61.90	10.33
27128056004	中央区	Chuo	大手前４丁目	0	0	0.00	0	0	0	0	0	0	0	0.00	24.17	4.03
27128046001	中央区	Chuo	大手通１丁目	204	379	26.93	39	10.29	106	51.96	188	50.4	15	38.46	100.00	56.70
27128046002	中央区	Chuo	大手通２丁目	214	377	23.35	53	14.06	119	55.61	204	45.89	11	20.75	38.05	42.95
27128046003	中央区	Chuo	大手通３丁目	100	187	12.42	32	17.11	49	49	96	48.66	7	21.88	100.00	51.83
271280680	中央区	Chuo	大阪城	0	0	0.00	0	0	0	0	0	0	0	0.00	0.00	0.00
271280370	中央区	Chuo	天満橋京町	76	151	3.31	24	15.89	30	39.47	79	47.68	9	37.50	34.22	39.53
27128029001	中央区	Chuo	安土町１丁目	78	141	5.31	44	31.21	43	55.13	51	63.83	20	45.45	100.00	64.41

27128029002	中央区	Chuo	安土町２丁目	0	0	0.00	0	0	0	0	0	0	0	0.00	100.00	16.69
27128029003	中央区	Chuo	安土町３丁目	70	118	4.44	16	13.56	36	51.43	61	48.31	6	37.50	100.00	53.55
27128001001	中央区	Chuo	安堂寺町１丁目	367	583	22.90	92	15.78	239	65.12	307	47.34	17	18.48	100.00	55.74
27128001002	中央区	Chuo	安堂寺町２丁目	986	1616	35.59	192	11.88	607	61.56	838	48.14	73	38.02	100.00	60.42
271280190	中央区	Chuo	宗右衛門町	79	103	1.91	30	29.13	62	78.48	42	59.22	11	36.67	100.00	66.53
27128010001	中央区	Chuo	島之内１丁目	1437	1864	13.05	226	12.12	1151	80.1	807	56.71	88	38.94	100.00	63.57
27128010002	中央区	Chuo	島之内２丁目	2750	3693	27.52	530	14.35	2126	77.31	1173	68.24	250	47.17	100.00	70.81
27128040001	中央区	Chuo	島町１丁目	143	250	18.92	19	7.6	85	59.44	135	46	3	15.79	100.00	49.92
27128040002	中央区	Chuo	島町２丁目	258	325	16.52	25	7.69	212	82.17	201	38.15	11	44.00	100.00	59.94
27128053001	中央区	Chuo	常盤町１丁目	162	231	11.03	53	22.94	119	73.46	71	69.26	31	58.49	100.00	73.82
27128053002	中央区	Chuo	常盤町２丁目	305	366	15.38	14	3.83	264	86.56	212	42.08	4	28.57	100.00	57.45
27128025001	中央区	Chuo	平野町１丁目	118	153	5.82	30	19.61	90	76.27	81	47.06	14	46.67	100.00	62.80
27128025002	中央区	Chuo	平野町２丁目	20	26	1.09	5	19.23	15	75	14	46.15	0	0.00	100.00	52.05
27128025003	中央区	Chuo	平野町３丁目	46	85	3.54	24	28.24	29	63.04	42	50.59	4	16.67	100.00	56.03
27128025004	中央区	Chuo	平野町４丁目	104	112	4.61	15	13.39	98	94.23	42	62.5	9	60.00	100.00	71.89
27128050001	中央区	Chuo	徳井町１丁目	132	213	18.09	28	13.15	78	59.09	92	56.81	7	25.00	100.00	55.77
27128050002	中央区	Chuo	徳井町２丁目	387	497	33.35	23	4.63	309	79.84	303	39.03	10	43.48	100.00	61.98
27128017001	中央区	Chuo	心斎橋筋１丁目	50	89	1.42	31	34.83	30	60	39	56.18	16	51.61	100.00	65.68
27128017002	中央区	Chuo	心斎橋筋２丁目	36	67	1.20	34	50.75	18	50	39	41.79	10	29.41	100.00	58.17
27128015001	中央区	Chuo	日本橋１丁目	771	1134	10.67	287	25.31	553	71.73	506	55.38	123	42.86	100.00	66.46
27128015002	中央区	Chuo	日本橋２丁目	1426	2195	23.99	552	25.15	941	65.99	803	63.42	246	44.57	100.00	69.16
27128030001	中央区	Chuo	本町１丁目	13	24	0.84	11	45.83	6	46.15	12	50	2	18.18	100.00	54.98
27128030002	中央区	Chuo	本町２丁目	0	0	0.00	0	0	0	0	0	0	0	0.00	100.00	16.69
27128030003	中央区	Chuo	本町３丁目	0	0	0.00	0	0	0	0	0	0	0	0.00	100.00	16.69
27128030004	中央区	Chuo	本町４丁目	45	53	0.90	10	18.87	38	84.44	31	41.51	7	70.00	100.00	68.03
271280540	中央区	Chuo	本町橋	466	766	10.79	86	11.23	275	59.01	414	45.95	13	15.12	100.00	49.76
271280600	中央区	Chuo	材木町	384	438	24.73	21	4.79	342	89.06	241	44.98	4	19.05	100.00	57.93
27128003001	中央区	Chuo	東平１丁目	550	1179	52.61	181	15.35	207	37.64	579	50.89	49	27.07	55.38	49.60
27128003002	中央区	Chuo	東平２丁目	370	567	23.19	90	15.87	254	68.65	264	53.44	18	20.00	100.00	58.28
27128016001	中央区	Chuo	東心斎橋１丁目	603	912	7.58	214	23.46	416	68.99	478	47.59	70	32.71	100.00	59.78

27128016002	中央区	Chuo	東心斎橋２丁目	106	164	2.55	61	37.2	72	67.92	74	54.88	23	37.70	100.00	64.56
271280430	中央区	Chuo	東高麗橋	704	936	22.54	91	9.72	567	80.54	547	41.56	28	30.77	100.00	59.13
271280060	中央区	Chuo	松屋町	815	1260	25.02	96	7.62	554	67.98	617	51.03	26	27.08	100.00	57.15
271280660	中央区	Chuo	松屋町住吉	548	715	21.88	48	6.71	447	81.57	386	46.01	7	14.58	100.00	55.65
27128072001	中央区	Chuo	森ノ宮中央１丁目	711	1251	12.07	238	19.02	425	59.77	635	49.24	84	35.29	100.00	58.45
27128072002	中央区	Chuo	森ノ宮中央２丁目	372	642	6.34	144	22.43	238	63.98	305	52.49	56	38.89	60.48	54.40
27128070001	中央区	Chuo	法円坂１丁目	518	978	5.76	383	39.16	230	44.4	453	53.68	117	30.55	23.42	47.34
27128070002	中央区	Chuo	法円坂２丁目	151	184	2.47	10	5.43	140	92.72	156	15.22	1	10.00	100.00	46.91
27128026001	中央区	Chuo	淡路町１丁目	91	147	6.06	17	11.56	55	60.44	59	59.86	8	47.06	100.00	59.71
27128026002	中央区	Chuo	淡路町２丁目	75	126	5.06	25	19.84	43	57.33	62	50.79	13	52.00	100.00	60.79
27128026003	中央区	Chuo	淡路町３丁目	80	139	5.65	14	10.07	36	45	83	40.29	5	35.71	100.00	48.10
27128026004	中央区	Chuo	淡路町４丁目	12	18	0.91	2	11.11	9	75	8	55.56	0	0.00	100.00	49.75
27128073001	中央区	Chuo	玉造１丁目	1048	2226	19.13	406	18.24	435	41.51	1037	53.41	98	24.14	100.00	53.13
27128073002	中央区	Chuo	玉造２丁目	1143	2167	10.98	429	19.8	633	55.38	1093	49.56	124	28.90	74.66	51.85
27128007001	中央区	Chuo	瓦屋町１丁目	753	1290	22.08	196	15.19	444	58.96	585	54.65	54	27.55	100.00	57.79
27128007002	中央区	Chuo	瓦屋町２丁目	1089	1909	25.43	296	15.51	582	53.44	760	60.19	109	36.82	73.35	56.06
27128007003	中央区	Chuo	瓦屋町３丁目	640	1073	27.11	158	14.73	384	60	383	64.31	48	30.38	100.00	61.46
27128027001	中央区	Chuo	瓦町１丁目	556	821	28.24	80	9.74	381	68.53	433	47.26	25	31.25	100.00	58.00
27128027002	中央区	Chuo	瓦町２丁目	13	22	0.90	8	36.36	8	61.54	9	59.09	2	25.00	100.00	59.75
27128027003	中央区	Chuo	瓦町３丁目	29	35	1.37	4	11.43	27	93.1	18	48.57	3	75.00	100.00	70.39
27128027004	中央区	Chuo	瓦町４丁目	37	44	1.66	7	15.91	33	89.19	23	47.73	5	71.43	100.00	70.94
27128039001	中央区	Chuo	石町１丁目	152	238	19.60	61	25.63	101	66.45	133	44.12	31	50.82	100.00	65.17
27128039002	中央区	Chuo	石町２丁目	222	319	23.77	68	21.32	159	71.62	180	43.57	28	41.18	100.00	62.93
271280650	中央区	Chuo	神崎町	241	453	21.12	60	13.25	113	46.89	238	47.46	20	33.33	100.00	54.14
271280640	中央区	Chuo	粉川町	666	1191	43.81	223	18.72	363	54.5	565	52.56	61	27.35	100.00	60.51
27128047001	中央区	Chuo	糸屋町１丁目	369	758	65.27	68	8.97	157	42.55	372	50.92	14	20.59	100.00	55.85
27128047002	中央区	Chuo	糸屋町２丁目	90	168	6.31	20	11.9	41	45.56	91	45.83	3	15.00	62.45	39.80
27128032001	中央区	Chuo	船場中央１丁目	0	0	0.00	0	0	0	0	0	0	0	0.00	100.00	16.69
27128032002	中央区	Chuo	船場中央２丁目	0	0	0.00	0	0	0	0	0	0	0	0.00	100.00	16.69
27128032003	中央区	Chuo	船場中央３丁目	0	0	0.00	0	0	0	0	0	0	0	0.00	100.00	16.69

27128032004	中央区	Chuo	船場中央４丁目	0	0	0.00	0	0	0	0	154	0	0	0.00	100.00	16.69
27128042001	中央区	Chuo	船越町１丁目	164	263	23.44	33	12.55	102	62.2	170	35.36	8	24.24	100.00	52.22
27128042002	中央区	Chuo	船越町２丁目	211	292	18.55	28	9.59	163	77.25	151	48.29	7	25.00	100.00	57.40
27128018001	中央区	Chuo	西心斎橋１丁目	222	301	3.57	60	19.93	166	74.77	169	43.85	20	33.33	100.00	58.81
27128018002	中央区	Chuo	西心斎橋２丁目	327	434	4.42	86	19.82	257	78.59	57	86.87	27	31.40	100.00	68.53
27128055001	中央区	Chuo	谷町１丁目	54	94	3.63	34	36.17	32	59.26	138	0	15	44.12	100.00	51.86
27128055002	中央区	Chuo	谷町２丁目	174	270	7.05	32	11.85	115	66.09	144	46.67	15	46.88	100.00	58.11
27128055003	中央区	Chuo	谷町３丁目	212	294	9.12	22	7.48	163	76.89	502	0	8	36.36	68.99	42.46
27128055004	中央区	Chuo	谷町４丁目	528	1009	21.14	141	13.97	253	47.92	544	46.09	47	33.33	100.00	53.96
27128055005	中央区	Chuo	谷町５丁目	625	1166	47.23	181	15.52	306	48.96	1414	0	52	28.73	100.00	48.27
27128055006	中央区	Chuo	谷町６丁目	1523	2878	20.62	761	26.44	757	49.7	881	69.39	173	22.73	100.00	61.65
27128055007	中央区	Chuo	谷町７丁目	870	1652	23.26	362	21.91	420	48.28	294	82.2	92	25.41	100.00	63.39
27128055008	中央区	Chuo	谷町８丁目	290	585	17.39	144	24.62	130	44.83	462	21.03	50	34.72	100.00	50.97
27128055009	中央区	Chuo	谷町９丁目	554	943	20.59	194	20.57	334	60.29	540	42.74	90	46.39	100.00	61.18
27128057001	中央区	Chuo	農人橋１丁目	545	1124	29.96	220	19.57	286	52.48	294	73.84	25	11.36	100.00	60.12
27128057002	中央区	Chuo	農人橋２丁目	306	558	14.35	88	15.77	163	53.27	65	88.35	28	31.82	100.00	63.14
27128057003	中央区	Chuo	農人橋３丁目	102	107	7.06	3	2.8	97	95.1	6	94.39	3	100.00	100.00	86.13
27128024001	中央区	Chuo	道修町１丁目	11	16	0.60	11	68.75	8	72.73	18	0	5	45.45	100.00	64.96
27128024002	中央区	Chuo	道修町２丁目	30	34	1.43	3	8.82	27	90	45	0	2	66.67	100.00	56.72
27128024003	中央区	Chuo	道修町３丁目	39	90	3.86	5	5.56	10	25.64	7	92.22	2	40.00	100.00	53.92
27128024004	中央区	Chuo	道修町４丁目	15	17	0.67	8	47.06	13	86.67	150	0	5	62.50	100.00	64.91
27128011001	中央区	Chuo	道頓堀１丁目	276	422	5.30	111	26.3	192	69.57	36	91.47	59	53.15	100.00	74.81
27128011002	中央区	Chuo	道頓堀２丁目	30	53	2.01	16	30.19	14	46.67	152	0	4	25.00	100.00	43.80
27128041001	中央区	Chuo	釣鐘町１丁目	164	259	20.05	38	14.67	110	67.07	172	33.59	12	31.58	100.00	55.56
27128041002	中央区	Chuo	釣鐘町２丁目	206	254	16.59	15	5.91	173	83.98	275	0	7	46.67	100.00	52.73
27128052001	中央区	Chuo	鎗屋町１丁目	129	267	23.80	31	11.61	55	42.64	128	52.06	8	25.81	100.00	52.02
27128052002	中央区	Chuo	鎗屋町２丁目	195	257	22.64	8	3.11	151	77.44	147	42.8	3	37.50	100.00	58.44
27128014001	中央区	Chuo	難波１丁目	23	57	1.67	16	28.07	10	43.48	19	66.67	4	25.00	100.00	54.91
27128014002	中央区	Chuo	難波２丁目	19	26	0.95	7	26.92	14	73.68	8	69.23	5	71.43	100.00	74.44
27128014003	中央区	Chuo	難波３丁目	23	40	1.08	15	37.5	12	52.17	17	57.5	5	33.33	100.00	59.42

27128014004	中央区	Chuo	難波４丁目	62	112	3.92	45	40.18	32	51.61	48	57.14	10	22.22	100.00	59.05
27128014005	中央区	Chuo	難波５丁目	0	0	0.00	0	0	0	0	0	0	0	0.00	100.00	16.69
271280130	中央区	Chuo	難波千日前	407	676	9.80	213	31.51	263	64.62	300	55.62	78	36.62	100.00	64.28
271280690	中央区	Chuo	馬場町	133	136	2.26	0	0	130	97.74	102	25	0	0.00	0.00	29.80
27128008001	中央区	Chuo	高津１丁目	611	915	15.22	152	16.61	424	69.39	326	64.37	63	41.45	100.00	64.93
27128008002	中央区	Chuo	高津２丁目	669	851	27.32	80	9.4	552	82.51	315	62.98	47	58.75	100.00	72.70
27128008003	中央区	Chuo	高津３丁目	1437	2271	24.25	430	18.93	899	62.56	969	57.33	170	39.53	100.00	64.33
27128022001	中央区	Chuo	高麗橋１丁目	394	620	20.90	68	10.97	252	63.96	354	42.9	22	32.35	100.00	55.68
27128022002	中央区	Chuo	高麗橋２丁目	123	133	5.68	11	8.27	116	94.31	99	25.56	6	54.55	100.00	61.94
27128022003	中央区	Chuo	高麗橋３丁目	0	0	0.00	0	0	0	0	0	0	0	0.00	100.00	16.69
27128022004	中央区	Chuo	高麗橋４丁目	7	8	0.26	4	50	6	85.71	4	50	2	50.00	100.00	73.05
271280620	中央区	Chuo	龍造寺町	238	427	18.94	106	24.82	135	56.72	223	47.78	44	41.51	100.00	62.25

Appendix 2.2. Principle component analysis output for Osaka City, Japan

Total Variance Explained

Component	Initial Eigenvalues			Extraction Sums of Squared Loadings			Rotation Sums of Squared Loadings		
	Total	% of Variance	Cumulative %	Total	% of Variance	Cumulative %	Total	% of Variance	Cumulative %
1	2.771	39.585	39.585	2.771	39.585	39.585	2.122	30.309	30.309
2	1.491	21.305	60.890	1.491	21.305	60.890	1.855	26.504	56.813
3	1.137	16.249	77.139	1.137	16.249	77.139	1.423	20.326	77.139
4	.667	9.528	86.667						
5	.363	5.185	91.852						
6	.311	4.443	96.295						
7	.259	3.705	100.000						

Extraction Method: Principal Component Analysis.

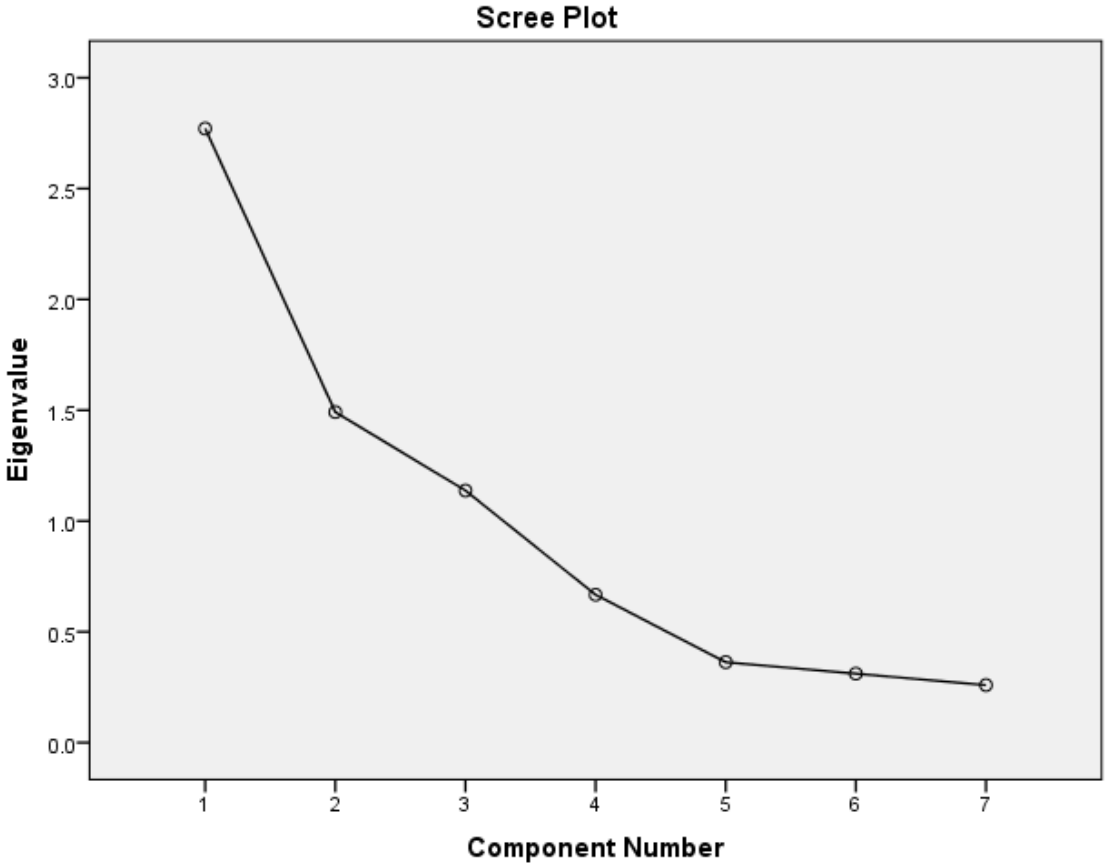

Rotated Component Matrix[a]

	Component		
	1	2	3
Age	.871	.120	.052
Unemployment	.699	.446	.282
Education	.909	-.062	-.003
Isolation	.010	.916	.109
Age_and_Isolation	.164	.884	.081
Density	.145	.099	.805
Lack_of_Green_Space	-.009	.083	.821

Extraction Method: Principal Component Analysis.

Rotation Method: Varimax with Kaiser Normalization.

Appendix 2.3. Heat wave vulnerability and exposure mapping for Osaka City, Japan: Supporting information

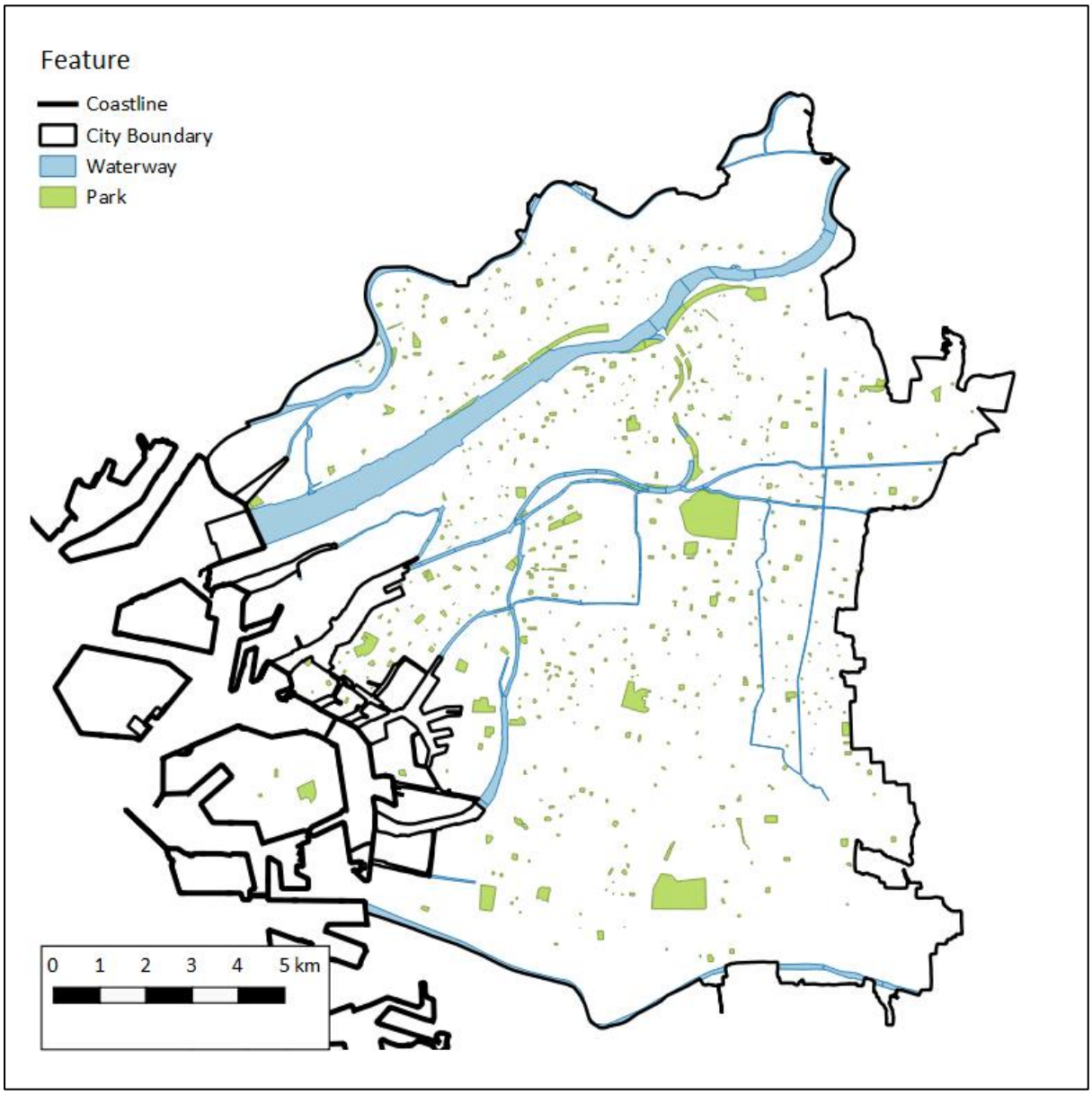

Figure 1: Location of parks, waterways and the coastline in Osaka City. Data accessed from: www.openstreetmap.org.

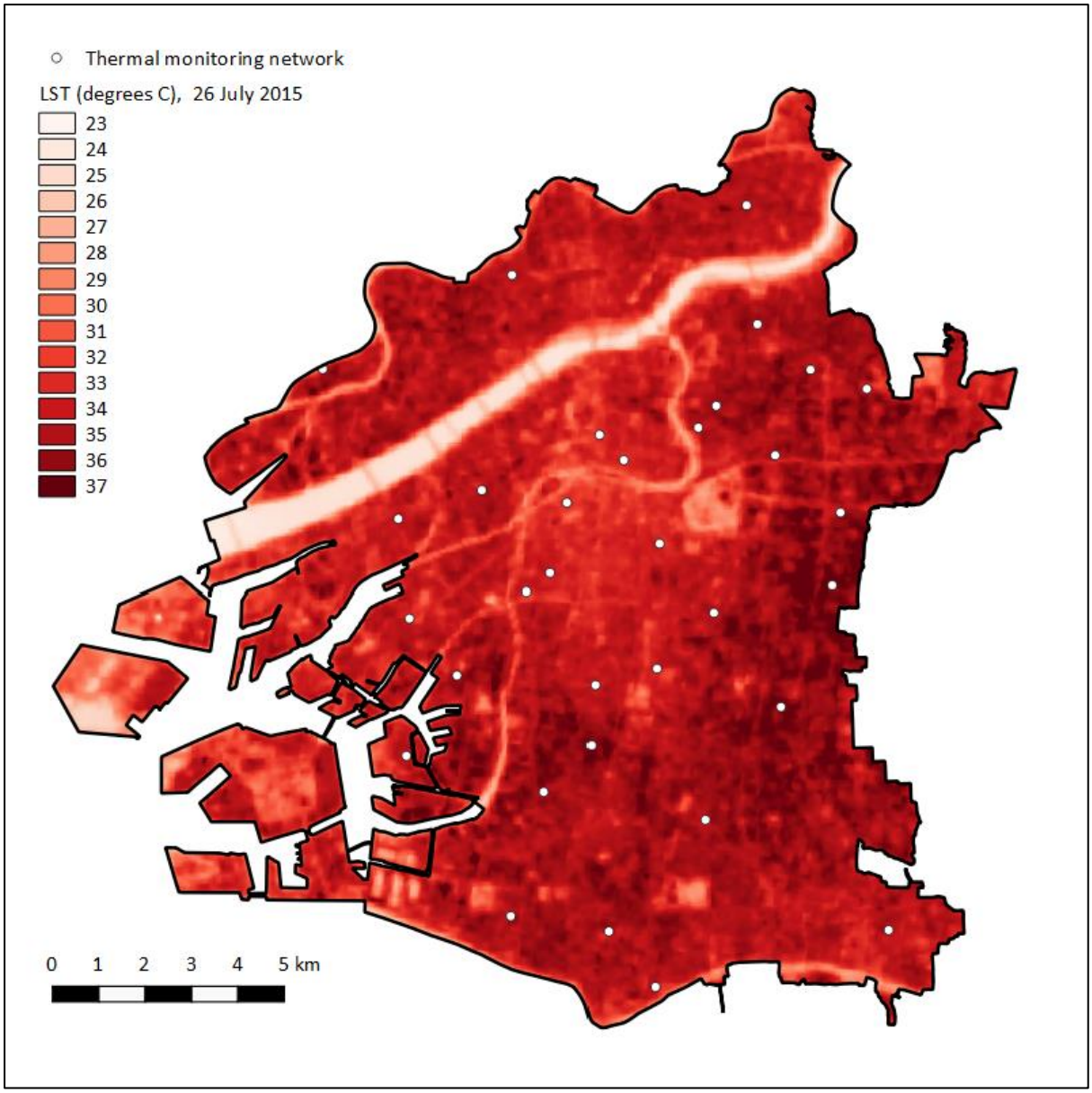

Figure 2: Landsat 8 Thermal Infrared Sensor (TIRS) image, with estimated land surface temperature (LST) at 30m^2 resolution. The image was taken at 10:34 AM on 26th July 2015. This image was selected as a representative of LST for Osaka City as it is the only 'hot day' image with zero cloud cover available from Landsat 8 (TIRS) for the study area. Data accessed from: http://earthexplorer.usgs.gov/.

LST is calculated from Band 10 wavelengths (thermal energy) in a two-step process:

Step one involves converting the unscaled data into Top of Atmosphere (TOA) radiance using the following formula:

$$L_\lambda = M_L Q_{cal} + A_L$$

Where L_λ is the TOA radiance (Watts/(m^2 * srad * μm)), M_L is the band-specific multiplicative rescaling factor, Q_{cal} is the unscaled data value and A_L is the band-specific additive rescaling factor.

Step two involves converting TOA radiance into at-satellite brightness temperature (an estimate of LST:

$$T = \frac{K_2}{\ln(\frac{K_1}{L_\lambda} + 1)}$$

Where T is the at-satellite brightness temperature (Kelvin), K_1 is the band-specific thermal conversion constant and K_2 is a second band-specific thermal conversion constant. Further details available at: http://landsat.usgs.gov/Landsat8_Using_Product.php.

LST is obtained by converting degrees K into degrees C (Buscail et al. 2012) (C = K – 272.15).

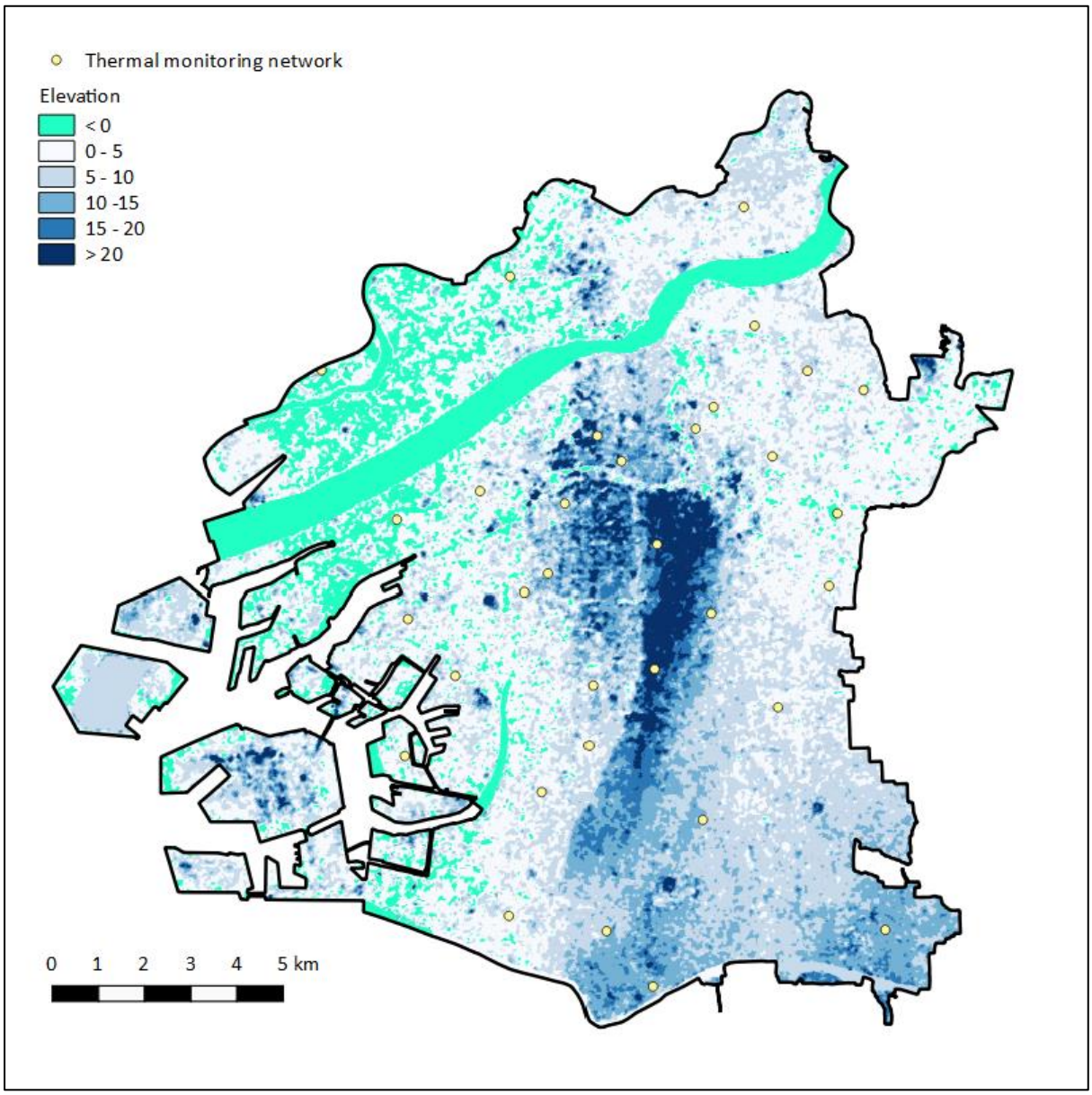

Figure 3: Terrain elevation at 25m² resolution in Osaka City. Data accessed from: http://nlftp.mlit.go.jp/ksj-e/gml/gml_datalist.html.

Appendix 3.1. Location of Osaka Prefecture, Japan

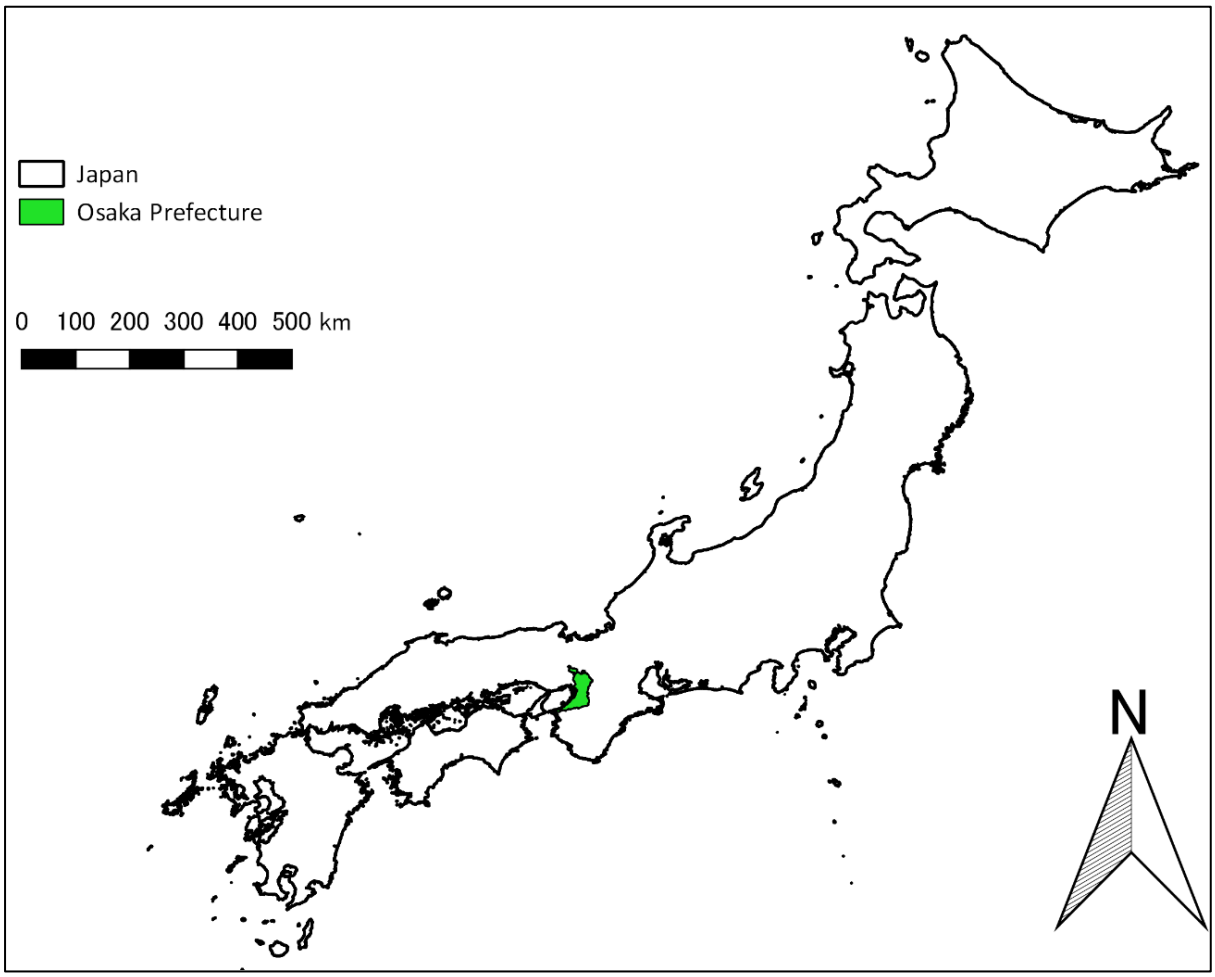

Appendix 3.2. Full study framework for Chapter 4

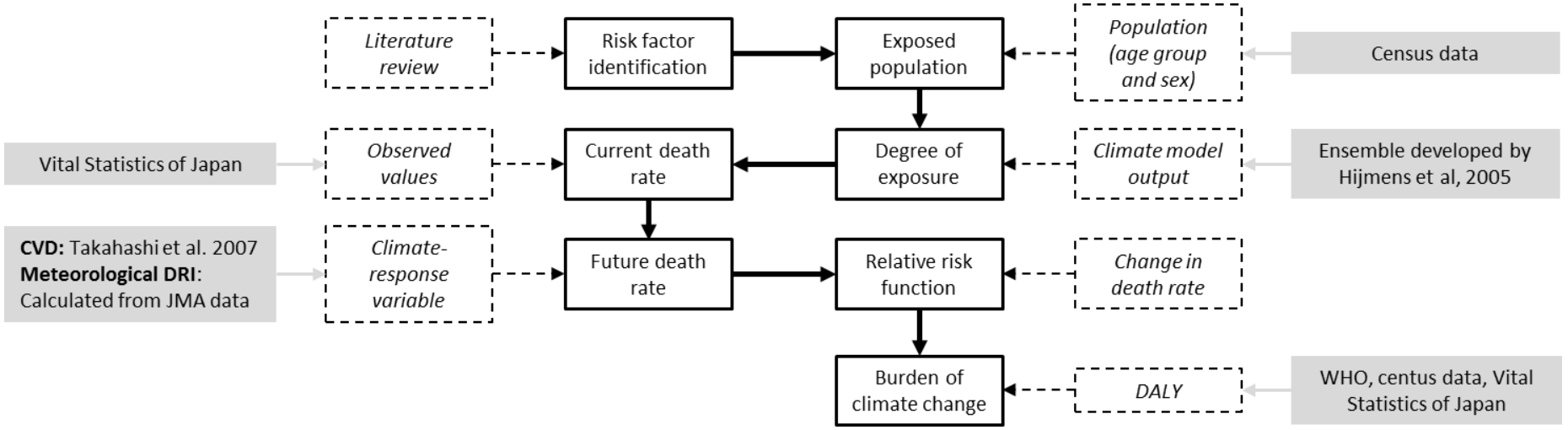

Appendix 3.3. Osaka Prefecture Digital Elevation Map

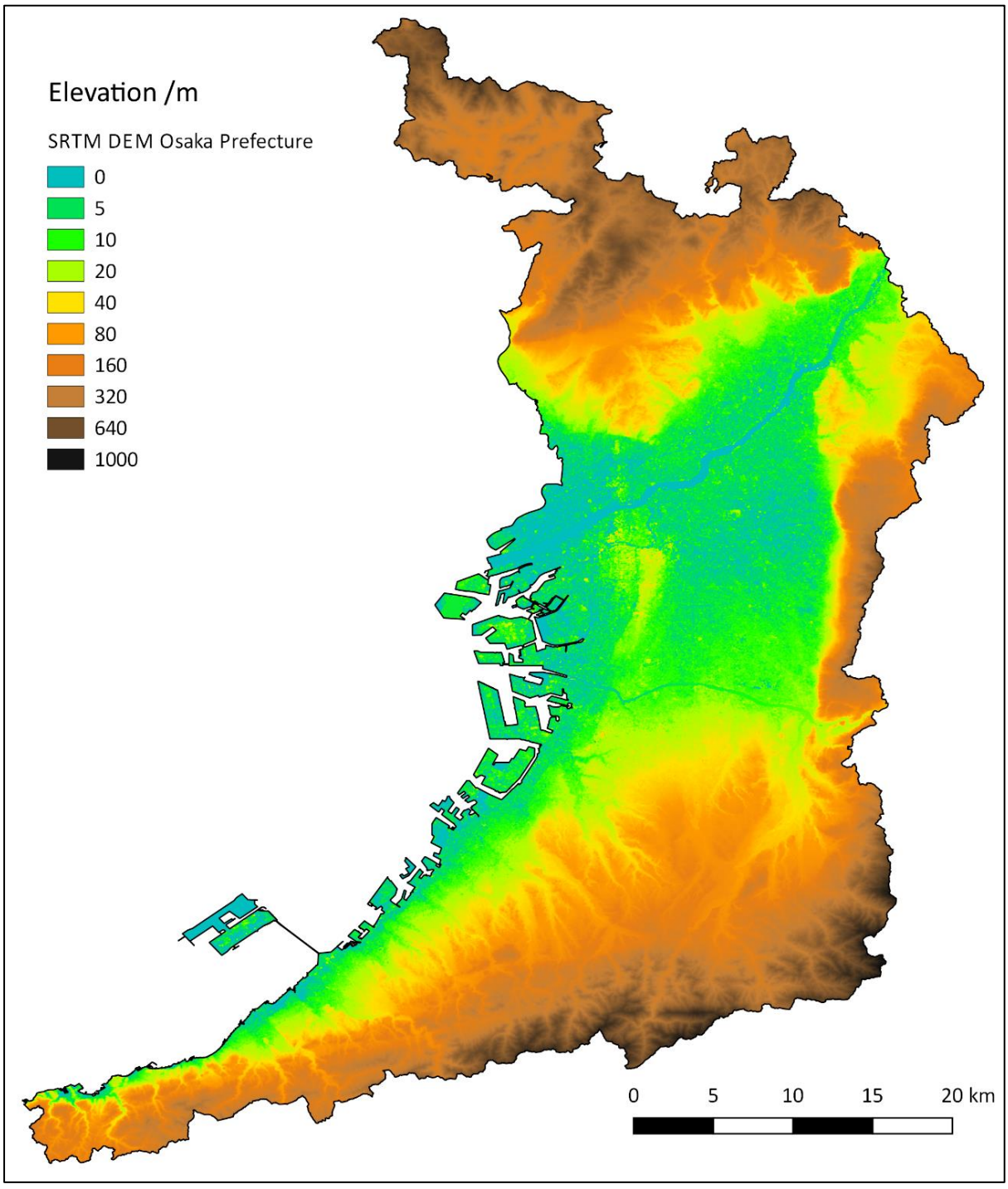

Appendix 3.4. 1km resolution interpolated observed temperatures for Osaka Prefecture 1980 – 2000

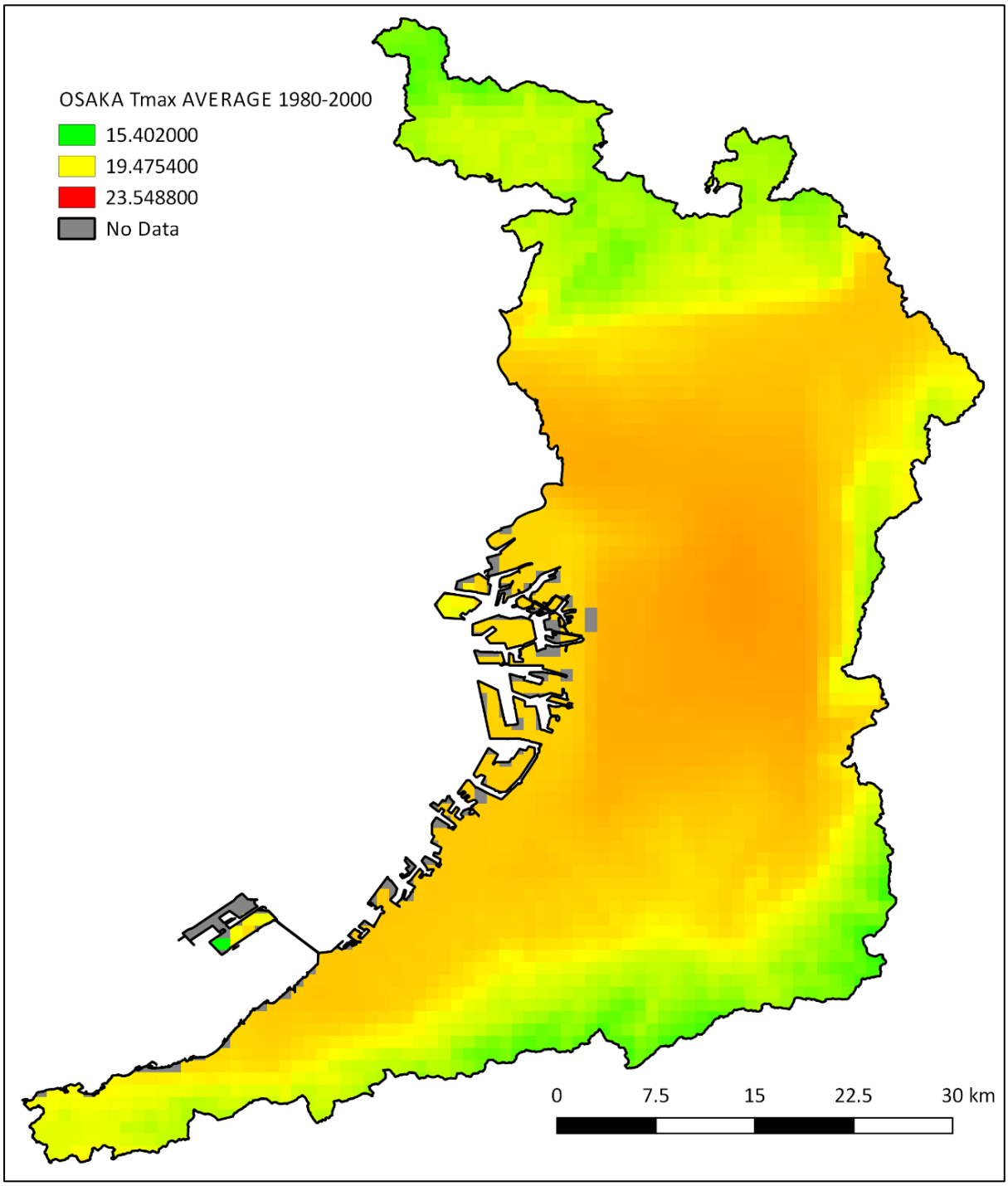

Source data from Hijmens et al. (2005) (Chapter 4 references)

Appendix 3.5. 1km resolution climate model output temperatures for Osaka Prefecture 2050

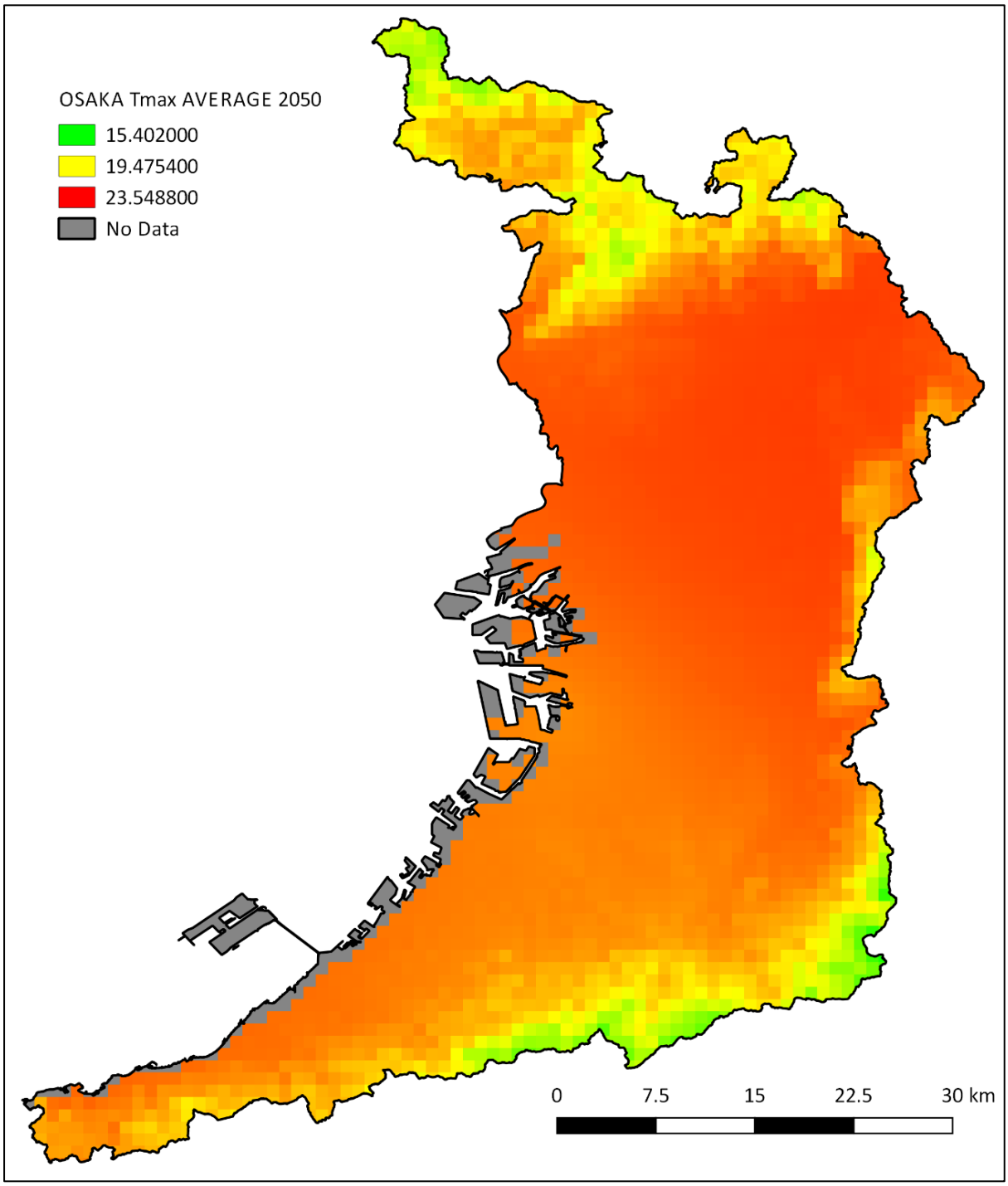

Source data from Hijmens et al. (2005) (Chapter 4 references)

Appendix 3.6. Projected change in mean annual temperature per administrative zone 2000 – 2015, in Osaka Prefecture, Japan

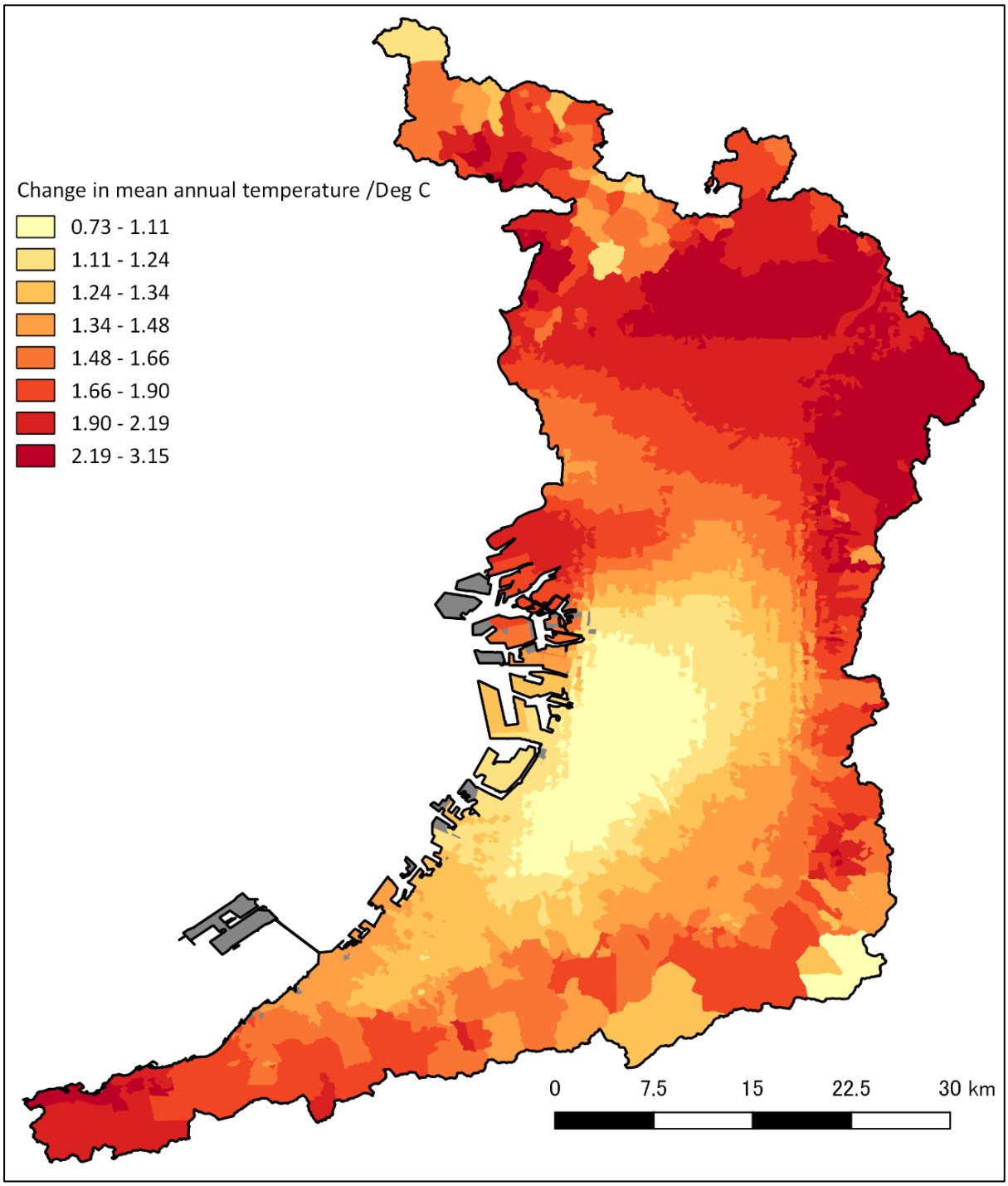

Appendix 3.7. Population per administrative zone in Osaka Prefecture

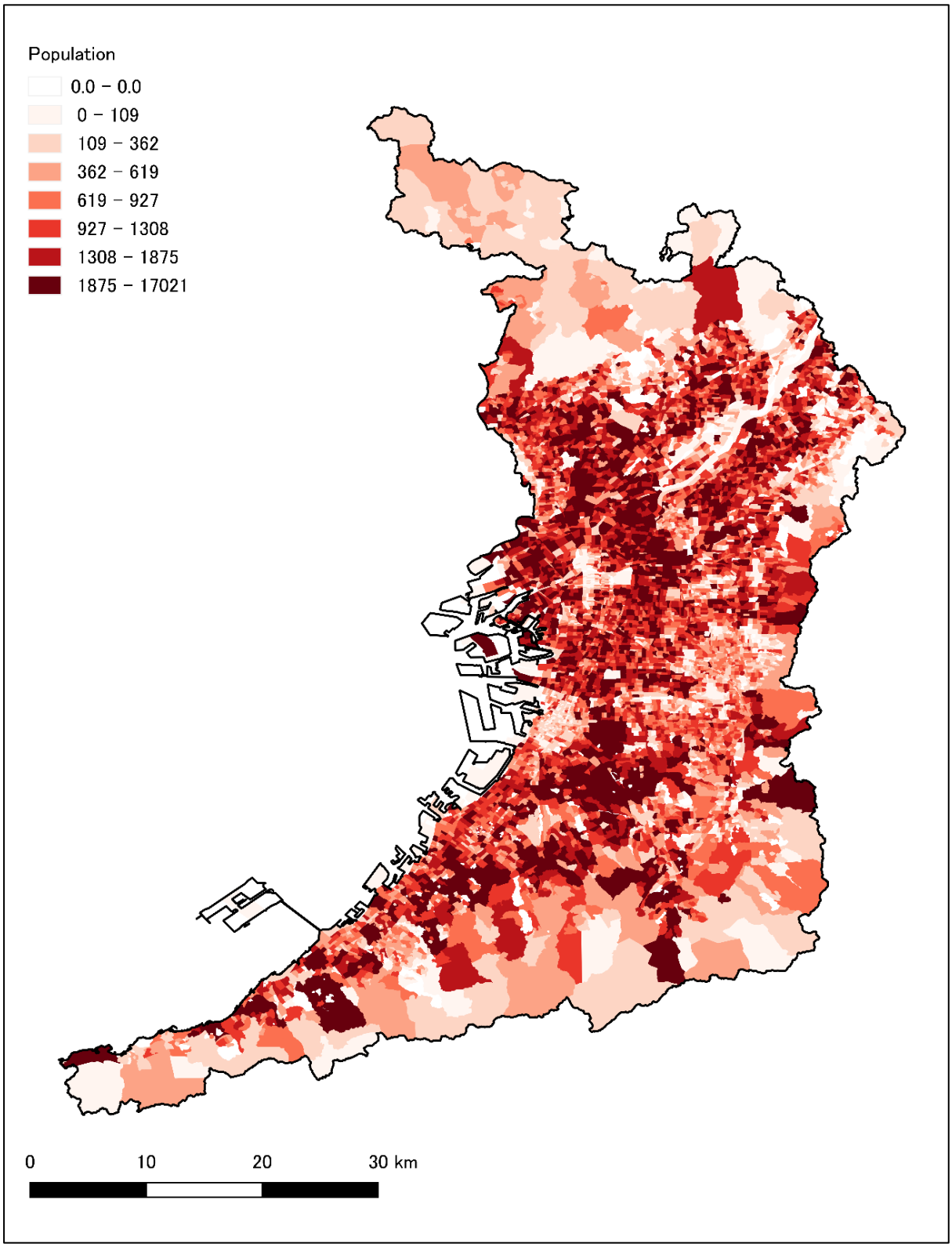

Appendix 3.8. Population density per administrative zone in Osaka Prefecture

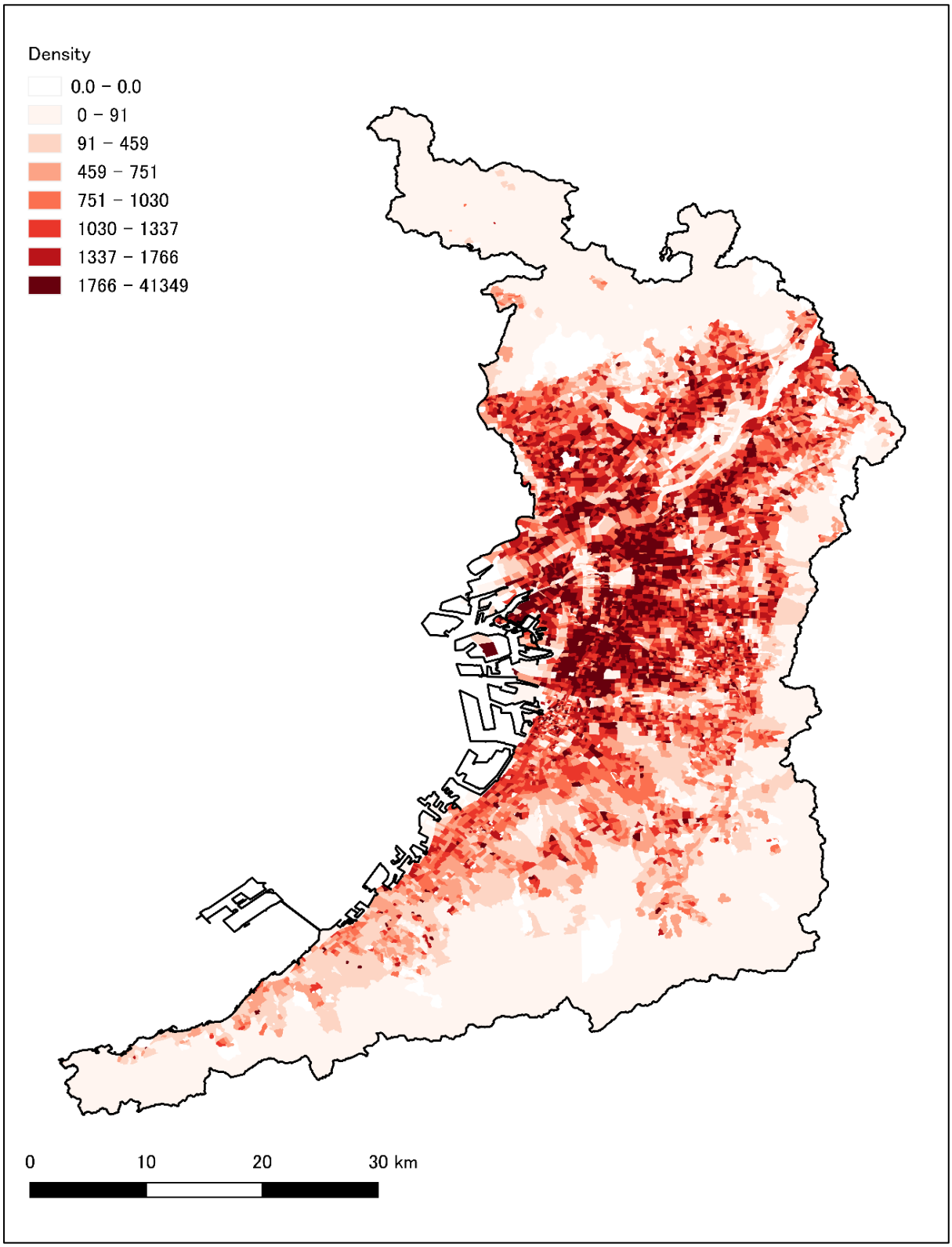

Figure 1: Population Density per km^2 for each administrative zone in Osaka Prefecture.

Appendix 3.9. Regression analysis of observed annual Tmax and the number of days above designated CVD risk temperature thresholds for Osaka Prefecture 1985-2015

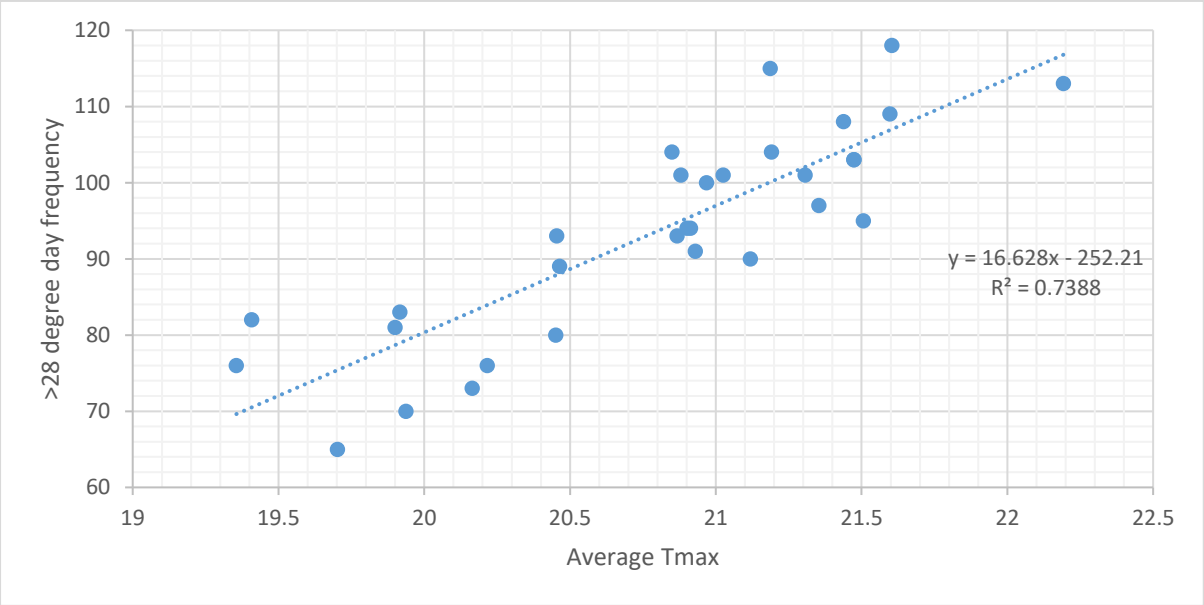

Figure 1: Average annual Tmax and the number of days above 28ºC

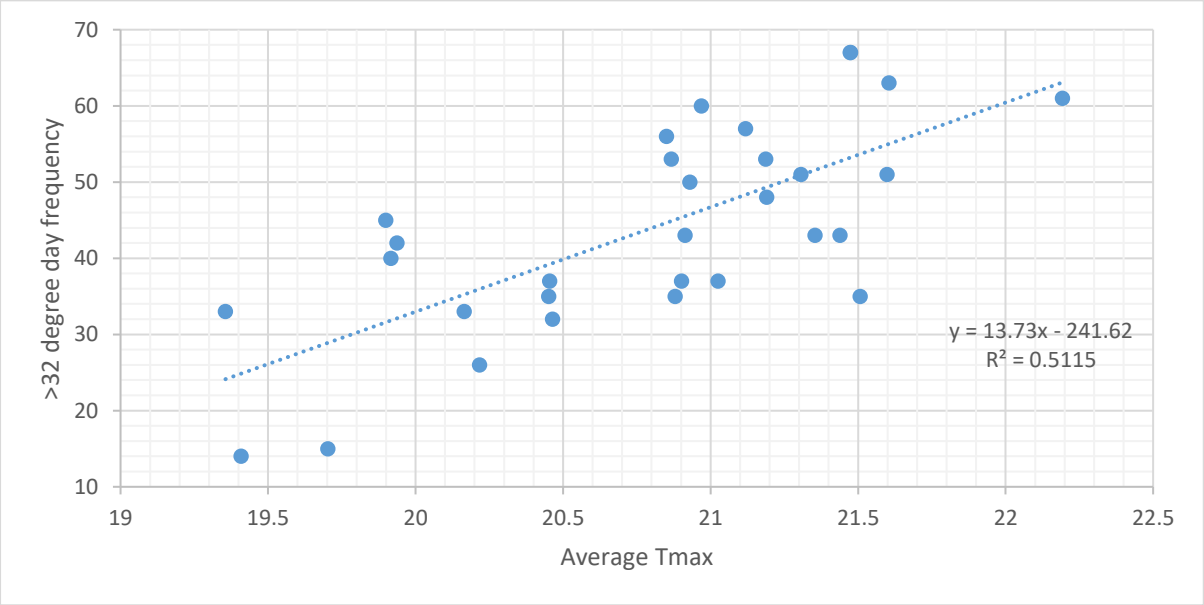

Figure 2: Average annual Tmax and the number of days above 28ºC

Appendix 3.10. Regression analysis of observed annual precipitation, the number of high intensity rainfall events and meteorological DRIs

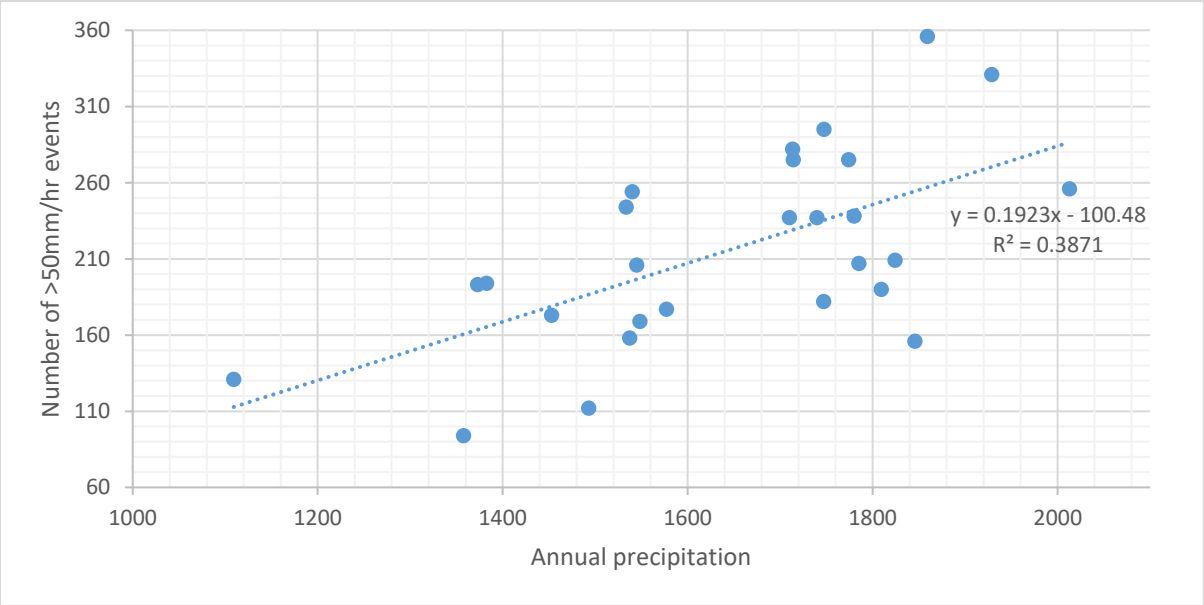

Figure 1: Annual precipitation and the number of > 50 mm/hr precipitation events in Japan 1989-2015

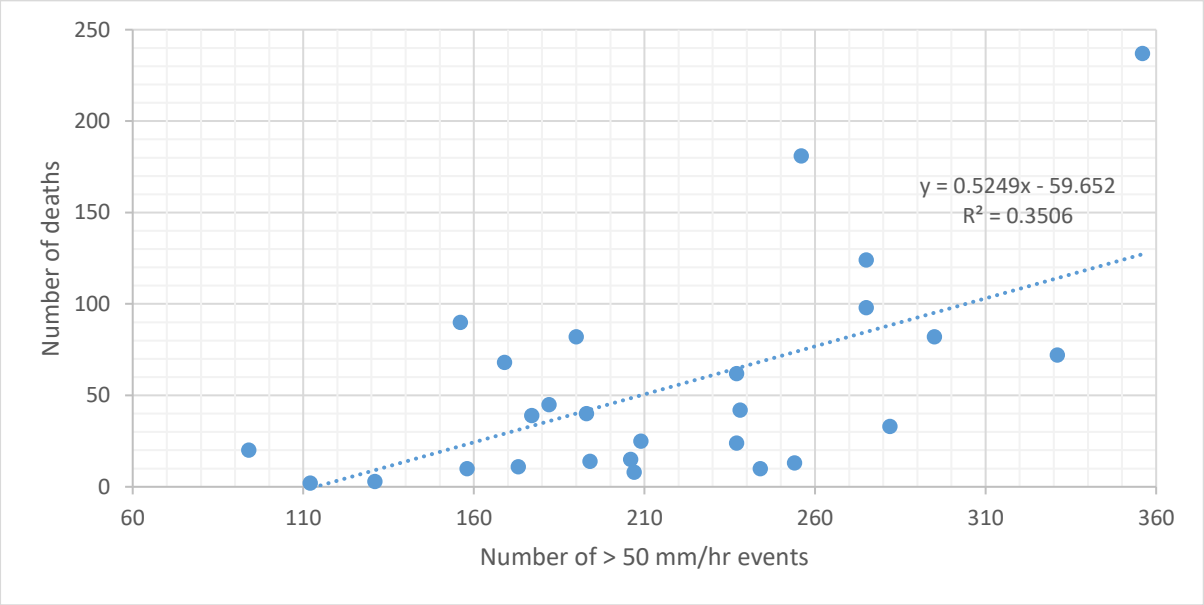

Figure 1: Annual number of > 50 mm/hr precipitation events and number of meteorological DRI deaths in Japan 1989-2015

Appendix 3.11. A selected portion of the climate change influenced cardiovascular disease risk database for Osaka prefecture

In total there are 8838 administrative zones in Osaka Prefecture. This table shows a portion of the total zones. The zones are identified by their individual Keycodes. The number of days above each threshold (Tmax > 28ºC and Tmax > 32ºC) are calculated Based upon the ratios observed in Appendix 3.6.

KEY_CODE	Total pop	Obs Tmax	2050 Tmax	2010 >28 DD	2010 28-32 DD	2010 >32 DD	2050 >28 DD	2050 28-32 DD	2050 >32 DD	CVD Deaths 2010	CVD DR 2010	Daily DR	2050 >28 excess DD	HAD 28-32 excess DD	2050 >32 excess DD	28-32 DD excess deaths	32 DD excess deaths	2050 excess deaths	2050 TOTAL DEATHS	2050 DR	2050 RISK RATIO	CVD DALY	CVD DALY /100k	2050 DALY	2050 DALY /100k	Change in DALY rate
27102014003	2253	21.39	22.61	103.50	51.41	52.10	123.80	54.94	68.86	6.553	290.83	0.01	20.30	3.54	16.76	0.00	0.03	0.031	6.584	292.	1.005	89.28	3962.834	89.71	3981.799	18.965
27102015005	1433	21.38	22.59	103.21	51.35	51.86	123.37	54.87	68.50	5.602	390.95	0.01	20.16	3.51	16.64	0.00	0.03	0.027	5.629	392.	1.005	64.71	4516.112	65.02	4537.575	21.463
27102015004	1688	21.36	22.58	102.97	51.31	51.66	123.17	54.83	68.34	4.761	282.05	0.01	20.20	3.52	16.68	0.00	0.02	0.023	4.784	283.	1.005	61.68	3654.430	61.98	3671.835	17.406
27102014002	1758	21.36	22.58	103.02	51.32	51.70	123.22	54.84	68.38	6.428	365.62	0.01	20.19	3.52	16.67	0.00	0.03	0.031	6.458	367.	1.005	75.77	4310.019	76.13	4330.539	20.520
27102014001	1831	21.36	22.58	102.94	51.31	51.63	123.17	54.83	68.33	6.135	335.08	0.01	20.23	3.52	16.70	0.00	0.03	0.029	6.165	336.	1.005	79.09	4319.567	79.46	4340.165	20.598
27102015002	4839	21.37	22.58	103.08	51.33	51.75	123.25	54.85	68.40	13.071	270.11	0.03	20.17	3.52	16.66	0.00	0.06	0.062	13.133	271.	1.005	179.5	3709.584	180.3	3727.226	17.642
27102015003	1249	21.35	22.57	102.84	51.29	51.55	123.02	54.81	68.21	2.120	169.72	0.00	20.18	3.52	16.66	0.00	0.01	0.010	2.130	170.	1.005	31.83	2548.523	31.98	2560.647	12.124
27102013003	1991	21.36	22.58	102.94	51.31	51.63	123.17	54.83	68.33	3.722	186.94	0.01	20.23	3.52	16.70	0.00	0.02	0.018	3.740	187.	1.005	53.88	2706.319	54.14	2719.224	12.905
27102013001	1702	21.37	22.58	103.08	51.33	51.75	123.25	54.85	68.40	31.341	184.13	0.08	20.17	3.52	16.65	0.01	0.14	0.149	31.490	185.	1.005	509.7	2994.688	512.1	3008.929	14.241
27102010003	1644	21.39	22.59	103.54	51.41	52.13	123.49	54.89	68.60	4.114	250.25	0.01	19.95	3.48	16.47	0.00	0.02	0.019	4.134	251.	1.005	49.99	3041.237	50.23	3055.544	14.307
27102015001	1412	21.34	22.54	102.56	51.24	51.32	122.60	54.73	67.87	5.650	400.12	0.01	20.04	3.49	16.55	0.00	0.03	0.027	5.676	402.	1.005	67.04	4747.923	67.35	4770.361	22.439
27102011002	1563	21.42	22.60	103.98	51.49	52.49	123.52	54.89	68.62	5.122	327.69	0.01	19.54	3.41	16.14	0.00	0.02	0.024	5.145	329.	1.005	67.55	4321.817	67.86	4341.730	19.913
27102013002	1219	21.32	22.56	102.37	51.21	51.16	122.92	54.79	68.13	3.180	260.90	0.00	20.55	3.58	16.97	0.00	0.01	0.015	3.196	262.	1.005	43.47	3566.170	43.68	3583.448	17.278
27102010002	1067	21.33	22.56	102.52	51.23	51.29	122.99	54.80	68.19	3.096	290.19	0.00	20.46	3.57	16.90	0.00	0.01	0.015	3.111	291.	1.005	38.78	3634.874	38.97	3652.412	17.538
27102012004	771	21.38	22.58	103.36	51.38	51.98	123.32	54.86	68.46	3.277	424.97	0.00	19.96	3.48	16.48	0.00	0.01	0.015	3.292	426.	1.005	38.29	4967.357	38.47	4990.732	23.375
27102010001	2366	21.32	22.56	102.30	51.20	51.10	122.89	54.78	68.11	4.761	201.21	0.01	20.59	3.59	17.00	0.00	0.02	0.023	4.784	202.	1.005	67.81	2866.145	68.14	2880.060	13.915
27102011001	1363	21.41	22.59	103.82	51.46	52.36	123.40	54.87	68.53	3.948	289.67	0.01	19.58	3.41	16.17	0.00	0.02	0.018	3.966	291.	1.005	50.79	3726.485	51.02	3743.689	17.204
27102012003	949	21.38	22.58	103.35	51.38	51.98	123.31	54.86	68.45	2.824	297.60	0.00	19.95	3.48	16.47	0.00	0.01	0.013	2.838	299.	1.005	34.46	3631.518	34.62	3648.600	17.082
27102009002	5044	21.36	22.57	102.90	51.30	51.60	123.13	54.83	68.30	6.001	118.97	0.01	20.23	3.52	16.70	0.00	0.03	0.029	6.030	119.	1.005	94.62	1876.016	95.07	1884.962	8.946
27102012002	2104	21.38	22.58	103.35	51.38	51.98	123.31	54.86	68.45	7.449	354.06	0.02	19.95	3.48	16.47	0.00	0.03	0.035	7.484	355.	1.005	89.67	4261.894	90.09	4281.942	20.048
27102009001	828	21.34	22.57	102.64	51.25	51.38	123.02	54.81	68.22	2.979	359.78	0.00	20.39	3.55	16.83	0.00	0.01	0.014	2.993	361.	1.005	36.19	4371.395	36.36	4392.405	21.010
											5	8							514		5		9			

271020											253.47	0.01								254.		79.70		80.09				
08001	2454	21.32	22.56	102.30	51.20	51.10	122.89	54.78	68.11	6.220	5	7	20.59	3.59	17.00	0.000	0.030	0.030	6.250	706	1.005	5	3247.967	2	3263.735	15.769			
271020											226.93	0.02								227.		140.1		140.8				
08002	4591	21.40	22.59	103.59	51.42	52.17	123.35	54.86	68.49	10.418	1	9	19.76	3.44	16.32	0.000	0.050	0.049	10.467	988	1.005	86	3053.493	39	3067.722	14.228			
271020											294.57	0.01								296.		54.56		54.82				
07001	1466	21.32	22.56	102.31	51.20	51.11	122.87	54.78	68.09	4.318	7	2	20.57	3.58	16.98	0.000	0.020	0.021	4.339	005	1.005	2	3721.798	6	3739.846	18.048			
271020											229.61	0.01								230.		64.99		65.29				
12001	2094	21.38	22.58	103.35	51.38	51.98	123.31	54.86	68.45	4.808	8	3	19.95	3.48	16.47	0.000	0.020	0.023	4.831	698	1.005	3	3103.757	8	3118.357	14.600			
271020											297.08	0.01								298.		84.38		84.79				
07003	2223	21.29	22.53	101.83	51.11	50.72	122.35	54.69	67.66	6.604	6	8	20.52	3.58	16.94	0.000	0.030	0.032	6.636	523	1.005	4	3795.971	3	3814.336	18.365			
271020											232.05	0.00								233.		30.50		30.65				
07002	932	21.32	22.54	102.28	51.19	51.09	122.61	54.74	67.88	2.163	4	6	20.33	3.54	16.79	0.000	0.010	0.010	2.173	166	1.005	9	3273.518	5	3289.208	15.689			
271020											379.81	0.02								381.		92.42		92.85				
07004	2071	21.37	22.56	103.12	51.34	51.78	122.95	54.80	68.16	7.866	6	2	19.84	3.46	16.38	0.000	0.040	0.037	7.903	592	1.005	6	4462.852	8	4483.726	20.874			
271020											305.52	0.01								306.		47.95		48.17				
07005	1324	21.35	22.56	102.78	51.28	51.50	122.91	54.79	68.12	4.045	0	1	20.13	3.51	16.62	0.000	0.020	0.019	4.064	969	1.005	1	3621.672	8	3638.857	17.185			
271020											354.63	0.03								356.		133.4		134.1				
04005	3038	21.28	22.52	101.71	51.09	50.62	122.21	54.66	67.54	10.774	6	0	20.50	3.57	16.92	0.000	0.050	0.052	10.826	350	1.005	90	4394.010	35	4415.245	21.235			
271020											504.67	0.01								507.		63.81		64.12				
06001	1247	21.28	22.52	101.70	51.09	50.61	122.20	54.66	67.53	6.293	0	7	20.50	3.57	16.93	0.000	0.030	0.030	6.324	109	1.005	7	5117.644	5	5142.379	24.735			
271020											193.82	0.01								194.		91.17		91.60				
05001	3265	21.34	22.55	102.61	51.25	51.36	122.79	54.77	68.03	6.328	2	7	20.18	3.52	16.67	0.000	0.030	0.030	6.358	745	1.005	2	2792.399	6	2805.688	13.289			
271020											404.16	0.02								406.		103.5		104.0				
06002	2095	21.36	22.56	102.96	51.31	51.65	122.89	54.78	68.11	8.467	7	3	19.93	3.47	16.46	0.000	0.040	0.040	8.507	066	1.005	93	4944.764	80	4968.000	23.236			
271020											348.64	0.02								350.		113.3		113.8				
06003	2694	21.35	22.56	102.76	51.28	51.48	122.89	54.78	68.11	9.392	0	6	20.13	3.51	16.62	0.000	0.040	0.045	9.437	295	1.005	22	4206.461	60	4226.430	19.968			
271020											298.57	0.02								300.		90.51		90.95				
04004	2415	21.24	22.49	101.01	50.97	50.04	121.78	54.59	67.19	7.211	4	0	20.77	3.62	17.15	0.000	0.030	0.035	7.246	036	1.005	2	3747.927	6	3766.284	18.358			
271020											300.90	0.00								302.		39.13		39.31				
04003	1021	21.32	22.54	102.35	51.20	51.14	122.62	54.74	67.88	3.072	3	8	20.28	3.53	16.74	0.000	0.010	0.015	3.087	341	1.005	0	3832.470	7	3850.791	18.321			
271020											269.72	0.03								270.		176.3		177.1				
05002	4611	21.37	22.56	103.07	51.33	51.74	122.89	54.78	68.11	12.437	7	4	19.82	3.45	16.37	0.000	0.060	0.058	12.495	988	1.005	23	3823.959	47	3841.831	17.872			
271020											259.07	0.00								260.		45.72		45.93				
03005	1243	21.41	22.55	103.73	51.44	52.28	122.79	54.77	68.02	3.220	2	9	19.06	3.32	15.74	0.000	0.010	0.014	3.235	237	1.004	9	3678.886	4	3695.419	16.533			
271020											354.66	0.00								356.		38.08		38.26				
04001	971	21.28	22.51	101.68	51.09	50.59	122.08	54.64	67.44	3.444	2	9	20.40	3.56	16.85	0.000	0.020	0.017	3.460	368	1.005	1	3921.819	4	3940.684	18.864			
271020											222.18	0.01								223.		58.62		58.90				
04002	1764	21.34	22.54	102.62	51.25	51.37	122.66	54.74	67.92	3.919	1	1	20.04	3.49	16.55	0.000	0.020	0.019	3.938	231	1.005	9	3323.653	6	3339.356	15.702			
271020											357.23	0.01								358.		54.16		54.42				
03004	1319	21.27	22.50	101.49	51.05	50.44	121.99	54.63	67.36	4.712	8	3	20.50	3.57	16.93	0.000	0.020	0.023	4.735	965	1.005	4	4106.445	6	4126.293	19.848			
271020											381.02	0.00								382.		20.63		20.72				
03003	406	21.43	22.55	104.05	51.50	52.55	122.74	54.76	67.98	1.547	4	4	18.69	3.26	15.44	0.000	0.010	0.007	1.554	703	1.004	2	5081.727	3	5104.125	22.398			
271020											251.26	0.00								252.		10.44		10.49				
03002	332	21.34	22.53	102.62	51.25	51.37	122.35	54.69	67.66	0.834	2	2	19.73	3.44	16.29	0.000	0.000	0.004	0.838	431	1.005	3	3145.580	2	3160.214	14.633			
271020											136.66	0.00								137.		32.43		32.59				
03001	1399	21.27	22.50	101.42	51.04	50.38	121.92	54.62	67.31	1.912	8	5	20.50	3.57	16.93	0.000	0.010	0.009	1.921	328	1.005	5	2318.457	2	2329.663	11.206			

Appendix 3.12. Flood and sediment risk zones in Osaka prefecture

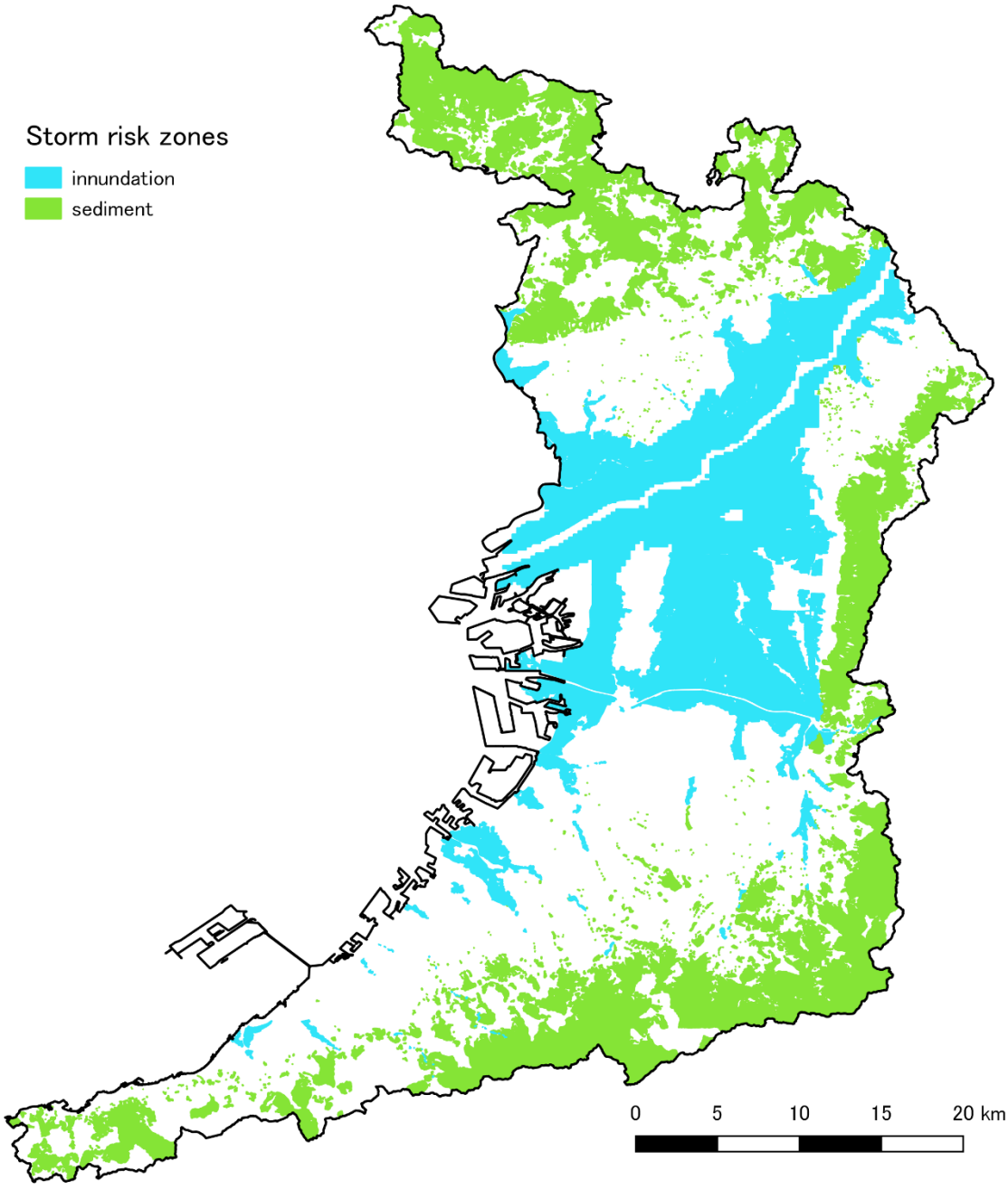

Data source: NLNI, 2016. National Land Numerical Information download service, Accessed online at: http://nlftp.mlit.go.jp/ksj/jpgis/jpgis_datalist.html [Japanese].